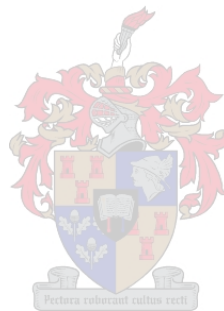# DEVELOPMENT CAPABILITY PROFILES OF SELECTED REVERSE ENGINEERING TECHNIQUES

Alexander Duss

Student Number: 14352508

Thesis presented in partial fulfilment of the requirements for the degree
Master of Science in Engineering (Industrial) at the university of Stellenbosch

Study Leader: Prof D. Dimitrov

U

Declaration

I, the undersigned, hereby declare that the work contained in this thesis is my own original work and has not previously in its entirety or in part been submitted at any university for a degree.

_____   _____

Signature: Date:

Synopsis

Reverse engineering (RE) has emerged as an important tool in the design stages of a product. The demand for better performance of hardware and software has spawned many different technologies that fall under RE. The diversity of technologies is linked to the different application areas of industry. It is critical to understand what the exact capability of each individual technology is, in order to choose the appropriate RE system.

The objective of this study is to develop capability profiles of different RE technologies available, such as: Coordinate Measuring Machine, Articulated Arm (Cimcore), Non-contact scanner (GOM), and contact scanner (Renishaw). To achieve the objective, the different characteristics of each technology are measured and quantified.

A capability profile can be regarded as defined criteria that represent the performance of a RE technology and in this study, is defined by quantifying the following characteristics:

- Accuracy
- Repeatability
- Speed of Measurement
- Work Envelope
- User-friendliness.

The significance of developing these capability profiles is so that they may be compared to one another. This is important, especially for the accuracy criterion, as each technology is manufactured by a different company, making an acceptable accuracy comparison amongst the different technologies impossible.

The study also suggests an evaluation tool which will help a decision maker choose the appropriate technology for a specified objective. Guidelines are also given to potential end users of RE technologies on how they should go about acquiring the right system.

On a more general level, the study contributes to research in recent trends, in the RE industry in terms of application, hardware, software and the selection of RE systems.

By developing these capability profiles, the study aims to contribute to its value in academia, as well as for industry partners and potential RE end-users.

Opsomming

RE het ontwikkel as n belangrike hulpmiddel in die ontwerp fase van 'n produk.   Die aanvraag na beter prestasie van hardeware en sagteware het gelei tot die ontwikkeling van baie verskillende tegnologie. Die diversiteit van die tegnologie gaan hand aan hand met die verskillende toepassings areas in die industrie. Dit is belangrik om die spesifieke eienskappe van elke individuele tegnologie te verstaan om die regte RE sisteem te kies.

The doel van hierdie studie is om die vermoë profiele van die verskillende beskikbare RE tegnologie te ontwerp: *Coordinate Measuring Machine, Articulated Arm (Cimcore)*, nie-kontak skandeerder (GOM) en kontak skandeerder *(Renishaw).* Die verskillende eienskappe van elke tegnologie word gemeet en gekwantifiseer.

'n Vermoë profiel kan gesien word as 'n vaste kriteria wat die prestasie van die RE tegnologie verteenwoordig en in hierdie studie word dit gedefinieer deur die volgende eienskappe:

- Akkuraatheid
- Herhaalbaarheid
- Spoed van meeting
- Meet volume
- Gebruikers-vriendelikheid

Die relevansie van die ontwikkeling van hierdie vermoë profiele is dat dit wedersyds vergelyk kan word. Dit is belangrik, spesifiek vir die akkuraatheids kriteria, omdat elke tegnologie by 'n verskillende maatskappy vervaardig word. 'n Aanvaarbare akkuraatsheid vergelyking onder die verskillende tegnologie is dus onmoontlik.

Die studie stel ook 'n evaluasie hulpmiddel voor wat die besluitnemer sal lei om die mees toepaslike tegnologie te kies vir die spesiefieke doeleindes. Verder word riglyne aan die potensiele gebruikers van RE tegnologie gegee oor hoe om te werk te gaan om die regte sisteem te kies indien die tegnologie nie in besit is nie.

Op 'n meer algemene vlak dra die studie tot navorsing by deur die nuutste tendense in toepassing, hardeware, sagteware en die keuse van RE sisteme in die RE industrie te beskryf.

Deur hierdie vermoë profile te ontwikkel beoog die studie om waarde toe te voeg aan die akademie, vennote in die industrie en potensiele RE gebruikers.

Acknowledgements

The author would like to thank the following people and organisations for contributing to the success of this study:

- Professor D. Dimitrov for being my study leader, giving me guidance, being patient and for helping me acquire financial assistance.
- Professor K. Schreve for his generous willingness to discuss ideas and procedures, and for giving me guidelines and support on the technical aspects of the study.
- My parents, for their faith in me.
- The 4th floor of the Department of Industrial Engineering. The staff and colleagues have really made my stay worthwhile by creating a friendly environment.
- Jesus Christ who gives me access to an almighty God to whom all things are possible.

Table of Contents

List of Figures

List of Tables

Glossary

CAD	Computer Aided Design
CAM	Computer Aided Manufacturing
RE	Reverse Engineering
STL	Standard Triangulation Language
NURBS	Non-uniform rational B-spline
CMM	Coordinate Measuring Machine
GOM	refers to the non-contact scanner used in the study
RENISHAW	Refers to the contact scanner used in the study
ARM	Refers to the articulated arm use in the study
CFD	Computational fluid dynamics
FEA	Finite Element Analysis
PET	Polygon Editing Tool
DMU	Digital Mock-up Unit
CTs	Computed Tomography scans
MRIs	Magnetic Resonance Imaging scans
DOF	Depth Of Field
CNC	Computer Numerical Control
AACMM	Articulated Arm Coordinate Measuring Machine
TC	Truncated Cone
CC	Coaxial Cylinder
S	Sphere
C	Cylinder
EP	Elliptical Pocket
T**SP**	Truncated Square Pyramid
H	Hole
VP	Vertical Plane
HP	Horizontal Plane
I	Inner
O	Outer
TP	Tilted Plane
R	Radius
GUM	Guide to the Expression of Uncertainty in Measurement
REX	Reverse engineering package for Pro/E
AHP	Analytic Hierarchy Process

1   Introduction

1.1   Background

Reverse Engineering (RE) has emerged as an important design tool in today's world, with the existing combination of CAD/CAM systems and computer measuring machines. Traditionally, a design drawing or CAD model is created before the manufacturing process. However, the original drawing is often unavailable, due in part to modification, poor manufacturing or the lack of communication between the manufacturer and the end user. As a result, RE techniques are integrated. This can be described as the process of digitising a physical object and making an electronic representation of it (Figure 1) [**1**]. Digitising, as a term, means measuring coordinates on the surface of an object. This can range from two points, digitising a line in space, to millions of points, digitizing a complex surface. In RE terminology, this set of points is referred to as a point cloud. In most Reverse Engineering techniques, the point cloud is not sufficient as a workable end-product, however impressive it may appear to the untrained consumer. Some kind of surface representation of the points needs to be created. The two most important surface representations in Reverse Engineering are Non-uniform Rational B-splines (NURBS) and Standard Triangulation Language (STL) [**1**]. The process of fitting the best represented NURBS onto a point cloud is, in most cases, the most time consuming, even with sophisticated software packages or experienced operators. A STL model is the triangulation of a point cloud and is done quickly and easily. However, the technique interpolates all the points of the captured data, including noise and holes. Nonetheless, new software packages have now made it possible to edit and manipulate STLs more easily. Both surface representing techniques involve some sort of objective decision making criteria, which can and will, have a direct impact on the accuracy of the representation. Once a surface representation of the digitized object is complete, the part can be remanufactured or modified using various techniques such as milling, 3D printing and other manufacturing processes. Although the concept of RE is easy to understand, the implementation of the available technology can be a long and tedious process, with some of the steps easily overlooked.

a: preparation of object   b:point cloud   c: STL surfacing   d: workable CAD model
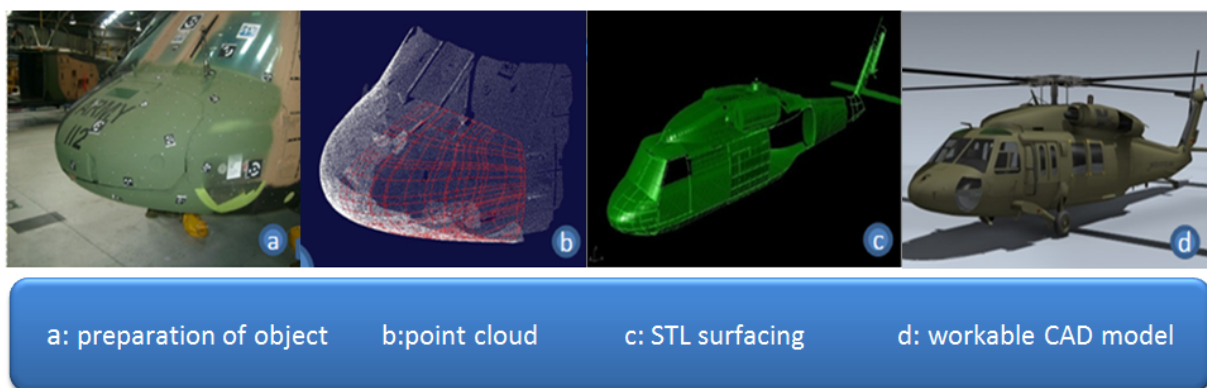
Figure 1: Reverse Engineering process chain

1.2   Problem statement

3D scanning, as well as software processing and modelling tools, have now entered the mainstream of design, inspection, product development, medical treatment, and additive manufacturing [**2**]. The Wohler Report is an annual trade report on additive manufacturing that includes a RE state of the art section. The report lists all the available 3D scanning systems and processing software packages as well as a list of companies that offer 3D scanning and data-processing services. All the technologies are quantified in terms of accuracy and work volume. However, there is a lack of standardisation in defining RE process capabilities, for example, accuracy. In one case it can be given as a single number, in another, it is given as a deviation to a set distance and sometimes even as a range. The accuracy of a machine can also be a function of time, volume or feature. The information supplied in the report originates primarily from the manufacturers themselves, thus making it a non-objective comparison. Another review describes the process of reverse engineering shapes [**3**]. It also identifies the purpose of reverse engineering and the main application areas; it outlines various digitizing strategies and describes the advantages and disadvantages of various data acquisition technologies.

The main research question of this study is: What are the real capabilities of the different RE hardware systems available for the study? The main criteria that make up the capability profile of each system are:

- Accuracy
- Repeatability
- Speed of Measurement
- Work Volume
- User-friendliness.

There are also other criteria that will be discussed, although in less detail. The available hardware systems for the study are a Coordinate Measuring Machine with touch trigger probe (CMM), an articulated arm with contact probe (Cimcore), a structured light non-contact scanner (GOM) and a CMM with analogue probe (Renishaw). The words in brackets will be used to refer to the different systems in this study.

The secondary problem is that capability profiles of different digitizing hardware have been done before but either lacked credibility or were difficult to compare with other results from similar studies.

1.3   Main objectives and research methodology

The responsibility of the researcher is to properly document all procedures executed during the study. This is so that other laboratories, which conduct similar tests, are able to compare their results to those of this study. This will eventually lead to better communication between metrology laboratories and may spark joint ventures or more effective measuring guidelines.

The main objective of the project is to develop capability profiles for the four available RE hardware systems. This will aid users in selecting the most suitable RE hardware system for their purpose or application. The steps that were followed to obtain this primary objective can be summarised as follows:

- Conduct a literature study of the current global situation regarding Reverse Engineering technologies in order to identify factors that could influence the different criteria.
- Investigate and develop suitable experimental procedures that will quantify the different criteria regarding the capability profile of all the hardware.
- Investigate, develop and manufacture a suitable benchmark part that is used as a base for the accuracy criterion.
- Validate the accuracy of the benchmark part. An important aspect of testing is that the accuracy criterion must be traceable to international standards. The CMM is calibrated by the designated governing body, which is the most accurate and will thus, act as the base for testing accuracy.
- Quantify other criteria with suitable experimental procedures or literature.
- Compare the quantified measurements amongst the different RE hardware systems for each criterion.
- Investigate and develop a suitable evaluation tool that will help the user in choosing a suitable system.
- Validate the evaluation tool by implementing it practically.
- Write a final draft of the thesis, documenting all developments, results, assumptions and recommendations.

On completion of the above specific steps, the main objective, defined in the project heading, will be achieved. More importantly, the study will make it possible for both system users, and the public, to compare their findings of different, or similar technologies, to that of this study.

2   Literature Study

2.1   RE applications in different industries

Reverse Engineering techniques are used in many different sectors of industry. They play a key role in the design stage, but it is important to mention that in general, RE is considered a part of the design stage, when looking at the process chain of the development of a product. Part inspection is used at the end of the process chain, to verify design constraint accuracies. Both RE and Part Inspection may use similar or the same hardware and / or software, however, the system's set-up differs. This project looks at the Reverse Engineering stage; reverse engineering applications in different industries are listed below and some are briefly discussed:

- Automotive industry - car bodies, cams, seals, gears, etc.
- Aerospace industry - turbine blades, impellors, ducts, aerodynamic parts, etc.
- Consumer products - phones, cameras, monitors, radios, etc.
- Tooling industry – moulds, dies, parts, etc.
- Medical device industry – teeth, body organs, bones, etc.

Each application may require different capabilities of the applied hardware and software. In mentioning some examples from different industries, it illustrates the point at which different applications require different hardware and software capabilities. It also shows that similar capabilities are used across different industry sectors.

2.1.1   Automotive industry

The modern automotive industry uses reverse engineering for several key reasons [**4**]:

1. to create free-form shapes that are difficult to model in CAD software;
2. to overcome obstacles in data exchange and data integrity;
3. to create complex geometries that might not have a CAD model;
4. to resolve and correct problems arising from discrepancies between the CAD master model and the actual tooling or as-built part;
5. to speed up innovation in such areas as ergonomic design, retro-inspired design, combustion design, and aerodynamics, where CAD modelling often adds an unnecessary step; and
6. to ensure quality and performance through computer-aided inspection and engineering analysis.

A new car is designed from a variety of specification groups. Surveys extract information from customers, mathematical simulations define the aerodynamics of a car, production defines manufacturing constraints and ergonomics make up the overall specifications. The car body is designed on a one-quarter scale clay model and reverse engineered. The reverse engineered model is then analysed by different departments to verify or re-model the design and if necessary, to achieve the overall desired specifications. Specifications from different departments are equally important, for example, with the increase in the price of petrol, the aerodynamics of a car has become very important. The aim is to reduce the drag on the car's body, in order to reduce the petrol consumption. The car, however, still needs to look attractive and be ergonomically

comfortable to sit in, as well as be viable for manufacture. The scaled model and life size model include complex spatial shapes and sharp edges. For this reason, the RE system needs to be capable of capturing high quality coordinate points in terms of precision and point density, and to convert this to clean usable CAD data.

The reverse engineering of engine blocks is also common in the automotive industry. This is often done as the original engine block's drawings are not available or there are discrepancies between the main cad model and built part. This falls under points 3 and 4 in the above mentioned reasons. In addition, the interior ducts are important for the CFD simulation, to optimize cooling, while a FEA simulation can be used to determine where material can be removed, without affecting the strength of the block. This reverse engineering method needs to be more accurate than in that of the previous example, the point cloud density may be reduced, the scanner must be able to measure deep holes, and difficult to reach, or interior cavities, may have to be captured, as mentioned in point 5 above. The following example shows how a local company in the automotive industry has used reverse engineering techniques to add value to their organisation.

Optimal Energy (Pty) Ltd. is a privately owned South African company based in Cape Town, with investments from the Innovation Fund (IF), an instrument of the Department of Science and Technology. The company is in the research and development phase of producing Africa's first battery-operated electric car (Figure 2). Reverse Engineering techniques are used to produce a complete Digital Mock-up Unit (DMU) of the car. The exterior body panels are reverse engineered for assembly purposes, while the interior mechanical parts are digitised to ensure a proper fit. The DMU is used to estimate the total weight and price of the car and to help the various departments within the company with the design stage. The hardware used is a Konica Minolta VIVID 9i laser range scanner; accompanied by a Polygon Editing Tool (PET) from Konica Minolta to produce a STL file. Surfaces, splines and features are then fitted using Catia or Solid Works.

Figure 2: Optimal Energy's car the Joule

2.1.2   Aerospace industry

The design stage of producing a plane, as in the automotive industry, is assisted by introducing reverse engineering. The two main goals in the design of a new aircraft are to increase the amount of passengers and to reduce the fuel consumption [**5**]. To reach these goals, the fuselage and wing designs are improved by introducing new geometries of composites, reducing the aerodynamic resistance and weight respectively. The development of this occurs in a wind tunnel using a scaled model. The improved model then needs to be digitised using reverse engineering techniques. Likewise, these techniques are used to verify the structural integrity of new wing designs during deformation tests. Here the wing is exposed to an applied known load and the deformation is captured using RE techniques. The RE techniques need to be capable of capturing free-form parts with high accuracy in real time.

The aerospace industry not only consists of airplanes but also guided missiles, space vehicles, aircraft engines, propulsion units and related parts, helicopters and so on. Many planes, helicopters and space vehicles in operation today, were designed decades ago and CAD models or technical drawings are therefore often difficult to come by. These aging vehicles need to be maintained to keep them in the air, so reverse engineering techniques are used to create a legacy part and hard tooling, for parts that do not have CAD models, and need to be manufactured. The task is made easier if the RE hardware is portable as this enables the part to be reverse engineered without removing it from the aircraft. The parts may, however, vary in geometry and the capability requirements of the RE hardware may thus differ. For example, exterior metallic aircraft panels may have to be replaced with composite ones [**6**] or precise turbine blades may need to be reverse engineered. The objects in these two examples vary in geometry which could necessitate a difference in the hardware's capabilities. When digitising a turbine blade, both contact and non-contact RE methods can be used in combination, to reverse engineer the part or its assembly, as neither is ideal when used individually. Combining contact and non-contact digitizers in a single point cloud is referred to as hybrid modelling and will be discussed at a later stage.

2.1.3   Medical device industry

In recent years, technological advances in the automotive and aerospace industries have made their way into the medical field. The combination of CAD and medical technologies (bio-CAD) is used in many applications such as computer aided surgery, structural modelling of tissue, design of orthopaedic devices and implants, design of tissue scaffolds and bio manufacturing [**7**]. As a result, the capturing of internal structure, as opposed to only surface generation, is needed. In conventional manufacturing, an internal structure is obtained with the use of destructive techniques. This is, as the word indicates, a technique that destroys the measured object and is thus not suitable for human part scanning. Instead, the medical industry uses ultrasonic scanning, one example of which, is called CT scanning (Computerized Tomography). This is a technique that captures 2D images of the cross sectional slices obtained from the ultrasonic or X-ray scan. The results are, however, not very accurate when compared to that of conventional RE techniques [**8**]. Another factor to consider in the medical industry, is that scans are done of patients, so the scan procedure needs to ensure that patients enjoy a certain level of comfort. For this the measurement repeatability, speed and access to object, forms part of the capability profile of such a system. The following example motivates the importance of the implementation of RE techniques in the medical field.

The hearing instrument market is estimated to be worth approximately $5 billion at retail level [**4**]. However, only 20% of people with hearing loss currently own hearing aids. Comfortable and discreet hearing aids need custom-made individualised shells. For decades this was done by sculptors but this technique made the manufacturing process into a craftsmanship, rather than an industrial process. Moreover, this method makes streamlining, and maintaining a manufacturing plant, difficult. In 2001, GN ReSound, the world's largest hearing instrument manufacturer, doubled its production in three months with a 75% reduction in labour, by implementing reverse engineering and rapid manufacturing techniques. This underlines the importance of RE techniques and research and development in the field.

2.1.4   Conclusion

The above examples illustrate that different tasks need different systems and that each application may have different RE capability requirements. Some need to capture high density free form point clouds, while others need to measure deep holes or internal cavities. Some need to be able to capture in real time where an object's volume can range from tooth size to a complete fuselage. Some need good repeatability and others need to capture internal objects, without using a destructive method. Different capabilities require different types of technologies and therefore different hardware. Furthermore, with different hardware, comes a variety of different software and strategies.

2.2   Reverse engineering - hardware

The different applications mentioned have developed various techniques over the years. Techniques exist that can almost instantaneously sample millions of points of an object, while others can sample only one point at a time. The hardware could, for example, be classified by the capability of the density output of the data. The scanning method is, however, normally classified either as non-contact or contact scanners [**1**]. This classification has also been used and is presented in Figure 3 [**3**] [**9**]. Note that some contact hardware can be modified for it to become a non-contact method and *vice versa*. For example, an articulated arm with a laser head becomes a non-contact scanner and a portable touch probe mount with light emitting targets affixed, becomes a contact one.
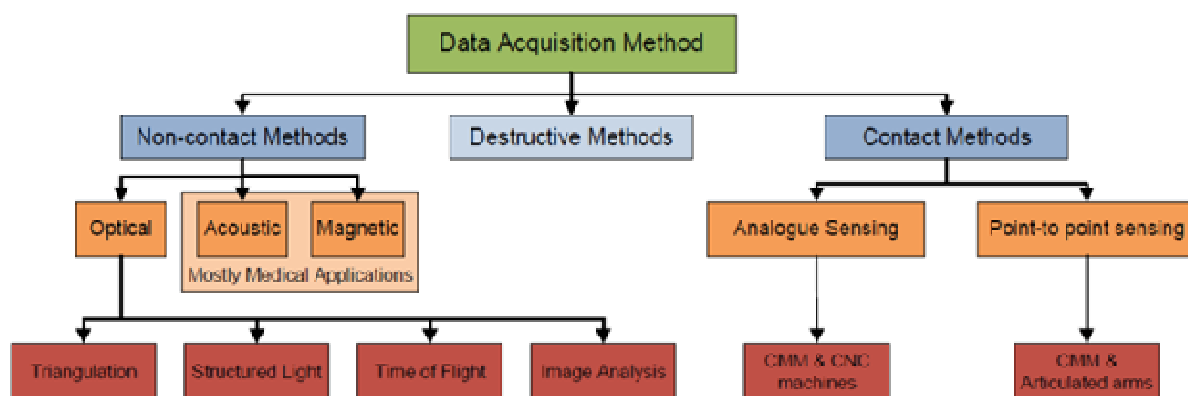
Figure 3: Classification of Reverse Engineering Methods (adapted from [3])

2.2.1   Non-contact methods

2.2.1.1   Optical

In the 1980's and 1990's several methods were developed to capture multiple sets of 3D points, without any contact or markers of the measured surface [**10**]. These methods are often fast and recent development has increased the accuracy in many of these technologies [**1**]. The main advantage of non-contact methods is that they can capture thousands or even millions of points almost instantaneously. The new methods were based on the following principles:

1. **Emit energy onto a physical object** (optical, sound or magnetic field)
2. **Capture the reflecting energy** with an electronic detection device (typically a camera)
3. **Compute the Cartesian coordinates** by analysis

The captured point cloud can be defined as a surface or volumetric representation of the object. For example, if X-rays are used as the emitting energy (magnetic) then the captured data will include internal hidden geometries and external visible surfaces (the shell), as mentioned. Alternatively when a laser is used as the emitting energy (optical), only the visible outer shell surface will be captured, therefore only that which is visible to the human eye. In volumetric 3D digitizers, such as CTs and MRIs, the emitting energy is either ultrasound or x-ray; the same as what is used during human body scans. The only difference is that the magnitude of the emitting energy is increased according to material density. Surface 3D digitizers use emitting energies such as visible white light, near invisible infrared light or a laser light to digitize the visible surface of an object. Optical surface 3D digitizers are the most well-known digitizers throughout all industries. They are often the safest, fastest, cheapest and easiest way to reverse engineer an object. As much as 90% of close-range digitizers, used in industrial applications, belong to this category under a method called triangulation [**10**]. The most commonly available non-contact reverse engineering methods are the following:

2.2.1.1.1   Triangulation based laser digitisers

Most laser scanners use straightforward geometric triangulation to determine the surface coordinates of an object [**4**]. The following diagram explains the triangulation-based approach, where *B, β* and *α* are typically known through system calibration. The range r, or distance, is calculated by means of geometric known distances and angles. Equation (1) refers to Figure 4 which evaluates the range consisting of the illumination angle *α*, and *B,* which is the baseline.

$$r = F(\alpha, B, i, j, \dots)$$ (1)

The variables *i* and *j* represent the horizontal and vertical position respectively, or the address of a pixel in the camera image. A pixel is generally thought of as the smallest single component of a digital image, which is arranged structurally. The image is represented electronically by a matrix with *i* and *j* components. The function is adapted to various cameras, lenses, mirrors and laser setups but the principle remains the same. The emitting energy is in this case a laser spot, which is transmitted onto the measured object, at a defined angle. The camera then detects the position of the reflected point and calculates the range. This is evaluated by finding the brightest pixel or spot which falls onto the image sensor of the camera. An alternative is to transform the laser beam into a projection

line at the laser source. The laser projected on the object and recorded on the camera is then a line and thus the technique is much faster.
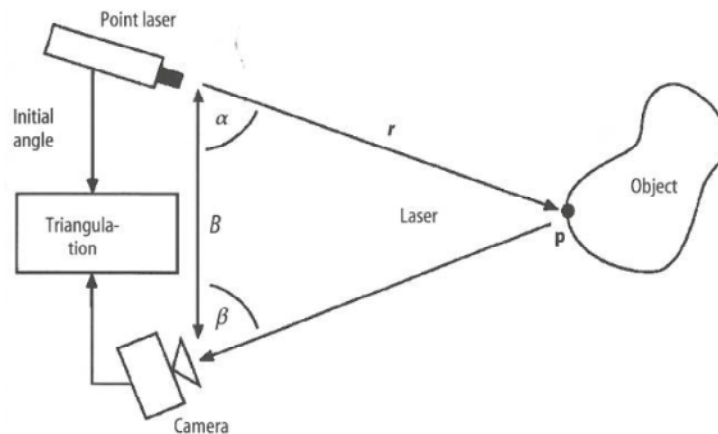
Figure 4: Triangulation-based approach example

Triangulation-based laser digitizers are close-range systems, as the distance between the instrument and digitized object is generally less than 1 meter. The depth of field, DOF, is usually in the range of 25 to 200 mm. This is the same term used in photography; the distance between the nearest and furthest plane, where an object seems sharp or in-focus. The camera can be interchanged with different lenses, for different 'focal lengths'. The quality of the camera and resolution, the quality of lenses and mirrors, mechanical mounting (tripod), saturation and lack of capturing light, as in photography, will determine the accuracy of the captured data. Each independent system might contribute a bias error.

2.2.1.1.2 Structured light

Structured light also uses triangulation to compute the basic geometry of the measured object, however, it does not use a laser. The energy used is a white light, emitted at a known angle and the reflected light is then captured by either one or two cameras. The captured image is analysed to produce 3D Cartesian coordinates of the measured surface. The light pattern can be a single point, a sheet of light (line), a strip, a grid or more coded complex light. The most commonly used pattern is a sheet of light [**4**]. This line sweeps along an axis (or the object moves on a conveyer belt), while a sequence of images is taken in discrete steps. The system denotes each image to the position of the line in a defined space. The strip or grid projected light system does not need to have a moving light source, as the projection normally covers the whole object. One of the advantages is that this method does not use a laser and the data acquisition is very fast.

Another technique using a fringe based light emitting approach is Interferometry (Moiré Effects).The Interferometry method is well known for dimensional inspection and deformation measurements. The Moiré technique has been around for a long time [**11**]. The projector also emits a structured white light onto the surface of the measured object, as in structured light and the reflected grating will be distorted, due to the topology of the surface, as in structured white light. The difference to structured white light is that the reflected image is filtered through a reference grid; this produces a

shadow moiré effect. The distance between the lines of the two grids is directly proportional to the height of the surface, at the point of interest and this is how the coordinates are calculated.

2.2.1.1.3 Time of flight

The principle behind time of flight is to measure the time it takes for the emitting light (laser), or sometimes sound pulse, to travel from the emitter to the receiver. The speed of light and time travelled is known, and from this, a simple distance-over-time equation is executed in principle. The angle between the transmitting and returning beam is neglected, as it is indifferent to the measurement [**4**]. The result is that the transmitter and receiver share the same axis in theory and therefore overcome two obstacles of triangulation based methods. The first one is that it is possible to measure close vertical walls with time of flight methods. The second is that it is possible to measure large and distant objects. The layout between the transmitter and receiver in triangulation determines the accuracy of the measurement. Here the standoff distance is important; with time of flight, the layout is neglected as stated above. The light emitted from the laser can be in a pulse or wave form. The pulse based time of flight, for example, is used to capture buildings and fuselages, the depth of a field being between 1.5 and 1000m, with a range of up to 25km [**10**]. Where the laser light is emitted as a waveform (laser oscillating at a known frequency), the phase shift between the emitting and receiving wave determines the time of flight. However, this has a lower depth of field, ranging between 1.5 and 80m. The accuracy (0.4mm) is better than that of the pulse-based timed system; however it is still less accurate than the close range systems.

2.2.1.1.4 Image analysis

Image Analysis is referred to as a passive method, as no emitting energy is applied. The method uses conventional captured images to determine the coordinates of an object (Figure 5). There are many different passive methods, including shape from shading, shape from stereo, shape from motion, shape from focus/defocus, shape from silhouette and volumetric reconstruction [**4**]. Image analysis has been around for a number of years and techniques have improved over time [**1**]. In 'shape from stereo' the 3-D representation is reconstructed from a single image, by analysing the shading information of the image. This can cause problems as the reflectance of an object is not consistent and shading intensity may be difficult to pick up. Another method, shape from stereo, photogrammetry is more accurate and flexible. The method uses either two cameras simultaneously, or two (or more) images from different viewpoints, to automatically find corresponding features in each of the images. Triangulation is then used to measure the distance to the object, by intersecting the lines of sight from each camera to the object. Markers or targets can also be placed onto the object to create a more defined feature, if necessary. This technique makes it ideal to measure large objects; it is also relatively inexpensive, compared to other techniques. The photography boom has ensured that high-end sensors are freely available, which in turn is responsible for the increase in accuracy of the technique.

Figure 5: Example of the Image Analysis method.

2.2.1.2   Acoustic

The two most common acoustic methods, used for revere engineering purposes are Active Sonar and Computed Tomography (CT scan), using ultrasonic sound waves. As mentioned, a CT scan can also be executed using X-rays, however, this falls under the magnetic classification. Active sonar is mostly used in the marine industry to map underwater ocean floors; this is often used for navigation or sub sea oil constructions purposes. Accuracy is often lacking, as they do not have high acquisition speed and noise often becomes problematic [**4**]. A CT scan, using ultrasound, is mostly used in the medical profession, however, it is also very low in accuracy. Most of the time acoustic CT scans are used for the scanning of unborn babies.

2.2.1.3   Magnetic

CT scans, using x-ray, is a form of electromagnetic radiation and thus falls under magnetic methods. They are also mostly used in the medical industry; however, they have also been adapted to accommodate industrial tasks. Nikon [**12**] and Toshiba [**13**] have developed numerous industrial X-ray CT scanners with relatively good accuracy and low noise components. Magnetic resonance imaging (MRI) uses magnetic fields and radio waves and thus also falls under the magnetic method. The technology is state-of-the-art and produces cross sectional images of the body without using radiation. Compared to CT scans, MRIs produce superior quality images of soft tissue such as organs, muscles, cartilage, ligaments, and tendons. Both CT and MRI are powerful techniques for medical and industrial practices; however, they are extremely expensive. Another well-known magnetic method is microwave radar (radio detection and ranging). This is well known in the aircraft industry and is used for long range remote sensing. For 3-D reconstructive purposes, radar is used to measure distances and map geographic areas

2.2.2   Destructive methods

In additive manufacturing processes, a part is built up layer by layer, destructive reverse engineering is the opposite of this. An object is machined down layer by layer in a given direction, normally in the z axis of a CNC machine. Each exposed cross sectional layer is captured by a camera. Software uses edge detection and other algorithms to evaluate the contours of each layer. The three dimensional image is then generated by interpolating each successive and equal incremented layer.

A destructive-based digitizer is always volumetric and the object after measurement will at this stage no longer exist. The method can work with machinable materials including aluminium alloys, plastics, steels, wood and others. Softer materials or thin walled objects may have to be infiltrated or cast in a resin based material; this will ensure the object remains intact. The software of such images will block out the colour of the resin and model it as void spaces. As the method is destructive it is often used for smaller parts. The method is also fast with acceptable accuracies and a repeatability of ± 12.7 μ. The layer thickness is from 0.0127-0.254mm [**4**].

2.2.3   Contact methods

Contact methods use sensing devices with mechanical arms and coordinate measuring machines (CMM) and computer numerical control (CNC) machines to digitise a surface [**4**]. There are two types of data collection technique classifications in contact methods:

- Analogue sensing with scanning probes and
- Point-to-point sensing with tough-trigger probes.

In analogue sensing, a scanning probe is used either on a CMM or CNC machine. The machine emits a continuous signal in time and magnitude and the probe moves and touches continuously along a surface. The continuous deflection output, combined with the machine's position, derives the location of the surface. The scanning speed is up to three times faster than point-to-point [**4**]. In point-to-point a touch trigger probe is installed either on an Articulated Arm or CMM to digitise points of a surface of an object. Most articulated arms are manually operated, portable and have six to seven axes of rotation, allowing for more freedom of movement, this makes it easy to capture complex surfaces on different planes. On the other hand, CMMs, which have been developed over a longer period of time, provide more accurate data, as they only have three Cartesian axes. A CMM can also be programmed to follow along a contour or planned path.

The advantages and disadvantages of contact methods, compared to non-contact methods, are as follows: [**4**]

Advantages:
- High accuracy,
- Low costs,
- Ability to measure deep slots and
- Insensitivity to colour or transparency

Disadvantages:
- Slow data collection and
- Distortion of soft objects by probe

2.2.3.1   CMMs

Coordinate Measuring Machines technologies have been around for a number of years in metrology, with well-developed capability profiles and advances. They are well accepted in industry, because they are very flexible and allow for the measuring of points in space with high accuracy. CMMs are flexible in that they are capable of measuring deep holes and cavities, are insensitive to the object's colour or texture and they can reposition an object with acceptable reference points. They are also very accurate as accuracies of up to 1 μ have been reported [**14**]. Well developed third party software is readily available and includes user-friendly interfaces with easy geometric property evaluation tools. The technology is not often used for complete reverse engineering purposes; however, the technology has dramatically improved in this regard over the years. Some machines are capable of measuring up to 200 points/s at a speed of 150mm/s [**5**], which makes it viable to measure large simple freeform parts. This is possible in a structured or random point cloud but at very low resolution; thousands of points, as opposed to dozen of millions to that of optical scanners, in terms of point density. A CMM is capable of analogue and point-to-point sensing. It can be converted into a non-contact scanner by replacing the touch-trigger or scanning probe with an optical scanner. A comparison study between accuracy findings of laser and contact CMMs has been documented [**15**].

A CMM, with a touch-trigger probe, typically works like an electrical switch as shown in Figure 6. The probe rests on three sensors and the circuit is broken as the probe makes contact with the measured object. The machine moves before the impact, thus a directional vector is converted into a lobing error and the machine knows the coordinate of impact. The machine then moves away from the object, the circuit is re-established and the next coordinate may be measured. The object measured may not deform when the touch probe makes contact; therefore clay models or parts including soft polymers cannot be measured, for example. The size or feature complexity of the part measured is also dependant on the probe. Different sized probes and probe extensions are available for specific applications.
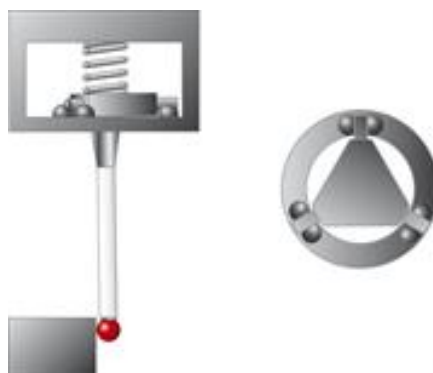
Figure 6: Tactile Probe Design Schematic

2.2.3.2   Articulated arms – portable CMMs

An articulated arm, for coordinate metrology, is a device similar to a robot arm; however, it is not controlled by servo-motors. An operator must move the often six axis arm to the required measuring point. A touch-trigger probe at the end picks up deflections, similar to a conventional CMM, and converts the six angular axes representation into a Cartesian vector (X, Y, Z). The biggest advantage to that of a conventional CMM is that the articulated arm is portable and can be used in the field or on site, for example on the production floors or in places where disassembling is sometimes not an option. Complex assemblies can be inspected on site without removing or disassembling it and measuring it conventionally in-house on a CMM. The accuracy is, however, not as that of a CMM. The accuracies of articulated arms can range between 50-250 µ. As an arm has 6 degrees of freedom, rather than three, each bias error is added to the overall uncertainty. The CMM is also often located in a laboratory with controlled temperatures, the AACMMs are sensitive to temperature and this may increase the machines' error, when measuring in extreme ambient conditions. The main disadvantage (only with touch probe) is that capturing freeform shapes is near to impossible or too time consuming and therefore not viable.

2.3   Reverse engineering - software

There is no single RE software that can completely satisfy the requirements of RE data processing and geometric modelling [**4**]. The selection of the RE software depends on the requirements or specifications of each individual project. The RE software's application can range from controlling the hardware to manipulation or construction of polygons, NURBS or basic CAD features. The different software operations can be classified into four different RE data processing phases. These different processing phases will be described below.

2.3.1   Data processing phase classification

There are four phases or classifications when it comes to reverse engineering data processing. Similarly to the hardware classification, software phases or strategies can be classified differently. The model used in Figure 7 is adapted [**4**]. Some software packages include the operations of all four phases, whilst others focus only on one or two. The software provided with the hardware, commonly allows editing of the point and polygon phase. The different phases are briefly described and discussed below.
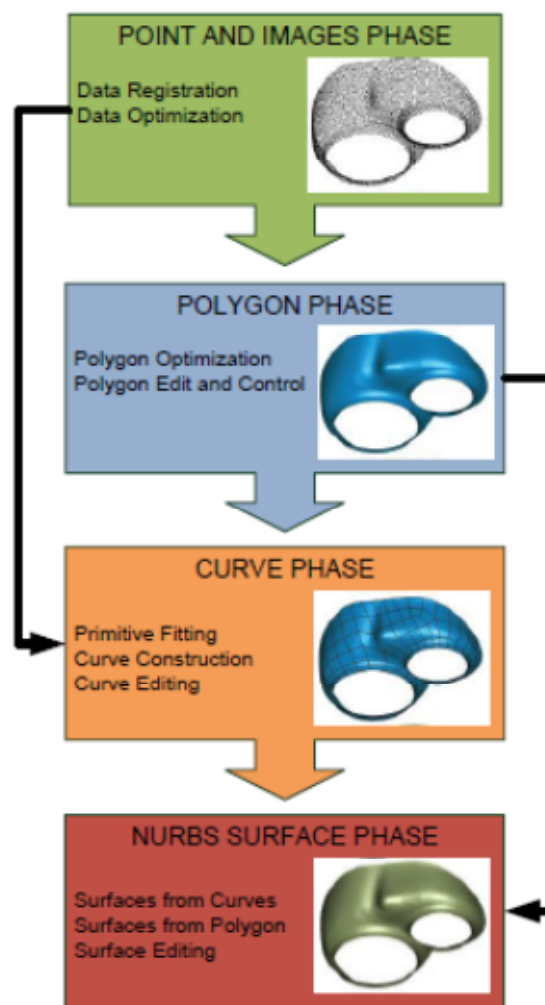
Figure 7: Phases in RE data processing

2.3.1.1   Point and image phase

Most reverse engineering software enables point cloud manipulation and editing. Most RE techniques such as triangulation, structured light, and time of flight and image, provide point cloud data. Image analysis is mostly used in medical applications. As discussed in the hardware classification, CT and MRI scans provide a large series of 2-D cross-sectional images. Regardless of whether points or images are analysed, the data need to be triangulated to produce a polygon mesh model. Once a point cloud is obtained, the arbitrary coordinate system, created by the software, often needs to be changed or moved. This is done because some point clouds are aligned with a CAD model (inspection), or numerous point clouds need to be overlapped. A well-defined coordinate system also makes working with CAD features more pleasurable, for example mirroring features. In addition, it gives a coordinate system that can be related to other models. One such example is that a typical car's coordinate system is located in the middle of the front axle [**16**]. The Z axis points to the top, the X axis to the back and the Y axis to the front right wheel. This makes comparing different cases with one another much easier. There are different transformation methods; these entail the operation of defining a coordinate system to a model. The method used the most in industry is called the 3-2-1 method. This refers to the 3 points that are needed to define the first plane (often the Z plane), 2 points define the first axis, lying on the first plane (often the X axis), and 1 point is needed to define the second axis (often Y axis) and the zero point of the first axis. This makes up the coordinate system and defines an origin at the intercepts of the plane and the two axes. The distance between each point should be as far away as possible, to minimize errors in the deviation of points. The transformation stage can also be constructed in the Polygon Phase.

2.3.1.2   Polygon phase

Polygonization means that the point cloud is converted into a non-overlapping mesh of triangles. Depending on the curvature of the object, the mesh has different densities [**16**]. This density can be adjusted, refined (increase of triangles) or decimated (decrease of triangles) [**4**]. The thinning or decimation should happen only on simple planes and refined at edges and complex geometries. The thinning process principle is illustrated in Figure 8. Refining is the opposite of thinning as the software creates an additional point within an already defined triangle and joins vertices to the other already measured or defined points. The density of the polygon mesh can often be adjusted in a typical polygonization wizard with software.
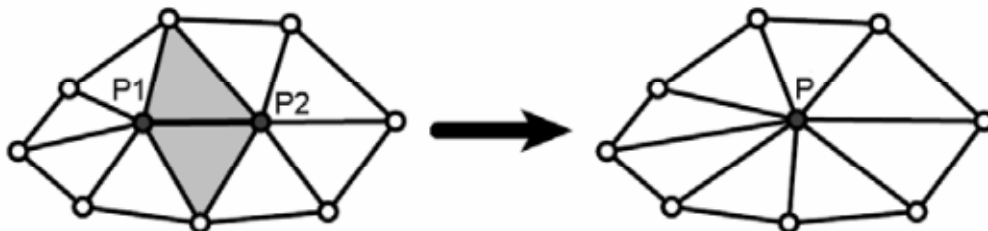
Figure 8: Thinning mesh illustration [16]

The original point cloud data may also be replaced with a newer calculated adjusted mesh. The software interpolates average points for point densities better, and eliminates noise. The software can create a complete new mesh grid using none of the measured data points. This is referred to as a regular mesh, as all points are equally spaced. A number of filters may be introduced. The polygon mesh may be smoothed or relaxed. An example of a regular and relaxed mesh is illustrated in Figure 9.

a) Original mesh   b) Regular mesh   c) Relaxed mesh
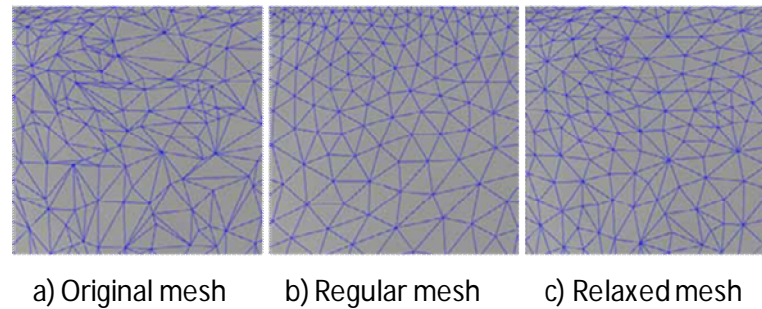
Figure 9: Various types of meshes [16]

The polygon mesh may have holes in the model, which might have been introduced during the scanning process, or because of an error in converting the point cloud to a polygon model. There are various techniques strategies to fill a hole but in essence they all serve the same purpose. The operator needs to decide the importance of the missing surface(s) or hole. There are strategies in how to deal with fairly large holes [**17**]. A simple illustration on how a hole is eliminated is depicted in Figure 10.

a) Mesh with hole   b) Mesh with filled hole
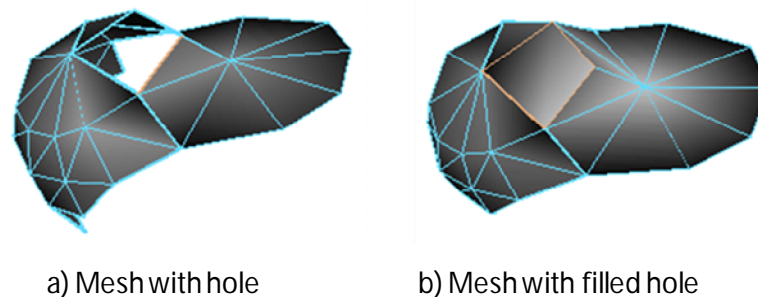
Figure 10: Filling a hole example

According to Wohlers [**18**], in 2005, major software improvements enhanced the speed of converting 3D data to 3D CAD parametric models. One such development is the detection of features by the program. The software picks up the original design intent and divides the model into different parametric regions for example fillets, edges or surfaces. Many studies have been done on this development, [**19**] and [**20**]. The mesh is firstly divided into segments. The software then decides if the edges are sharp or soft (fillet) and assigns different segments, before applying surfaces onto the model.

The last common feature mentioned in the polygon phase is that primitives can be created, for example; points, lines, circles, planes and spheres, directly from the point cloud. This is often done to help register the part to a specific datum or for part inspection.

2.3.1.3   Curve phase

Curve phase is a technique or phase which is well known in the boat building industry and most reverse engineering packages include it as a feature. The designer defines and then divides up the mesh into different curves. This can be done automatically or with a sketching tool. These curves can be section curves, boundary curves, silhouette curves or feature curves. The curves may then be used to construct a conventional featured base parametric solid model using loft, sweep, extrude or revolve. The designer's experience will impact the accuracy and quality of the final CAD model. A common strategy is to reduce the 3D point cloud to 2D planes along an axis and then create splines from the data on each axis, see Figure 11. Only data points that fall onto the defined planes are captured, the rest are emitted. This technique reduces the data point cloud considerably and the computing power required is much lower. Each curve on each plane can be edited. The number of points making up the curve can be reduced, increased, spaced equally or edited completely. The individual sequential curves are then lofted through each plane to create a solid 3D model. A study explains how a part is typically reverse engineered, by lofting a set of curves on 2D planes into a 3D model [**21**] [**22**]. The planes do not necessarily have to be along a straight line, a circle or boundary curve is also used for instance.
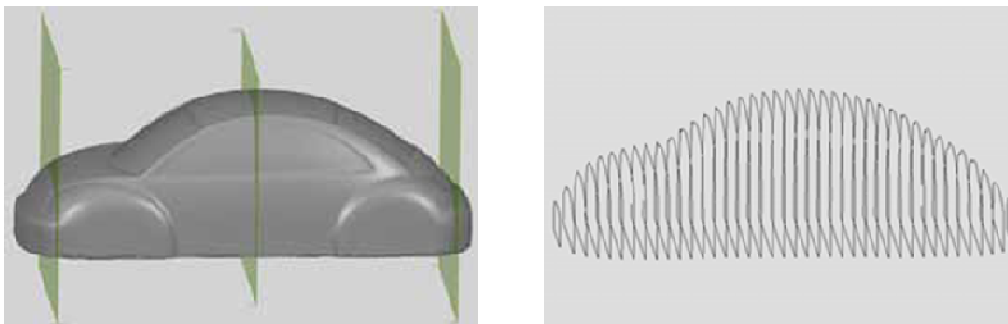
Figure 11: Parallel cutting planes and curves [16]

2.3.1.4   NURBS surface phase

The manner in which the NURBS surfaces phase is executed depends on the steps taken. As depicted in Figure 7, the arrow on the right indicates automatic freeform surface modelling, in which no curves are created or defined. This technique is mainly used for RE modelling of organic shapes, including consumer products such as toys, and medical shapes such as human/animal organs, bones and blood vessels. Human organs are extremely complex, as there are no recognizable geometries and the intricate details are usually expressed by stitching quantities of surface patches. The process of surface creation is simple and often automatic. Modification of such models in a 3D CAD software package is almost impossible and the surface representation or smoothness between stitched

surfaces is not of high quality. The other technique involves curvature or feature detection, as mentioned in the polygon phase. If the features are not identified in the polygon phase, curves are inserted and created manually in the curve phase. The identified features are then used to build NURBS surfaces. The individual sub features are then automatically or manually extended, trimmed or sewn into a solid 3D CAD model (surface). Unlike solid modelling CAD software packages, which focus on making water-tight solids, RE software packages typically output surface models. These surface models, however, can in most cases be converted into a watertight model. Another strategy to consider is whether a part is symmetrical along a plane, therefore whether the surface fitting can be done on only one side of the object and then mirrored in the splitting plane [**23**]. Another strategy is to identify a repeated feature within a model and replicate it by using the pattern feature (Figure 12).
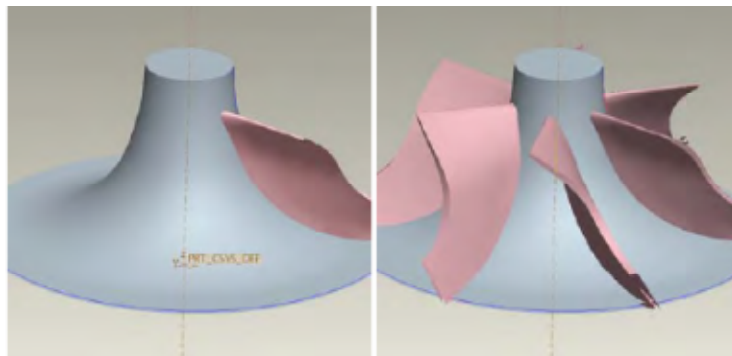
Figure 12: Pattern replication – impellor pump

2.3.2   Conclusion

Most operations, conducted in each phase method, involve the knowledge of experienced metrologists. It is important to define the specifications of each RE project, as this can limit the number of operations and therefore save time. Some projects only need profile or contour curves, while others need accurate freeform surfaces. Hybrid methods can be described as the combination of two or more point clouds, obtained from different RE methods [**1**]. This is done due to the fact that the one point cloud may define the freeform, while the other defines the exact boundary curve of the shape. The methods used vary from metrologist to metrologist [**4**] [**24**]. For most RE projects at least two software packages are used, one for data manipulation (point and polygon phase) and the other for geometric modelling (curve and NURBS phase). An important factor, which plays a role in the decision-making process, is the availability of equipment.

2.4   Selecting a reverse engineering system

The system selection process, for a major system, should comprise of two components [**4**]. The first is choosing the most suitable hardware and software from a technical capability point of view. The other consideration is from a commercial perspective. Possible questions which could be asked are for instance, does the vendor or company have a good representation, reputation and support outlets? Technical consideration may be done internally, amongst senior managers or project leaders, or the entire technical evaluation can be done using a consultant. The latter option is expensive but eliminates the entire selecting process; however, the consultant may be biased towards a particular system. Hiring internal members on the other hand could increase the sense of 'ownership' amongst members. Regardless of what method is chosen, the attributes of the reverse engineering system need to be defined. Some of the common criteria or attributes are mentioned and discussed:

- **Accuracy –** This is a very sensitive attribute and is discussed in more detail in section 2.4.1.
- **Resolution** – This is often given with non-contact scanners, as resolution can have an impact on accuracy. A higher resolution is desired for freeform parts.
- **Part dimensions -** Different systems have different working volumes. This can range from 'Shoe box' sizes to entire fuselages.
- **Shape complexity –** Some systems are designed for quick freeform capturing, while others tend to be better with basic geometric shapes.
- **Material and surface –** As some systems are dependent on the reflection of the emitting light back to the sensor, the surface reflection properties are important.
- **Traceability/Calibration –** Most touch-trigger systems, especially CMMs, are well calibrated and traceability systems and standards are properly in place. Some systems need to be calibrated before each measurement, which can be time consuming, whereas others are calibrated only once a year.
- **Flexibility –** A system that is ideal for the measurement of freeform surfaces is often not suitable for the measurement of deep holes. It needs to be decided if both these attributes are equally important or if the one is more important than the other.
- **Speed –** The time it takes to measure a part needs to be considered more carefully, especially if numerous and similar objects need to be measured. For single once off measurements, the speed of the measurement is not crucial.
- **Portability –** Some systems can be used in the field, which allows for inspection without removing the part from the assembly. This can obviously save time, although these systems are not always very accurate, as they are operated in non-controlled environments.
- **Initial Capital Costs –** The initial capital cost, to implement a reverse engineering system, can range anywhere from as low as R25 000 to as high as R2m. The budget needs to be known and an asset payback analysis needs to be made. Sometimes it is better to outsource the job than to acquire an in-house system; due to the fact that there are many expenses and considerations, which make outsourcing a better option, for instance the acquisition of expensive machinery, or the training of staff, and then there is the ongoing maintenance to keep the system in place.
- **Commercial/Technical support –** This is the second component, distinguishable from the technical capabilities. During the training stage of implementing a new system, the technical

assistance or reputation of the vendor, needs to be considered. Choosing the cheapest system might not be the best option as there are other considerations to keep in mind, for example, whether there is a vendor representative in your country.

A good reference or starting point for choosing an appropriate technology, after evaluating the criteria, is to look at literature [5]. The following table indicates different technologies with a weighted limited capability profile:

Figure 13: Literature capability profile of different technologies [5]

Two approaches, on how to evaluate a reverse engineering system, are shown below. The one relies on the information provided by the vendor or company. The other uses a fabricated benchmark part.

2.4.1   Vendor model

The table below is an example of what is found in the Wohler report [**18**]. Most manufacturers of RE equipment are listed below, in a tabular form. All the information in the table is supplied by the manufacturers and the comparison is therefore not entirely objective. The table however acts as a good starting point to find a suitable provider or product. The complete table is presented in Appendix A.

Table 1: Example of Wohler report's RE table [18**]**

Company	Product	Technology	Work Volume	Accuracy	Speed
GOM **gom.com**	ATOS I	Structured white light (fringe)	40x30-1000x800 mm	n/a	1m pts / 7 sec
Renishaw, Inc **renishaw.com**	Cyclone Series 2	CMM with contact or laser probe	600x500x370	5 µm (repeatability)	400 pts/s
Mitutoyo **mitutoyo.co.jp**	(multiple models)	CMM	varies	varies	n/a
Romer, Inc **romer.com**	INFINITE LSI	Articulated arm w/laser scanner	9-foot envelopes (typical;others available)	±0.0006 in (6-feet envelope)	> 23,000 pts/s

Note that the accuracy is not represented in a standard form and most vendors represent their accuracy as a single number. Reducing a device's accuracy to a single number might be misleading, as a complete accuracy assessment is a complex issue [**4**]. The accuracy of all measurement systems will vary, depending on where within the work volume, the measurement was taken. Examples of this are in triangulation, where the accuracy is dependent on the standoff distance, the accuracy decreases, with the increase in distance from the light source. Similarly an articulated arm will deflect more when the arm is fully extended. Any error in the system is magnified, proportional to the distance of the taken measurement, this is the deflection principle. The same is the case for any other contact based scanner. The touch probe may be extended by a stylus, each extension adding an error to the system. Some vendors as a result may give the accuracy as a mean value; others will quote the root mean square, giving a better indication of the mean and standard distribution. Other factors may also influence the accuracy of a system. Although the resolution of the system and accuracy are not directly related, the resolution of a system can influence its accuracy. An example is that if the resolution, representing a sharp edge, is poor the surfaces or curve, representing the edge, introduce an error. The repeatability is also sometimes given with the accuracy and it must be noted that measurements taken in controlled laboratories have higher repeatability. This might be completely different in a real scenario, as temperature and humidity can dramatically influence the repeatability of measurements. All these observations on accuracy are mentioned to show that the right questions need to be asked when the topic of accuracy is discussed. The accuracy of any system must always be investigated but the real question should be if the system's accuracy is fit for its intended purpose.

Once the other capabilities of the reverse engineering system are identified and quantified, it is a good idea to make contact with some of the companies listed in the complete Wohler's table. This should be done after having a look at each potential vendor on the internet first, as it could give a good idea as to the general attitude or move towards different technologies and vendors in the industry. Forums and journals give feedback on tried systems; this saves time by eliminating some vendors and increasing general knowledge on the topic. A preliminary investigation should list as many suppliers of RE products as possible. Contact should be made with these companies and a

document, listing all requirement criteria should be sent to them. From the responses the list can be reduced. At this stage it would be good to negotiate a company visit with the vendor, or request a sales assistant to visit the potential customer. A sense of company service can, through this process, be established.

To compare different systems meaningfully, it is necessary to list the importance of each criterion or attribute, defined within the system's specification. The importance is normally ranked on a scale of 1-5 where 5 is 'essential' and 1 is 'not at all important'. When the system is being demonstrated or evaluated, each member within the company should form his own opinion of the capability of the system or vendor, in terms of each criterion. The values may be averaged or discussed and mutually agreed upon. Each score is then multiplied with the importance of each attribute. All weighted scores are then added to give a final score. The vendor or system with the highest score is chosen. Note that the sensitivity of each score and weight should be done, as the results are subjective. This overall process is illustrated in Figure 14.
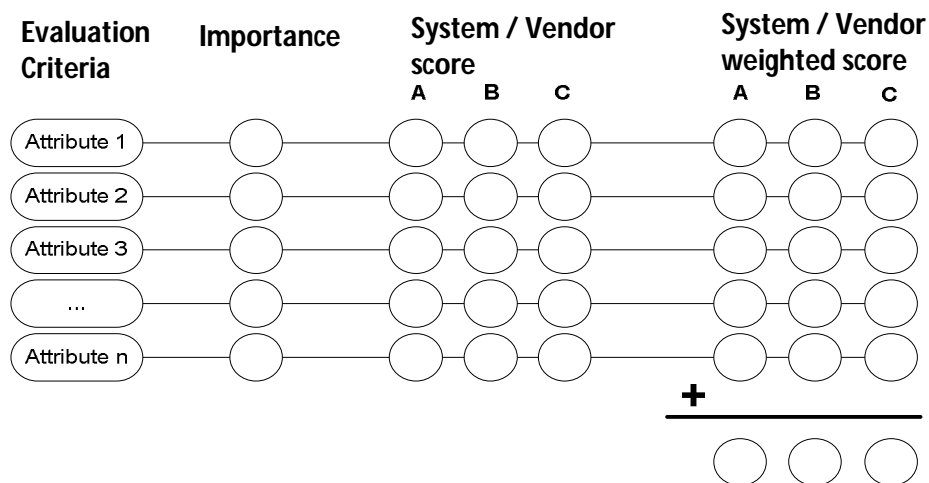
Figure 14: Example of a rank weighted grid

To quantify each score in a more objective manner, a benchmark part has to be introduced.

2.4.2   Benchmarking

Comparing and choosing between different systems is quite an arduous task because, at the moment, there is no standard procedure internationally recognized and accepted for qualifying and evaluating the performance of 3D scanners [**25**]. For this reason benchmark parts have been introduced. There are many common benchmark parts made available by accredited metrology laboratories. A laboratory, well known in the international metrology community, will design a benchmark part, measure it and publicly show all results and findings. The benchmark part design is then made public, for other laboratories to try and re-produce the results; this process is often discussed in journals.

If the Vendor Model has not pointed towards a definite solution, a benchmark part may be introduced. The vendor is then asked to scan a component, to produce a desired output. It could be achieved by means of a point cloud to decide on an appropriate software vendor, a CAD model for manufacturing purposes or an input file for a rapid prototyping process. It is important that the team, handling the matrix of capability attributes, is present during the entire stage, in order that they are aware if scores need to change in the capability matrix. This will lead to a firm technical decision in terms of each systems capability and a commercial evaluation can also be conducted, when dealing with the different vendors, during the benchmark part process.

2.4.3 Conclusion

Choosing a system is not an easy task. It is not possible to provide a generic approach that will fit all situations exactly. The decision making process is a dynamic one and should be adapted and updated throughout. The internet makes it easy to gather data but there is no substitute for visiting the vendor or witnessing a demonstration, perhaps at a trade show. Note that the vendors are well prepared for the trade show thus asking them to RE a representative part, different to their own, is suggested. The matrix of capability attribute evaluation model is a good tool for channelling the information gathered during the evaluation period. Producing a benchmark part will further the depth of the matrix and will give more concrete data in evaluating the scores of each attribute. However a benchmark part is not always needed.

3   Benchmark Part

As mentioned in the previous chapter, the introduction of a benchmark part makes it possible to compare different digitizers. For this reason a benchmark part is introduced in this study. There are multiple benchmark parts available, thus designing a completely new one would diverge from the idea that a guide or standard, in the future, needs to be developed to compare 3D scanners.

3.1   Benchmark part description

The benchmark part used in this project, has been designed and used for contactless scanner comparison [25]. Five out of the 47 defined parameters were altered. Three holes were added, to verify the inspections and accuracy of deep holes. The benchmark part was designed, with reference to moulds, like production tools. The original decision, in terms of the size, was to make it easily transportable and make it fit into the working volume of small contact digitizing systems. As stated in [25] the common geometric features of moulds and sculpted surfaces were considered in the design phase, to make the benchmark representative of a variety of production tools and wide consumption products. The part is measured using different digitizing techniques thus a comparison is only achievable if the simple classical dimensions are well defined. Simple geometries are represented in both concave and convex form (hole and boss), in order to consider all possible cases and because most tools consist of both the female and male features. The following features are represented in the negative and positive form [25]:

- two quarters of hemispheres (S) with radii of 40mm.
- two quarters of a cylinder (C) with radii of 60mm.
- two quarters of a truncated cone (TC): they connect the quarter of the cylinder with the spheres. The cone angle is 43.6°, adjoined to the 60 and 40mm top and bottom circles.

The terminology and acronyms used will be the same as in the study of [25], to simplify referencing and comparisons. The convex geometries are referred to as the 'OUTER' (O) and the concave geometries are referred to as the 'INNER' ones. A complete list of notation can be found at the end of this section. The other classical geometries found in the benchmark part are as follows:

- Two coaxial cylinders (CC), each 10 mm high. The smallest has a radius of 8mm and lies over the bigger one whose radius measures 16mm.
- An elliptical pocket (EP), minimum and maximum radii measure 15 and 25 mm respectively.
- Three tilted planes (TP)
- Some planes are vertical (VP) and others are horizontal (HP).
- A truncated square pyramid (TSP). The edge of the top face measures 20mm and the side faces are tilted towards the top one at different angles of: 0°, 5°,10° and 15°.
- Three deep holes (H): 15, 10 and 5mm in diameter.

The position and centre axis of all the features are measured and referenced in the same coordinate system of the benchmark part.

Notation	Meaning
TSP	Truncated square pyramid
TSP1	Top plane of the truncated square pyramid
TSP2	Lateral vertical (α=0°) plane of the truncated square
TSP3	Lateral vertical (α=5°) plane of the truncated square
TSP4	Lateral vertical (α=0/10°) plane of the truncated square
OS	Outer sphere (convex geometry)
IS	Inner sphere (concave geometry)
OC	Outer cylinder (convex geometry)
IC	Inner cylinder (concave geometry)
OTC	Outer truncated cone (convex geometry)
ITC	Inner truncated cone (concave geometry)
CC1	First coaxial cylinder
CC2	Second coaxial cylinder
HP	Horizontal Plane
HP1	Bottom horizontal plane of benchmark geometry
HP2	Top horizontal plane of benchmark geometry
HP3	Top horizontal plane of the elliptical pocket
HP4	Bottom horizontal plane of the elliptical pocket
EP	Elliptical pocket
TP1	Big tilted plane
TP2	Tilted plane near the elliptical pocket
TP3	Small tilted plane
TP	Tilted plane
VP	Vertical plane
VP1	Vertical plane near the elliptical pocket along the X
VP2	Vertical plane near the elliptical pocket along the Y
H1	Top hole (Ø 15mm)
H2	Centre hole (Ø 10mm)
H3	Bottom hole (Ø 5mm)
α	Tilted angle of the feature
X	X-axis coordinate of the feature position
Y	Y-axis coordinate of the feature position
Z	Z-axis coordinate of the feature position
R	Radius of the Feature
X_c	X-axis coordinate of the feature centre
Y_c	Y-axis coordinate of the feature centre
Z_c	Z-axis coordinate of the feature centre
X_a	X-axis coordinate of the feature axis
Y_a	Y-axis coordinate of the feature axis
Z_a	Z-axis coordinate of the feature axis

Figure 15: Definition of classical geometric shapes of benchmark part

Complex shapes are widely used by designers to improve the aesthetic value of a product; a free form shape is therefore introduced into the benchmark part. The freeform surface is represented as a NURB surface, joining the two eights of a sphere. NURBS are generally used to represent freeform surfaces [**5**]. As NURBS are shown using parametric surface representation some of the benefits are:

- It is easy and convenient to define and control shapes and curves within a CAD program.
- The surfaces and curves are independent of any coordinate system, so the choice of reference will not alter the shape of the surface or curve.
- Their mathematical representation is easily expressed in matrices, thus computing power is used efficiently and making large data manipulation editing more convenient.
- As they have the ability to represent large surface patches, they are easily manipulated or edited and can at the same time represent simple analytical shapes. The exact geometry of a NURB surface is unknown to the CAD designer when editing in the design program. After exporting the object in the IGES (Initial Graphic Exchange Specification) format the

mathematical surface representation is created. Only then may the theoretical coordinates of every single surface point be computed and the model may be used for inspection purposes.

3.2   Benchmark part fabrication

The manufacturing of the benchmark part was conducted by IAT (Institute of Advance Tooling), at Stellenbosch University. The stock aluminium block measured 195x165x70mm and was machined by means of the Hermle C40U five axis CNC machine. The part was drawn up in Pro Engineer and the milling path was computed in PowerMill from Delcam (see part drawings in Appendix B). The total time to machine the part took 5 hours. The 5-axis CNC machine and finished part can be seen in Figure 16. It was decided not to post hand polish the part, as this might introduce measurable deviations from the CAD model. The surface roughness was measured with the Mitutoyo Surftest-211 handheld device. This can only be conducted on flat surfaces, where the device may rest on the same plane. Ten measurements were taken, each over a distance of 5mm. The mean value of the Ra measurement is 0.82μm with a standard deviation of 0.13μm. This value is much smaller than the expected measured values in this study. The surface roughness is assumed to be less than 1μm for the remainder of the part.

a) Hermle C40U 5 axis CNC   b) Fabricated benchmark part
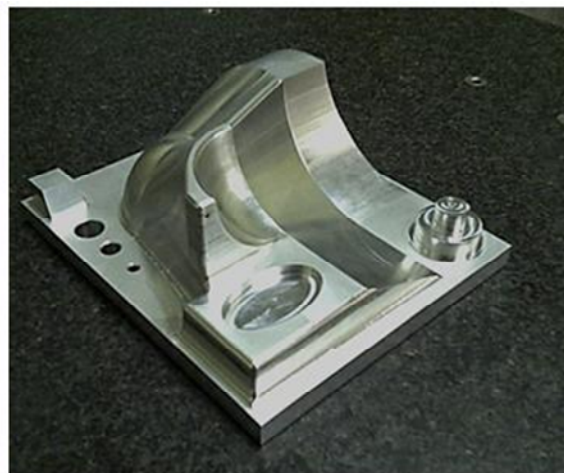
Figure 16: Benchmark fabrication

3.3   Benchmark part inspection and CAD model comparison

After manufacturing, the benchmark part was inspected by means of a CMM. This was done to assess the final real geometry of the part as 'fabricated'. All measurements are conducted in the metrology room of the RPD Laboratory. The room has no windows to the outside and it is artificially illuminated. Although the room's temperature is controlled, some lighting may have an effect on the surface temperature. This will be discussed later on. The CMM results will act as the base measurement for all the classical geometries of the benchmark part.

3.3.1   Approach

The classical geometries were measured using the Mitutoyo Bright 710 CMM. The machine is calibrated annually and is traceable back to the International Committee of Weight and Measurement. The CMM is certified with a current uncertainty of 3μ. The machine's particulars and tractability are discussed later on. The accuracy of the CMM is far superior to that of the other digitizing devices and thus these results will act as the reference values for the classical geometric features. These values will be taken as the real 'fabricated' dimensions of the benchmark part. The benchmark part was measured three times, to evaluate a mean and standard distribution of all the length and angle dimensions. The overall absolute mean, of all the length devistions, was found to be 0.041mm, when compared to the CAD model. All results are listed in Appendix C in detail and a distribution Histogram is shown below for the length dimensions (Figure 17).
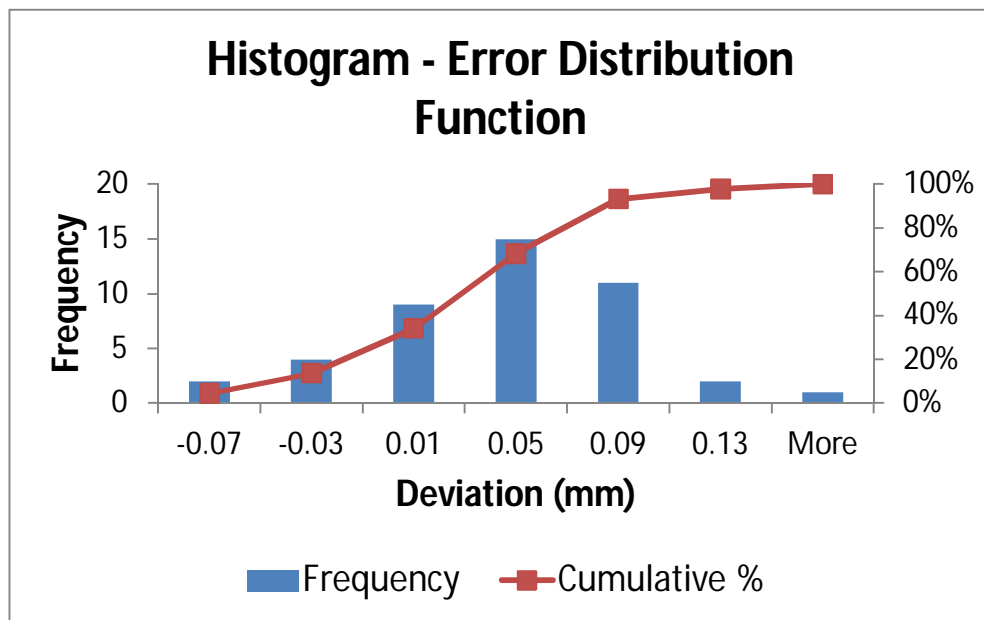
Figure 17: Histogram of error distribution

3.3.2   Feature measurements and deviations

Horizontal planes

There are 7 horizontal planes in total. All measurements were taken by moving the probe in the z direction. The flatness given by the CMM as the 'd' coefficient is very low (0.002). Out of the seven planes, three are spread over a relatively large area, while the other four are spread over a small one. The large horizontal planes are measured to be very close to the CAD model, the absolute average difference being only 7μm. The four smaller planes have an absolute average deviation of 51μm, when compared to the CAD model.

Vertical planes

There are three defined vertical planes within the benchmark part, two in line with the Y axis and one in line with the X axis. The two planes along the Y axis have a smaller and similar deviation, when compared to the plane along the X axis. This might be because the CMM's working axis is

longer in the Y direction than in the X direction and thus the error might be a function of length. But this is not confirmed.

Tilted planes

These dimensions are compared to each other in terms of degrees and not length. There are four angle dimensions along the truncated square pyramid and another three tilted planes within the benchmark. The absolute average mean of the seven planes is 0.08°, with a standard deviation of 0.085°. This is fairly small and the trend is that the smaller planes are further out than the larger planes.

Holes

All measurements with the CMM were taken using a 2mm ball tip probe that is 20mm long and has a 40mm extension. This made the accessibility to all surfaces easy, especially the three holes. The holes were measured automatically by a four point representation. The roundness of all three holes is satisfactory and is given as 0.007 by the CMM. The average error or deviation of the diameters of all three holes is around 40μm. This could be due to the fact that the holes were not drilled but machined, movement of the end mill is restrictive. The positions of the holes' axes were on average out by 70μm. This can be explained because the holes were first machined from the bottom of the stock block and then the aluminium block was turned around and the data was set again, before running the CAM program. An alignment error might have come in here.

Coaxial cylinder

The cylinders were also measured automatically by a four point representation. Both diameters of the coaxial cylinder have sound roundness properties. The diameter is also better than that of the holes, with an average absolute deviation of 20μm. The position of the axis of the cylinder is also better than that of the holes, this being at 40μm. The position deviation in the longer direction is surprisingly smaller than the one in the shorter distance. This contradicts the theory that an error is introduced as a function of length.

Ellipse

The ellipse was measured in the XY plane by eight point representations. Both smaller and larger radii, that represent the ellipse, are 5μm different to that of the CAD model.

Spheres, Cones and Cylinders

Up to now all dimensions were captured manually by moving the CMM probe. The six features (2 spheres, 2 cylinders and 2 cones) were initially also measured manually by 10 random points per quarter feature. As these results had a much higher deviation to the CAD model, when compared to all other previous results, the six features were analysed in more detail. Each quarter feature was obtained automatically, by a program that measured 25 points on a 5x5 grid over each surface of every feature. The schematic representation of the placement of these points can be seen in Figure 18. The dimensions of each feature are then calculated, by means of the least square method. Using algorithms, the software computes the best geometric fit of the mathematically given shape. In this case a sphere, cone and cylinder. The resulting geometric features were then compared to the initial results of the manual measurements. The difference between the manual and automated method can be seen in Table 2. It was decided to replace the originally manually obtained dimensions, with

the automated measured ones, as 14 out of the 20 dimensions were closer to that of the CAD model. It is questionable if it is closer to the 'real' manufactured value and still needs to be determined.

a) Automated point measurements   b) Best fit alignment
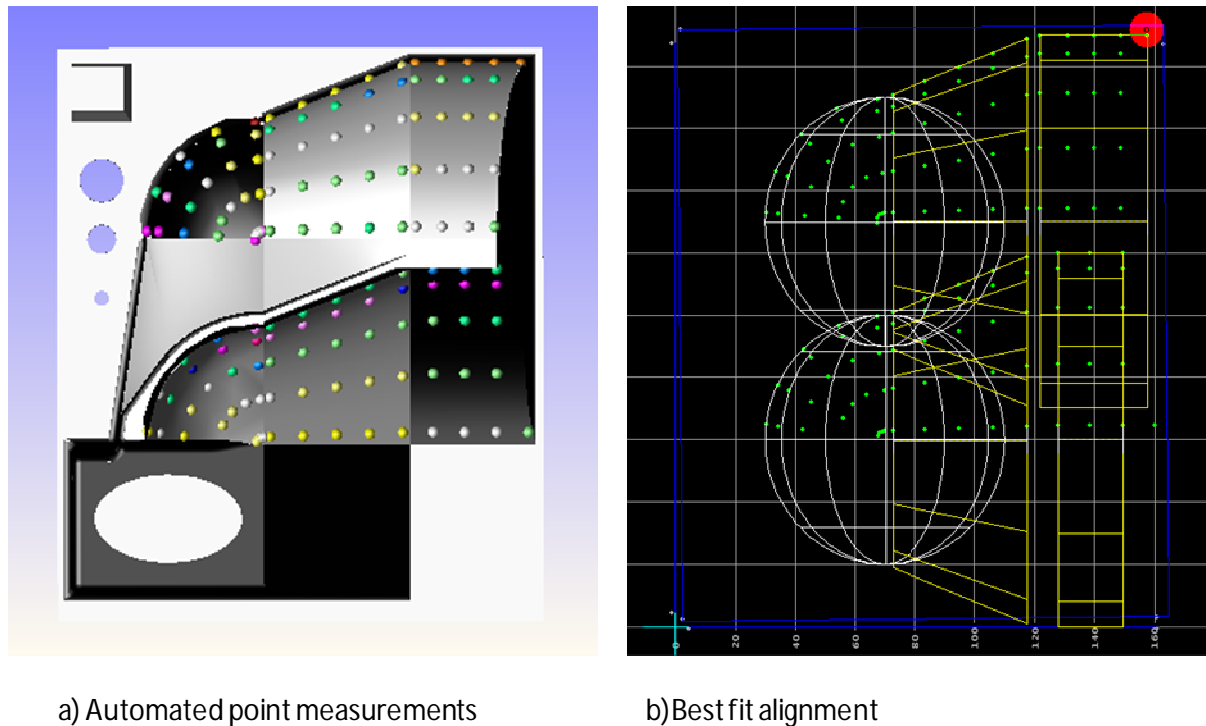
Figure 18: Best fit features of automated measurement

Table 2: Manual vs Automatic comparison

OS	Manual (n=10)		Automated (n=24)		IS	Manual (n=10)		Automated(n=23)	
	Mean	Deviation	Mean	Deviation		Mean	Deviation	Mean	Deviation
R	80.005	-0.005	80.021	-0.021	R	80.108	-0.108	80.047	-0.047
X_c	69.932	0.068	59.943	0.057	X_c	69.969	0.038	69.985	0.015
Y_c	129.933	0.067	129.942	0.058	Y_c	59.889	0.111	59.916	0.084
Z_c	0.007	-0.007	-0.011	0.011	Z_c	60.042	-0.042	60.003	-0.003
OTC	Manual (n=10)		Automated (n=25)		**ITC**	Manual n(=10)		Automated(n=25)	
	Mean	Deviation	Mean	Deviation		Mean	Deviation	Mean	Deviation
deg	43.456	0.144	43.529	0.071	deg	43.494	0.106	43.618	-0.018
Y_a	129.948	0.052	130.011	-0.011	Y_a	59.848	0.152	59.872	0.128
Z_a	-0.006	0.006	0.040	-0.04	Z_a	60.068	-0.068	60.045	-0.045
OC	Manual (n=10)		Automated (n=21)		**IC**	Manual (n=10)		Automated (n=15)	
	Mean	Deviation	Mean	Deviation		Mean	Deviation	Mean	Deviation
R	119.976	0.024	119.845	0.155	R	120.110	-0.110	120.088	-0.088
Y_a	129.971	0.029	130.037	-0.037	Y_a	59.901	0.099	59.920	0.08
Z_a	0.017	-0.017	0.064	-0.064	Z_a	60.046	-0.046	60.027	-0.027

NURBS

As mentioned previously, only after converting the NURB surface to an IGES file, may each location on the surface be represented by a coordinate point. An IGES file of the benchmark part was imported into the CMM inspection software. The coordinate system was established, as was done for the other measurements. 400 points were then taken from the surface to compare to the CAD model; the results with the deviation legend are shown in Figure 19. A best fit function was not executed, as this was not done to the other measurements and because the points are located on only one side of the benchmark part. The majority of the points were out by 32µm, this was due to the fact that the absolute mean value had an overall standard deviation of 38µm. The largest deviation point in the negative direction was 39µm, represented by one of the orange dots. The three black points are seen as random error, as the data clearly shows a trend along the measuring direction. The larges error in the positive direction was 84µm.

a) Scanned results   b) Machined path
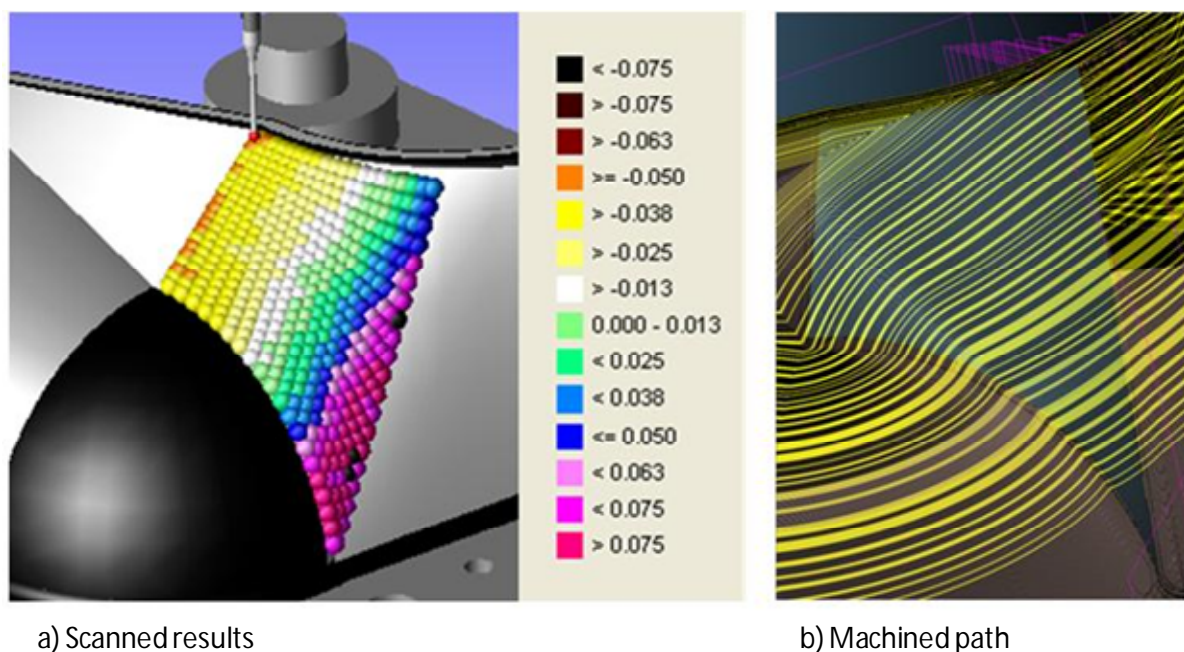
Figure 19: NURB analysis

After looking at the scanned results, it is clear that there is a trend in the NURB measurement. The machined tool path was consulted, to see if this caused the trend. The machined tool path is shown in Figure 19 b) and it correlates with the tool path visible to the naked eye, as expected. The direction of the tool path verifies that the measurement trend is not influenced by the tool path, as they run in different directions. The radical change in the direction of the tool path, in the top left corner of the NURB, is not picked up by the CMM. This also motivates the statement.

3.4   Benchmark measurement validation

3.4.1   Traceability

Results throughout all measurements need to be conducted according to an international governing body, this gives the results credibility. The term that needs to be introduced is traceability. Measurements done on the benchmark part may differ when conducted in different laboratories. There are several factors that can influence this. Results may differ even if a standardized uncertainty calculation is implemented, according to accredited guidelines. In today's metrology world, an exercise without the verification of traceability becomes pointless. Comparing measurements between industries becomes futile without globally agreed upon traceability and primary standards [**26**]. This, in essence, means that an experiment conducted within a laboratory is traceable, according to standards, when a globally accredited laboratory approves the methods. This study looks at a common and straightforward parameter 'length', where traceability is generally achievable. Only the traceable device in this study is the CMM. For this reason all other measurements in the study will be compared to that of the CMM. The traceability chain is seen in Figure 20:
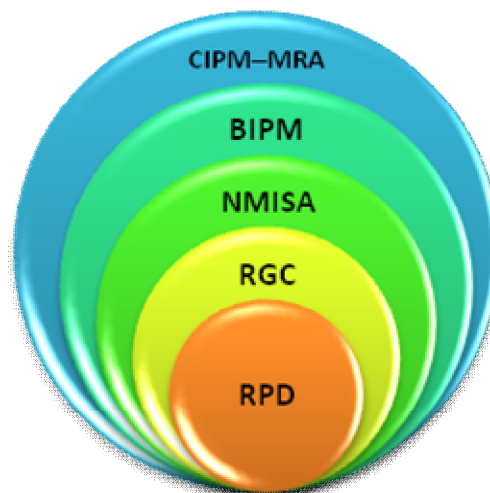
Figure 20: Traceability Governing Bodies

The international institute or primary standard, which is at the top of the hierarchy or traceability ladder, is the International Committee of Weight and Measurement – Mutual Recognition Arrangement (CIPM – MRA). The secondary standard or national body is the NMISA (National Metrology Institute of South Africa), which is accredited by SANAS (South African National Accreditation System). The NMISA Dimensional laboratory is a participant to the MRA through the International Bureau of Weights and Measurements (BIPM), by participating in international key comparisons, through the Consultative Committee for Length (CCL). The accredited laboratory, which calibrates the reference machine, is located in Johannesburg, RGC Engineering. All measurements are conducted at the RPD Labs (Rapid Product Development Laboratories), which shows an accepted traceability chain to the CIPM-MRA.

3.4.2   Uncertainty

In metrology a common mistake by those not familiar with its terminology and principles, is to assume that an instrument's accuracy and precision is one and the same thing. Accuracy is a characteristic of a measurement result, as is precision. Accuracy is the degree of closeness of a measurement to the absolute value. The precision of a measurement is also defined as the repeatability or reproducibility. The difference can be seen graphically in Figure 21. Accuracy is a generic concept of precision, related to the closeness of agreement between the average of one or more test results and an accepted reference value, which is often the 'true value' or absolute [**27**] [**28**]. The 'true value', however, may not be a practical concept since the 'truth' is never known. This introduces the question whether it is possible to determine or calculate (in)accuracy. If we could determine (in)accuracy then we could calculate the 'true value' from measurement results. Another term needs to be introduced to the study, namely measurement uncertainty [**29**].
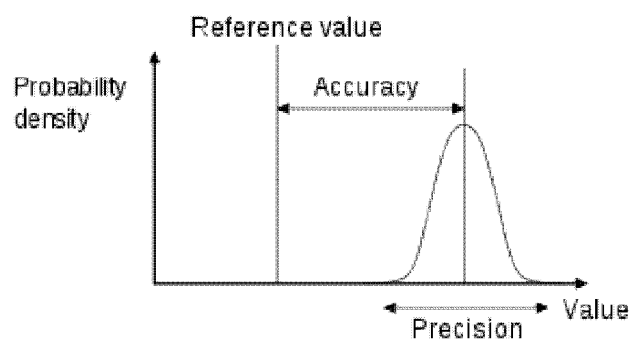
Figure 21: Accuracy versus Precision illustration

In 1995 the Guide to the expression of Uncertainty in Measurement (GUM) was published and rapidly established itself amongst universities and research centres, as well as industry [**30**]. A 'guide' normally has a lower status than an 'international standard', GUM, however, is an exception [**26**]. It implies a revolution in the way measurement results should be presented, in terms of uncertainty. When conducting an experiment, different types of errors show up in the measurement results, such as systematic and random errors, drift and outliers (Figure 22).
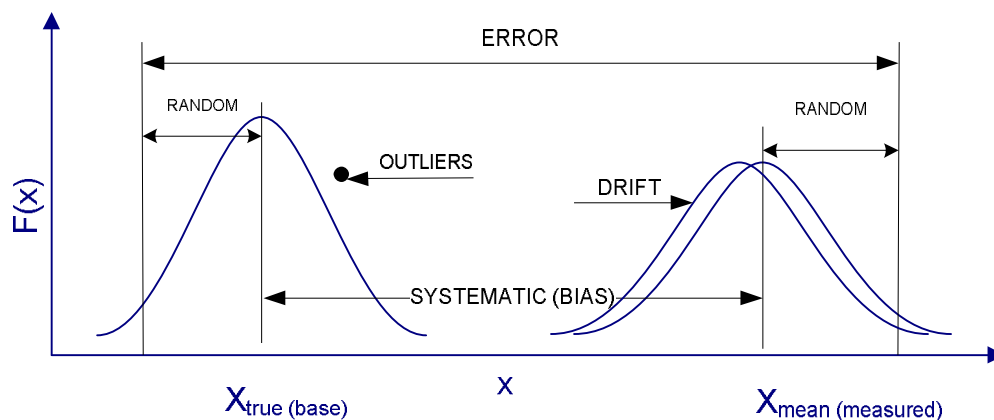
Figure 22: Types of Errors in Measurements

All errors are naturally systematic, as they can be characterized as the difference between the measured result and true value. Random errors are caused by non-controlled unsystematic influence. A random error can be characterized by the standard deviation and the type of distribution. Drift is often a time or wear effect, for example the results of a device may 'drift' throughout an experiment as the components, within the device, warm up or wear down. Outliers are mostly caused by human error and are often emitted when analysing a measurement result. Errors or uncertainties in a measuring process will be a mix of known and unknown errors from a number of sources or error components [**31**].

- Environment (humidity, vibration & noise, ambient pressure and temperature, etc)
- Measurement equipment (time since calibration, probe system, reading system, etc)
- Software and calculation (algorithms, rounding & quantification, filtering, etc)
- Metrologist (education, experience, training, etc)
- Measuring procedure (strategy, clamping, number of points/measurements, etc)

As stated, the uncertainty of the CMM is calibrated to 3μm. This is however difficult to accept as, when calibrating a probe in different positions or times a probe calibration error of 4μm of the same probe can be evident. This is due to the probe diameter and positioning uncertainty. It does not include the additional uncertainty in the measurement itself. Thermal expansion of the part itself introduces a measurement uncertainty. The following example quantifies this statement:

The room, in which all measurements are taken, is in a controlled environment. The temperature can however fluctuate within 2 degrees, as observed during measurements. This can be considered an uncertainty in the experiment. The longest dimension measured on the benchmark part is 145mm (l), the linear expansion coefficient of Aluminium is $\alpha=2.3\times10^{-5}$/°C and temperature variation is $\Delta t = \pm2°C$. The uncertainty due to thermal expansion (u_{Texp}) can be calculated as follows:

$$u_{Texp} \approx u_{\Delta t} = \frac{\partial f}{\partial \Delta t} u(\Delta t); \qquad\qquad \Delta l = l \cdot \alpha \cdot \Delta t; \qquad\qquad (2)$$

$$u(t) = \frac{\Delta t}{\sqrt{3}} \ for \ a \ normal \ distribution; \qquad\qquad \frac{\partial f}{\partial \Delta t} = l \cdot \alpha;$$

$$u_{\Delta t} = l \cdot \alpha \cdot \frac{\Delta t}{\sqrt{3}} = 145 \cdot 2.3 \cdot 10^{-5} \cdot \frac{2}{\sqrt{3}} = 0.0039 \ mm$$

$$u_{Texp} \approx 4\mu m.$$

Another important element, noticed within the laboratory, is that the extra lighting installation for the CMM bed can rise the surface temperature between 2 and 5 °C. This is an additional uncertainty and the eight 50W halogen light bulbs were replaced with low heat emitting LED lights.

The overall uncertainty of the CMM needs to be investigated, thus combining all uncertainty components. This was done using three certified gauges from the National Metrology Institute of South Africa. The three gauges are as follows:

- A ring with a diameter of 79,37557mm and uncertainty of ± 0,14 µm
- A sphere with a diameter of 24,99992mm and uncertainty of ± 0,15 µm
- A gauge block with a length of 100mm and uncertainty of ± 0,1 µm

Each gauge was measured five times to look for measurement deviation. The ring was computed five times using 5, 10 and 20 points to mathematically compute its radius. The sphere was measured 5 times with 10 and 20 points to compute the spherical representation. The gauge block was measured 5 times using a length representation of two points, two lines and two planes. The results are listed in Appendix D. They show that the more points used to measure the ring and sphere, the closer the results are to the real value. The best results for the gauge block were obtained from the point to point method. These results will be used in the uncertainty analysis and the sample calculation can be found in Appendix D.

GUM recommends the implementation of mathematical models of the measurement process whenever possible. There are two different types of classification of uncertainty evaluations, according to the standard, Type A and Type B. Type A will in most cases result in a more accurate estimate of uncertainty components, compared to Type B. Type B estimations are often difficult to compute numerically and are heavily dependent on the experience of the evaluator. An example of a Type B uncertainty is the uncertainty of the metrologist's experience. The Type A method evaluates the uncertainty component, u_{xx}, mostly by statistical means. The random error or the uncertainty component from repeated measurements can be calculated as follows and according to [31]:

Suppose n number of measurements (that is, n repetitions) of X are made, each measurement represented by X_i, where i = 1, 2,..., n and n is finite, the estimate of the true mean, $\bar{x}$ can be computed by:

$$\bar{x} = \frac{1}{n} \times \sum_{1}^{n} X_i \tag{3}$$

The standard deviation, S_x, of the distribution of the sample based on n measured values can then be computed as follows:

$$S_x = \sqrt{\frac{\sum_{1}^{n}(\bar{x} - X_i)^2}{(n-1)}} \tag{4}$$

The standard distribution which is calculated using finite measurements can be weighted to represent infinite measurements. A new variable is introduced as the t-estimator or safety factor, which is calculated, based on the Student-t distribution. The uncertainty component, calculated from measurement results, u_{xx}, obtained using single readings of the component concerned, is calculated as follows:

$$u_{xx} = S_{x,n} \times t_{v,P} \tag{5}$$

v is the degree of freedom and is given as $n-1$ and P is the probability in percent.

Addition of uncertainty parameters

The different uncertainty components, u_{xx}, are added geometrically to equate the combined standard uncertainty, u_c, using the expression as in [**31**]:

$$u_c = \sqrt{u_{x1}^2 + u_{x2}^2 + u_{x3}^2 + \cdots + u_{xn}^2}$$ (6)

The expanded uncertainty, U, is calculated as:

$$U = u_c \times k$$ (7)

where unless otherwise specified, the coverage factor is $k = 2$.

U and u_c are not stochastic variables and should not be treated as standard deviations, but as constant (unknown) errors. In literature, systematic errors are added geometrically to random errors, often represented with the following expression [**32**]:

$$u_x = [B^2 + (t_{v,P}P)^2]^{\frac{1}{2}}$$ (8)

where B is referred to as the Bias (systematic) uncertainty and P the standard random uncertainty, as calculated with the use of equation 5. It is more appropriate to add the systematic error arithmetically, rather than geometrically, in order to calculate the extended uncertainty, U [**8**] [**33**]. The combined expanded uncertainty becomes:

$$U = k \cdot u_c + |b|$$ (9)

where b is the overall systematic or bias error and is given as:

$$b = \bar{x} - x_b$$ (10)

This is the difference between the mean of the measurement as calculated with equation 10, minus the reference or base of the measurement (in this case this is the value of the gauges given by the NMISA). The complete procedure, with a sample calculation, is presented in Appendix D. The different computed uncertainties of the gauges are calculated as follows:

- U_{Ring} = 0.016mm
- U_{Sphere} = 0.027mm
- U_{Block} = 0.017mm

The average of the three measurements is 20μm, far greater than the certified 3μ. This observation does not give the study less credibility; it notes that the ideal and desirable expected measurements will have a larger uncertainty value than initially expected.

4   Criteria Evaluation

In the previous chapter, an already existing benchmark was modified, fabricated, measured and validated with a CMM. This chapter introduces the alternative hardware available for the study. The different software packages available are also classified and mentioned. The accuracy criterion makes good use of the measurements obtained in the previous chapter. Other criteria are also analysed and discussed.

4.1   Reverse engineering hardware available

The following text describes the characteristics and workings of the different reverse engineering hardware available during the study. The list consists of a conventional CMM, a CMM with an analogue scanning probe, an articulated arm and an optical structured white light scanner (GOM).

4.1.1   Mitutoyo bright 710 CMM

The accuracy of this machine, as stated by the manufacturer, is 6μm, however, from the previous chapter it can be deduced that there is a strong possibility of lower accuracies. The measuring tool is controlled by three primary moving, axis using servo motors. The air-bearings and granite mounting table help to achieve good accuracies. The work envelope is 900x1000x700 mm (X, Y, Z). The axis can move between 433 mm/s in fast mode and 26 mm/s during the actual measuring process. The machine comes with a remote joystick control panel, which allows for close-up inspection and control, or the machine can be controlled by entering coordinates or paths on the computer. This is done by writing a probe-path inspection program and setting up a jig for easy part alignment and clamping. The three axis machine can be extended to a 4 or 5 axis, depending on the probe head controller used. The CMM in this study has 5 axes (Figure 23).
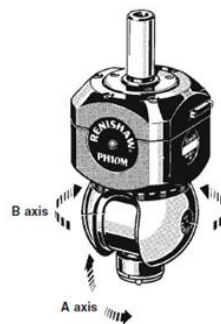
a)   Mitutoyo Bright 710 CMM   b) Renishaw probe head controller
      (3 axis)   (2 axis)

Figure 23: 5 axis CMM

Renishaw Probe Head controller of CMM

The motorised PH10M Renishaw head controller allows inspection at different and hard to reach angles, without having to re-orient the measured object. The additional 2 axes make it easy to inspect side holes, undercuts or overhangs. The probe head is compatible with a range of contact and noncontact scanning sensors and touch-trigger probes. It can achieve 0.5µm repeatability at a radius of 62mm. The A-axis has a range of 105 ° and the B-axis a range of ± 180° (Figure 23); both have steps of 7.5°, giving it a total of 720 positions to measure from.

4.1.2   CimCore infinite articulated arm

The six axis CimCore Infinite 5018i is the Articulated Arm CMM used for the study. The arm, also known as mobile CMM, has a 2-2-2 configuration; a shoulder, elbow and wrist, each equipped with two rotary encoders (Figure 24). With the help of a mathematical model, the software produces conventional Cartesian coordinate system, represented in the X,Y and Z direction. Each encoder's physical range is 360° with 20 000 electronic increments, giving each axis a resolution of 0.018° [**34**]. The arms connecting the joints are manufactured from carbon fibre tubes and the joints are machined from a light weight alloy. The arm is operated manually with three touch-probes. The arm has an optional laser scanner head; however, this was not available for the study. The Ø6mm diameter probe was always used in this study.

Figure 24: CimCore Infinite Articulated Arm

4.1.3   GOM ATOS I white light optical scanner

The ATOS system is also a portable scanner that consists of two cameras, a projector, stand, control unit and Linux laptop (Figure 25). During scanning, a fringe pattern is projected onto the object within seconds, the software calculates the high-precision 3D coordinates of up to 800 000 object points, hence each photo of the camera has a 0.8 megapixel resolution. The measuring area ranges from 40-30mm^2 to 1000-800mm^2 depending on which camera lenses are attached. The lenses, used during the study, captured a 485-389mm^2 (500x400) sharp image with a depth of field of 389mm and thus made the work envelope a total of 485x389x389mm. When measuring large objects, the work volume may exceed up to 3 times the above mentioned work volume, providing the neighbouring work volumes have 3-4 common reference points. However, this will induce an error to the overall accuracy of the system. The stated accuracy is 20 µm, as given by the manufacturer.

a) Control unit, stand and scanner   b) Scanner (cameras and projector)

Figure 25: GOM ATOS I white light optical scanning system

4.1.4   Renishaw cyclone analogue contact probe scanner

The axis travel or work envelope of the 3 axis scanner is 600x500x400mm, with an accuracy of 50µ and a 7µ resolution. The scanning speed is 3 meters per minute and up to 6m a minute for rapid scanning, with a scanning or sampling rate of 140 points per second. The machine is primarily designed and used for the mould and die mould industry. There are two measuring approaches; one method captures the contour of an object in a two dimensional plane. The alternative method is where the probe scans a two dimensional surface of an object incrementally by selecting a pitch. As with the other touch probe digitizers, edge detection can be a problem. Another limitation is that the probe cannot be tilted, in order to measure overhangs, or the 'floor-side' surfaces. The object would have to be turned around, re-aligned and then measured from the top. However, since the scanner is designed for the tooling industry, the cavities of a mould are often measured so there is no need for this strategy.

Figure 26: Renishaw Cyclone analogue scanning CMM

4.2   Software Interaction

4.2.1   PRO/E

This software was used to draw the benchmark part and is the only modelling package used in the study (Figure 27). The module is a conventional parametric-based CAD modelling package for the creation of solids and surfaces. The REX extension module allows for a complete reverse engineering process to be performed, from point cloud to solid model. This package will, however, not be used to evaluate the accuracy of the scanned data. It is not possible to execute a least square best fit of a sphere to a domain of point, therefore this missing feature does not allow for the analysis of the INNER and OUTER sphere. Nevertheless, the 'automatic surface generator', amongst other neat tools, makes REX a very functional and user-friendly package for reverse engineering tasks in industry.

Figure 27: Software Interaction

4.2.2   COSMOS (mitutoyo CMM)

This software was installed with the CMM's computer when it was acquired. It is an inspection software that not only controls the CMM, but also manages the files and includes the measurement program. A module, within COSMOS, GEOPAK, allows for the manual and automatic inspection of geometric features, contours and surfaces. IGES CAD files may be imported for the comparison of measurements. The software also allows for easy exporting of measurement points and reports into excel and word documents. This is the only module of the four that allows for the inspection of ellipses. For each ellipse evaluation of the other systems, eight points act as inputs to the built in function within COSMOS.

4.2.3   DELCAM power inspect (articulated arm)

As the name suggests, this software is typically used with CMM or AACMMs as an evaluation tool to verify tolerances or geometric properties. The software allows for easy measurement of geometric shapes and point cloud data can also be captured. An original CAD model is often imported and aligned for inspection purposes. The results can be exported as a test report in a tabular form or can be represented graphically with point deviations. This software is only used with the Articulated Arm.

4.2.4   ATOS (GOM)

This software is provided with the GOM and allows for a scanner to be calibrated and also controls the measurements. Furthermore, it was used both for the CAD alignment and the evaluation of

geometric properties of the measurements. It also allows for typical CMM inspection functions to be performed after scanning with the software. Classical geometries can be fitted to the scanned data; not only was this done with the data, captured with the GOM, but the data, captured with the Renishaw, was also analysed using this software.

4.2.5 Tracecut 24 (renishaw)

Tracecut 24, is the controlling software of the Renishaw but has no features that allow for geometric inspection. The software is installed on a Pentium 2 and files, ranging between 20-100MB in size, can take up to 12 hours to capture, making software operations time consuming, depending on computing power. The data points or splines, captured with this software, are always exported into additional secondary software for evaluation or design purposes. In this study, the data points are exported to the ATOS software for geometric inspections.

4.3   Accuracy comparison

The three remaining alternative RE hardware systems were used to measure the benchmark part and compared to that of the CMM. The alternative systems are the Articulated Arm (CimCore), optical scanner (GOM) and contact scanner (Renishaw).

4.3.1   CimCore articulated arm

The first comparison, with the benchmark part, was that of the Cimcore articulated arm. Studies have indicated that the error in the Z direction is greater than in the Y and X direction [**34**]. In this study, the benchmark part was placed in a position that facilitated ease of measurement for the operator and so that there were no arm restrictions. In addition, no encoders were overly extended. The images CAD model was imported and the features were created, as shown in Figure 28. The 3-2-1 transformation principle, as mentioned in Chapter 2, was used to create the origin of the coordinate system. All data was collected within the program except for the elliptical feature as has been explained. Here, eight points were measured and imported into COSMOS to compute its properties. The probe used was a ball probe of 6mm with a calibration value of 5.9mm with a 35μ standard deviation. Once the program was written, it was executed three times and the results are discussed and presented in Appendix E.
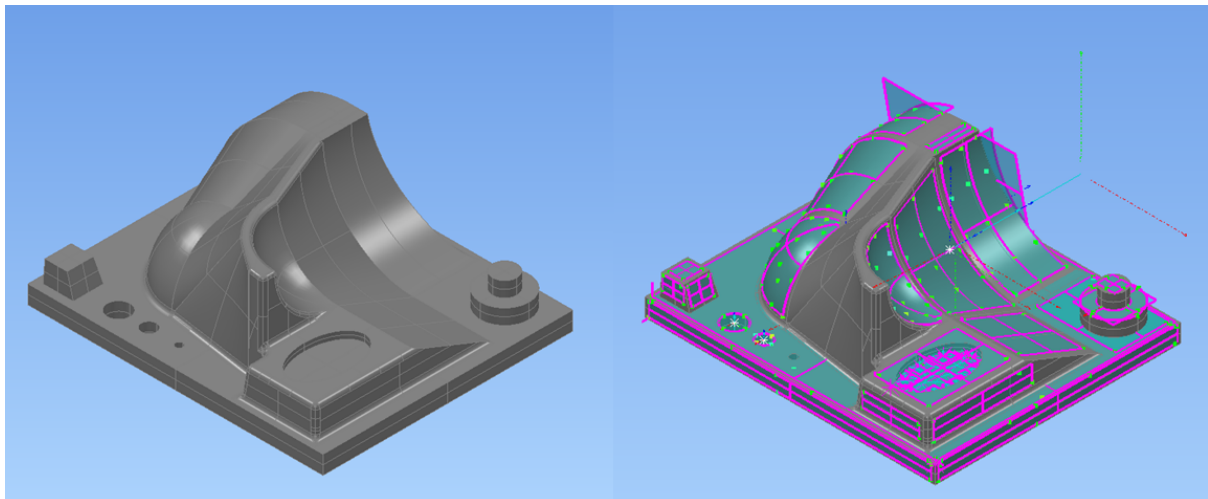
Figure 28: CAD model and created features

Horizontal planes
From the seven horizontal planes, which were measured three times, giving a total count of 21 measurements, one outlier was detected and ignored. The resulting absolute mean deviation comes to 21μ with a mean standard deviation of 35μ.

Vertical planes
The three vertical planes have an absolute mean deviation of 59μ to that of the CAD model with a standard deviation of 35μ.

Tilted planes

In the comparison of the 9 tilted planes, the absolute mean deviation to that of the CAD model, is 0.058° with a standard deviation of 0.05°. This result is closer to that of the CAD model reference than the results of the CMM. However, if this is closer to the absolute, machined values cannot be concluded.

Holes

Since the smallest ball probe available during the study was only 6mm, the smallest hole of 5mm could not be measured. Smaller probes are, however, available on the market to allow for finer measurements. The Cimcore arm is one such tool, allowing the measurement of smaller holes to be done quickly and efficiently. The absolute average deviation of the two holes is 10µ, with a positioning average of 73µ, giving standard deviations of 16 and 28µ, respectively.

Coaxial cylinder

The absolute deviation of the two circular bosses differs more in relation to that of the CAD model, than to the holes. The diameter deviation is at an average of 42µ with a positional error of 26µ. It should be mentioned when measuring holes or cylindrical bosses that the measurement in the z direction may be taken at different heights. If the z-depth varies considerably, the radius is calculated from a more 'oval' shape geometry, while the centre points would be the same.

Ellipse

The PowerInspect software does not allow for the evaluation of ellipses. Eight points were taken and imported into COSMOS, the CMM software, to evaluate the ellipse's two radii. The absolute deviation, to that of the CAD model, is 15µ.

Spheres, Cones and Cylinders

This refers to the 6 quarter features: the INNER and OUTER sphere, the cone and the cylinder. There are 14 dimensions that define the axes of all these features. These are always grouped to give an overall feature positioning accuracy, in this case 120µ. The radius deviation mean of the two spheres and cylinders was 180µ. The inner and outer sphere was calculated at 18 points, while the cones and cylinders at 15 points. The angle of the two cones was therefore out by 0.1 degree.

4.3.2 GOM ATOS I

The second comparison is the optical scanner, the ATOS 1 by GOM. The benchmark part was fitted onto a black wooden board with reference markers. The benchmark part was sprayed with liquid spray developer which leaves a white opaque powder. This helps with light reflection problems, typically encountered with shiny metallic objects. Such a layer does not alter the results of measurements taken where no contact is made [**35**]. The scan was performed under very low lighting conditions. The scan consisted of 8 overlapping images, with the GOM always remaining stationary, and was rotated on its wooden board with markers through 45 degree increments (Figure 29). The complete point cloud consisted of an average of around 42 000 points and the polygonisation raster was set to 1:4, with post processing set to 'very smooth'.

a) Benchmark on board   b) Complete point cloud   c) Primitive fitting
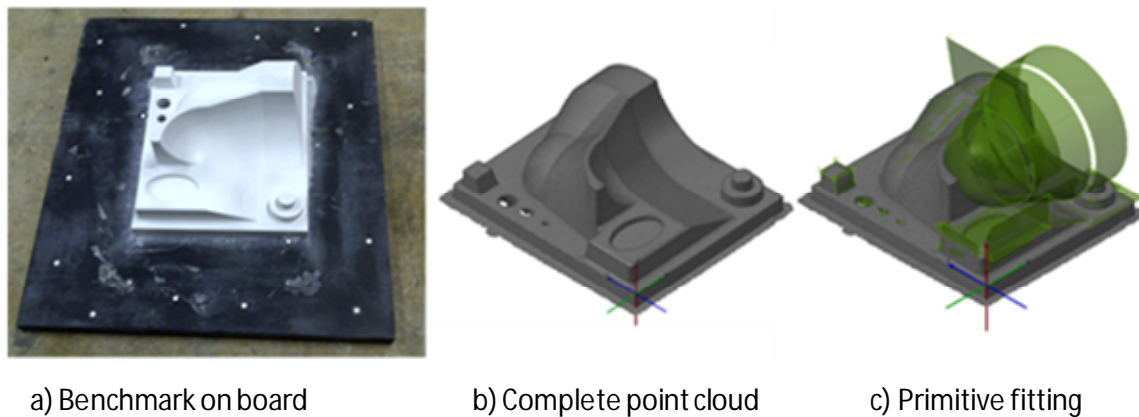
Figure 29: Measurement process of optical scanner

In this instance, the 3-2-1 transformation principle was also applied. The primitives were added to the cloud and most of the data could be extracted from within the ATOS program. This was done until all the parameters, as defined and quantified, could be evaluated. The whole process was executed three times in order to obtain a standard deviation and to evaluate the precision or repeatability of the device. The different geometric groups are evaluated individually, and are discussed. Measurement results are presented in Appendix F.

Horizontal planes
The absolute mean deviation of all 7 horizontal planes is 46µ, with a standard deviation of 29µ. There was no direct correlation to the error and size of the horizontal plane, as was seen with the CMM results. The perpendicular positioning of the camera, at just under 60° from the vertical position, gave it a good line of sight, while still remaining within the recommended angle guidelines.

Vertical planes
Surprisingly, the three vertical planes had a smaller absolute mean error than the horizontal planes. The mean was 33µ, with a standard deviation of 22µ. The capturing angle of the scanner was set to just under 60°, which is the recommended angle for measuring vertical planes. In addition, the camera did not have to be moved again in order to capture horizontal planes. This meant that only the benchmark had to be moved in-between measurements, and not the scanner itself.

Tilted planes

There are two outliers in this group, as per the definition given earlier in this chapter. Plane TSP4 and TSP5 are in their own scanning position in the background. The deviations to the CAD model were 0.728 and 0.432 degrees, respectively. The plane, with the next greatest error, was plane TP3 with an error of 0.249°, which was to be expected. The absolute mean deviation of the remaining six tilted planes was found to be 0.085°, with a standard deviation of 0.088°.

Holes

The recommended angle to capture holes with the GOM, is given at between 0 and 30 degrees. The angle was not changed since the holes where computed by their inner walls, rather than the edge detection of the hole. While this project is examining the performance of the hardware and not the software, this method was decided upon. Edge detection is greatly enhanced by using post processing in software solutions. The three holes have quite a large error, at 166μ, but the positioning error is at an absolute average of 24μ. This confirms the advice found in the literature, that measuring holes with optical scanners, is not recommended.

Coaxial cylinder

The measurements of the protruding cylinders were also better than that of the holes; the absolute mean of the diameters was 62μ, with a positional error of 43μ.

Ellipse

The ATOS software does not allow for the evaluation of ellipses. Therefore, eight points were recorded and imported into COSMOS, the CMM software, in order to evaluate the ellipse's two radii. The absolute deviation, to that of the CAD model, is at 26μ.

Spheres, Cones and Cylinders

The six features where fitted with a best fit approach, selecting all the points within each feature and assigning the right primitive to it. The grouping was done as with the Arm. The positioning accuracy was at 67 μ, the radius absolute mean 89μ, and the angle of the cones was out by 0.099 degrees.

4.3.3   Renishaw cyclone

The benchmark was scanned with the contact scanner, using a Ø4mm probe tip. The scanning grid consisted of two 45° overlapping cross scans, each with a nominal pitch of 0.1mm and a step over distance of 0.5mm. Different measurement procedures, with different scanning grids, were tested with similar results. Each scan took more than 5 hours, which is similar to the above mentioned study but the point cloud density was at roughly 750 000, rather than 1 150 000, and exceeded 70 MB. After the data had been captured, the stl files were imported to the ATOS software for analysis and to measure the classical geometrical entities. As can be seen in Figure 30, the probe was unable to capture many points on the vertical surfaces. However, the slightly tilted planes seemed to give more resistance to the probe's force input, and could thus be captured. According to the overall measuring procedure comparison, the Renishaw is less accurate as a result of the vertical component features of the surfaces. The results are discussed in more detail and are presented in Appendix G:
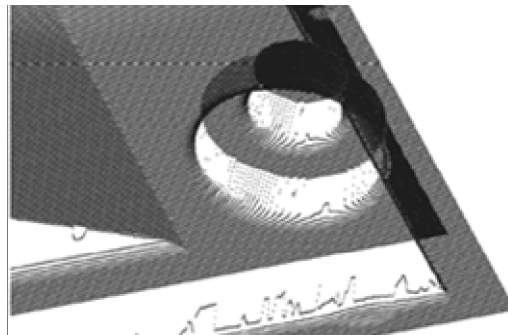
Figure 30: Point cloud showing poor vertical surfaces

Horizontal planes

As is shown in Figure 30, the point gathering on the horizontal planes is much denser than on the vertical planes. The reason for this is unknown and further investigation into the matter needs to be done. As a result, the horizontal surfaces have a very good mean absolute deviation from the CAD model: the seven horizontal planes have an error of only 9μ, with a standard deviation of only 7μ.

Vertical planes

As has been mentioned, the data gathered from the vertical planes, was very poor. The 3D scan performed on the benchmark part took approximately 6 hours and although it would have been possible to conduct a contour profile, in addition to the 3D scan, it was felt that this defeated the point of evaluating the accuracy of the 3D scanning capability and would not be viable in terms of time. The absolute mean error of the three vertical planes was 154μ, with a standard deviation of 83μ.

Tilted planes

The larger tilted planes had more point representation than the smaller tilted planes, making up the truncated square pyramid. The large error in angularity was as a result of this. The average absolute angle error is around 0.2°, with a standard deviation of 0.12°.

Holes

As holes are made up of vertical planes to determine their properties, these featured were also captured with low accuracy. The absolute mean error was at 80μ, with a standard deviation of 145μ.

Coaxial cylinder

The vertical planes of the coaxial cylinder, as seen in Figure 30, could also only be measured with an absolute mean error of 43μ and a standard deviation of 108μ.

Ellipse

The ellipse was again evaluated in the COSMOS software after importing 8 points. These results were poorly captured with similar results as for the holes and coaxial cylinder.

Spheres, Cones and Cylinders

The six features were fitted with a best fit approach, selecting all the points within each feature and assigning the right primitive to it, the grouping being performed in the same way. The positioning accuracy was at 38μ, the radius accuracy at 61μ, and the angle of the cones was out by 0.021 degrees.

4.3.4   Summary of results

The following table is a summary of the previously mentioned and discussed results of the benchmark part. The 6 quarter features refer to the INNER and OUTER sphere, cylinder and cones. The mean of the 6 quarter features comprises of all the dimensions that define the position and shape of all six features, 18 dimensions in total. The numbers in the brackets for the other features shows the number that makes up the mean. As for the ellipse, the mean is the average of the three repeated measurements and *S* refers to the standard deviation mean of the three repetitive measurements. All the results are in μ, unless indicated in degrees.

Table 3: Summary of measurement of benchmark

	Horizontal planes (7)		Vertical planes (3)		Tilted planes (9)		Holes (3)		Coaxial cylinder (2)		Ellipse (1)		6 quarter features	
	mean	S	mean	S	mean	S	mean	S	mean	S	mean	S	mean	S
CMM	32	8	51	17	0.09°	0.092°	41	5	20	1	5	2	42	68
CimCore	21	35	59	35	0.058°	0.05°	10	16	42	6	15	6	133	73
GOM	46	29	33	22	0.213°	0.1°	166	24	62	43	26	17	72	43
RENISHAW	9	7	154	83	0.201°	0.115°	117	145	42	160	40	138	45	24

4.3.5   Comparison to CMM

The comparison amongst the different hardware alternatives, in terms of accuracy, was evaluated by using only the length dimensions. The nine angular dimensions were not included when calculating the average deviation. The remaining 45 dimensional representations were used as an average to evaluate the final deviation from that of the CAD model. In each alternative, the three worst scores were omitted since in each case, there were clear outliers in the data set. Table 4 shows the scores for all the hardware results. The results are also represented graphically in Figure 31.

Table 4: Deviation error averages

	CMM	CIMCORE ARM	GOM	RENISHAW
avg. dev. to CAD	41µ	57µ	51µ	43µ
avg. dev. to CMM	NA	16µ	10µ	2µ
st. dev.	11µ	41µ	47µ	61µ

The difference between the machined part dimensions (absolute) and CAD data was not investigated in detail, however, an uncertainty of roughly 20µ, can be expected, as was shown in Chapter 3. There are, however, other factors that could influence this difference, for example alignment, transformation, error in file conversion in software, machining or inspection operator uncertainty. The results of the CMM are taken as the base and the other alternative measuring devices are compared in Figure 31. Although the Renishaw has poor evaluation of the components with vertical features, it makes up for it with the geometric components and horizontal features. It is also quite clear that the precision of the CMM is far superior to that of any of the other digitizing hardware. As only three measurements were taken for each feature in order to evaluate a mean, a further investigation was done into the validity of the repeatability of all the devices. The gauge ring, used earlier to evaluate the CMM's uncertainty, was used to evaluate the repeatability of all four of the systems.
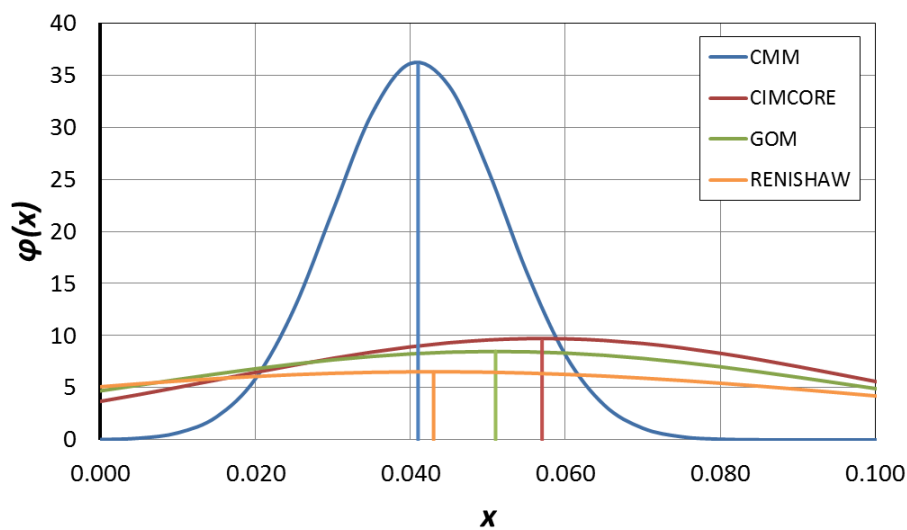
Figure 31: Error distribution and averages of accuracy results

4.4 Repeatability comparison between all digitizers

An analysis of the accuracy can already show a trend of what values can be expected for the repeatability criterion. The measurements included a standard deviation and this gave some indication of the repeatability. A separate exercise was executed to evaluate the repeatability of the different RE hardware. In this test, the flexibility, in terms of what type of features can be captured, is not as important. This test indicated the repeatability of the hardware if numerous objects of the same type needed to be measured. The gauge ring, that was used earlier, was measured 20 times with all four measuring devices. All the circles were computed, using only three points at 120 ° intervals. The study is also able to indicate the accuracy of the device (as the ring is calibrated and traceable @ Ø79.37557mm) under ideal circumstances, however, this is not typical for the variety of features found in production tools. The data from the repeatability exercise can be found in Appendix H.

The circumference was calculated using three points of the ring since the ATOS software only allows for 3 point circle primitive construction. This was to ensure consistency in the results. The CMM measurements were executed automatically and the Arm measurements were taken successively. However, the arm and joint movements are different for every measurement as the device is only manually operational. This already introduces a larger repeatability uncertainty since the z depth of every point is not consistent. In addition, a further component of uncertainty was introduced since the GOM measurements were analysed after four quarter images of the ring were taken and the data aligned to an axis. The Renishaw data was exported to Inventor to draw a 3 point arch and measure the circumference. Uncertainty could thus, also have been introduced by the use of additional software. The comparison of the four results is illustrated in Table 5 and in Figure 32 below.

Table 5: Repeatability results are given by the standard deviation (std.)

	CMM	*ARM*	*GOM*	*RENISHAW*
avg.	79.377	79.384	79.419	79.369
st. dev.	0.001	0.018	0.030	0.007
dev.	0.002	0.009	0.043	-0.007
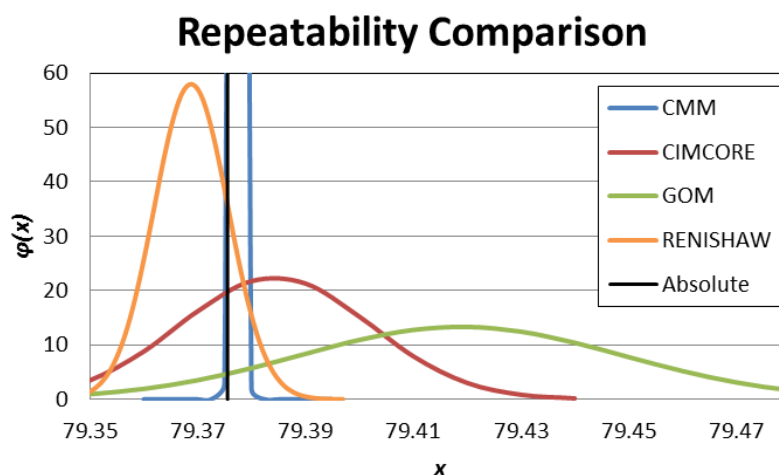
Figure 32: Graphical illustration of repeatability results

4.5   Measuring speed comparison

The measuring speed was only concerned with the speed of the acquisition of the data in order to evaluate the defined geometries in the accuracy section of the benchmark part. A complete CAD model was not generated and did not represent the end time zone for the RE procedure. This is because the capabilities of the hardware were only examined, and not the software as this is beyond the scope of this project. The investigation, performed as part of this study, was done after the accuracy testing and after the operator had familiarised himself with the hardware and software procedures and was aware of potential problems. The acquisition time signified that no technical difficulties were experienced and that absolute effective use of both software and hardware had been made. In other words, the operator had gone through the learning curve. The time results do not necessarily represent the absolute time but can be seen as comparison ratios.

Two out of the four hardware systems were portable and these are assumed to be permanent installations in the laboratory. The set up time for these machines was not investigated and all four devices were completely ready for use after being switched on. As these times are fairly similar for all devices, this step is not measured. The complete time study was broken into four stages: the calibration, transformation, software interaction and physical measurement stages. These are mentioned and discussed for each hardware device. The results of the time study can be seen in Table 6.

Table 6: Speed of measurement results

Time	CMM	ARM	GOM	RENISHAW
Calibration	4:30 min	2:10 min	10:10 min	3:00 min
Transformation	3:10 min	2:50 min	0:30 min	1:40 min
Software interaction	3:50 min	2:50 min	7:10 min	7:10 min
Physical measurement	18:00 min	5:10 min	3:50 min	5:35 hours
TOTAL	29:30 min	13:00 min	21:40 min	5:47 hours

4.5.1   Calibration

The CMM used a sphere of Ø 19.980mm to calibrate the Ø2mm ball probe. This nominal size sphere was measured three times, each sphere being represented by 5 points, in an automated process prior to this, the probe was defined in the probe data management window; the whole calibration took 4:30min.

The Cimcore Arm was calibrated in a similar manner. The nominal size sphere for calibration was a Ø25mm ceramic sphere. The desired probe calibration could only take place after calibrating the reference sphere with a Ø15mm ball probe and each measurement of the reference sphere could have as many point representations as desired. The whole process took 2:10 min.

The GOM took over 10 minutes to calibrate, making this the longest. First, both lenses needed to be adjusted to the right angle, then the right apertures had to be set up with the right focus before the calibration could begin. A special cross with multiple markers was used for the calibration. This cross had two scale bars with coded reference points, which needed to be adjusted to the correct height and angle with multiple scans, as instructed by the software. This procedure took 10:10 min.

The Renishaw was calibrated with machine initialization. This device is calibrated in a method similar to the CMM. The entire process was automated since the hardware needed to scan an Ø5mm calibration sphere three times, taking five points each time. This process took 3:00 min.

4.5.2   Transformation

All four methods defined the origin of the coordinate system after defining a plane, line and point. The plane is indicated by the Z origin, the line defined the X axis and the point the X and Y origin. The only difference between the four methods was that the GOM registration only occurred after the measurement had been taken. Of the four techniques, this process was completed in the shortest time. The times are indicated in Table 6 and range from 30 sec to 3 minutes.

4.5.3   Software interaction

The software interaction is the phase that the operator uses to define the geometries and input the program steps that are needed to execute the entire measurement. The method and software for the GOM and Renishaw are the same, hence the identical times. The user-friendliness of the software, used for the CMM and Cimcore arm, ensured that the time spent on defining parameters was kept to a minimum. In general, all software used to operate the hardware is very user-friendly, easy to learn and flexible in terms of process flow and procedure.

4.5.4   Physical measurement

The actual physical measurement is the process that separated the different methods. The only automated process was that of the Renishaw, however, this took the longest by far. The indicated time of over 5:30hours can also fluctuate considerably. The computer that was used was a Pentium 2 and computing power did slow down the measurement at times. As stated, in the accuracy part for the Renishaw, the benchmark part was measured with two 45 degree grids, each with a step over distance of 0.5mm and a nominal pitch of 0.1mm. It would, however, be possible to almost halve the time if only one of the 45 degree scans was used. This would not present considerable accuracy differences but a scan of 2:30 hours would still be much more time consuming than any other method. The second slowest time is that of the CMM, with 18 min. It should be noted, that this is the time taken for only one measurement. If, on the other hand, a benchmark part needed to be measured multiple times, then this time would be faster and the CMM the only device that would allow for automated scanning. The other factor that should be mentioned is that the method with the fastest time, the arm, is not capable of capturing the freeform NURB surface. Conversely, the GOM is capable, with additional software operations, to execute a complete Reverse Engineering CAD file. Capabilities like these, and others, are mentioned and some are quantified in section 4.7 under user-friendliness.

4.6   Work envelope comparison

This criterion was evaluated using the literature as well as tested for its validity. The work volume of the Cimcore arm was not found in any material supplied by the manufacturer. The Arm's rotating section is able to capture a spherical work volume with a radius of 960mm. The spherical work volume had a cylindrical void area of about Ø150mmx450mm starting from the centre point of the sphere. The GOM had a calibrated work volume of 485x389x389, however, the manufacturer stated that a work volume of 2-3 times that size would be allowed. Nonetheless, the following guidelines should be adhered to: each individual scan should capture at least four identical markers and overlap the previous scan by 30-40% in size. The following table summarises the different work volumes.

Table 7: Work Volume (mm^3)

CMM	ARM	GOM	RENISHAW
700x1000x500mm	*sphere radius of 960mm*	*485x389x389mm exceeded to 1455x1167x1167mm with overlapping*	*600x500x400mm*

4.7   User-friendliness

During the investigations of the criteria, several other findings were made in terms of the capabilities of the different techniques. These are mentioned in this section; however, no technical evaluation to quantify the criteria was done. The results are subjective, but they are nonetheless useful for the evaluation tool that is introduced in the following chapter. The star rating is used to indicate the quality of the capability, * being of a very low quality and ***** being of the best. The summary can be seen in Table 8. For measuring holes, the contact scanners perform better than the non-contact scanners (GOM). The scores, obtained from the scanning of the vertical walls, represent the findings of the accuracy study. In terms of the freeform shapes, the GOM scores higher than the Renishaw, because it is easier to use. The CMM and Arm are currently not ideal for capturing free forms. The only negative of the surface limitation, is that the GOM needs the right surface reflection to capture the object, a white powder is thus often applied to the object, prior to scanning. The other three alternatives are contact-based scanners. Here the surface texture, colour or reflective properties are not important however deformable objects on probe impact cannot be measured accurately.

Table 8: Other criterions

	Holes	Vertical Walls	Freeform surfaces	Surface limitations	Mobility
CMM	*****	*****	**	****	NA
ARM	****	****	*	****	*****
GOM	**	****	*****	**	****
RENISHAW	***	*	***	***	NA

5   Application of an Evaluation Tool

One of the objectives of the study was to implement an evaluation tool that helps a potential user of digitizing hardware to make a decision. This section incorporates the findings of the experiments with a decision making approach. The criteria have been quantified and are thus not intangible; however, additional criteria may be added, even if they are of a subjective nature. The decision making method or tool, gleaned from literature, which is applied in this project, is the Analytic Hierarchy Process (AHP) [**36**].

5.1   The analytic hierarchy process

5.1.1   Method description

The Analytical Hierarchy Process is a structured technique developed by Thomas L. Saaty in the 1970s but has been broadly studied and since then refined. It has also been implemented in various settings, one such example is that of British Airways which used the AHP method to choose the entertainment system for its entire fleet of airlines [**37**]. The technique has also been implemented for decision making in government, business, industry, healthcare and education systems. The AHP helps the decision maker to find a solution that best aids an understanding of the problem. This method provides a more structured approach in determining the scores and weights, as opposed to the method described in Chapter 2, a simple weighted multicriteria scoring model [**36**]. The hierarchy starts with the problem or objective of the task at hand. In this case the objective is 'Choosing the Appropriate Digitizing Hardware'. The hierarchy then branches off into the different criteria, in this case these are:

- Accuracy
- Repeatability
- Speed
- Work Envelope
- User-friendliness.

The different criteria can be tangible or intangible, carefully measured or roughly estimated, well- or poorly understood; they can thus be anything the decision maker feels will influence the objective. As a result, the addition of intangible criteria to the hierarchy can easily be included. Some are listed as an example.

- Commercial/Technical support
- Flexibility
- Shape complexity
- Learning difficulty
- Technology stigma
- Edge detection (or any criterion not quantified yet)

In essence human judgement, and not just fully quantified underlying information, can be used to execute the AHP. This distinguishes the AHP from other decision making techniques. One of the criteria may be very subjective, for example the 'trendiness' of the product.

The sub-sections or criteria are analysed and investigated individually, after they have been evaluated. It might be that certain sub-sections have to be broken up into smaller more understandable functions. For example user-friendliness can be broken up into smaller or different sub-sections that define the user-friendliness of the specific objective. From the different sub-sections or criteria the hierarchy branches into the different alternatives (Figure 33). In this study the alternatives are:

- Mytotoyo CMM
- Renishaw Cyclone
- ATOS GOM
- CIMCORE Arm
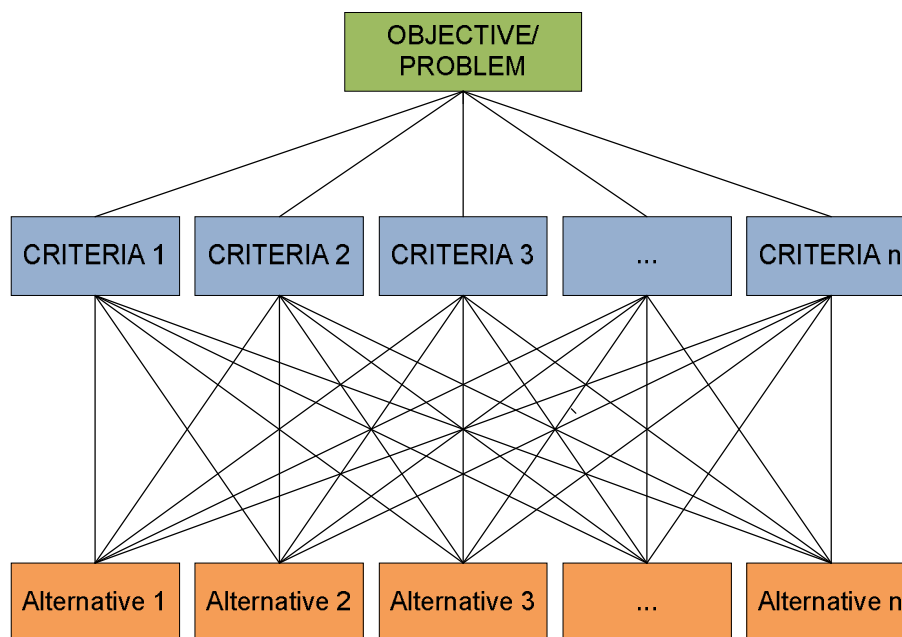
Figure 33: Analytic Hierarchy Process Flowchart

Once the hierarchy is built, the decision maker systematically evaluates each alternative, in respect of their impact on an element above them, in the hierarchy. This stage is called the pairwise comparison. After evaluating the comparison, normalising the comparison and checking for consistency, the different criteria are weighted. Each of these stages will be discussed below. In the final step the process calculates a numerical priority and assigns it to each of the alternatives. The value represents its ability to achieve the decision objective or answer to the problem, therefore a straightforward course of action can be taken.

Cost is often emitted in the first iteration of an AHP, as the benefits of all alternatives should be evaluated. The decision maker, possibly the financial sign-off division, at times, is not the same as the person executing the AHP and thus the equipment cost could overshadow all the other criteria, thus nullifying the entire exercise. A completely technical evaluation needs to be executed, before looking at the objectives from a purely economical perspective.

There are several firms which supply computing software to assist in the use of an AHP, however, the technique is straightforward and does not use immense computing power. Excel was used in this study. The AHP is executed as per definition and a sample calculation is exhibited in Appendix I [**36**].

5.1.2   Pairwise comparison

The first step, after evaluating the hierarchy, is to create a pairwise comparison matrix for each alternative on each criterion [**36**]. The following procedures need to be executed in terms of all the criteria individually. Let *n* be the number of alternatives in the hierarchy; a matrix of *n*x*n* is then created for each criterion. The values shown in Table 9 denote the extent to which the decision maker assigns a value to which alternative *i* is preferred to alternative *j,* where P_{ij} is an entry into the matrix. For example if the decision maker believes, or from a scaled deduction assigns, the value 5 to the matrix entry P_{ij} strong preference is given to alternative *i* when compared to alternative *j* within that criteria. The value of P_{ji} is the reciprocal of P_{ij} so the general rule is:

$$P_{ji} = \frac{1}{P_{ij}}$$

(11)

Table 9: Scale of pairwise comparisons in AHP

Value	*Definition*
1	Equally preferred
2	Equally to moderately preferred
3	Moderately preferred
4	Moderately to strongly preferred
5	Strongly preferred
6	Strongly to very strongly preferred
7	Very strongly preferred
8	Very strongly to extremely preferred
9	Extremely preferred

The value 1 is entered along the diagonal of each matrix as comparing one alternative to itself is equally preferred because they are the same (Table 9). All entries of all criteria matrixes are completed this way.

5.1.3   Normalising the comparison

Once each pairwise comparison matrix for all criteria is completed, the matrixes are normalised. In statistics, normalization refers to the division of multiple sets of data by a common variable, to eliminate that variable's effect on the data. It is thus possible to compare different underlying data, as it allows data on different scales, by bringing them on a common scale. This is in the form of a ratio comparison, rather than interval measurements between them. To normalise the pairwise comparison matrix, each entry is divided by its column sum. The normalised matrix is then used as the scores for each alternative on the criterion under consideration, after adding each alternative's row to make up its total score. The scores indicate the relative desirability of each alternative to one another in respect of the specific criterion.

5.1.4 Consistency

The values initially assigned to the pairwise comparison matrix should be consistent in its preference rating. For example if there are alternatives X, Y and Z, the decision maker prefers criteria 1 of X to that of Y, and strongly prefers the same criterion of Y to that of Z, it would be inconsistent for the decision maker to make alternative X equal to Z for criteria 1. Therefore before using the normalized comparison matrix it should be checked for its consistency. The consistency measure is done for each alternative. Here the numerator in each of these calculations multiplies the normalized matrix's score with the corresponding original pairwise comparison matrix and then the sum is taken of each row. The denominator is simply the score of the alternative, from the normalized matrix. The consistency measure index is equal to the number of alternatives, if the decision maker is perfectly consistent in the decision making, this is, however, practically difficult to achieve. If the inconsistency is not excessive, the scores obtained from the normalized matrix will be reasonably accurate. To determine if there is excessive inconsistencies the following quantities need to be calculated:

$$Consistency\ Index\ (CI)\ = \frac{\lambda - n}{n - 1}$$ (12)

$$Consistency\ Ratio\ (CR)\ = \frac{CI}{RI}$$ (13)

where:

  λ = the average consistency measure for all alternatives
  n = the number of alternatives
  RI = the appropriate random index from Table 10

If the pairwise comparison matrix is perfectly consistent, then λ=*n* and the consistency ratio will be 0. The values of *RI* in Table 10 give the average value of *CI,* if all the entries of the comparison matrix are chosen at random, the diagonal entries are equal to 1 and Equation (11) is implemented. The rule is that if the consistency ratio is smaller than 0.1 then the degree of consistency in the pairwise comparison matrix is satisfactory. However if CI>0.1 the AHP might not yield meaningful results.

Table 10: Values for RI for use in AHP

n	*RI*
2	0.00
3	0.58
4	0.90
5	1.12
6	1.24
7	1.32
8	1.41
9	1.45
10	1.51

Once the decision maker arrives at this stage the same process must be repeated for all the other criteria that were identified in the hierarchy tree.

5.1.5   Obtaining criterion weights

At this stage the decision maker should have a consistent and normalised matrix for each criterion. These matrixes indicate relatively how one alternative compares to another. The next step is to evaluate the weights assigned to each criterion which indicate the relative importance of each criterion to the decision maker. The same method, which is used for the pairwise comparison matrix, is used that is, normalizing it and checking it for consistencies. By this time, values assigned to the alternative comparison were quantified in a scientific manner, before adapting or adjusting them to the AHP scale. The weights on the other hand are more intangible values and thus the decision maker needs some sort of understanding of the entire problem or objective. The same scaling is used for the weights criterion.

5.1.6   Results and discussion

After acquiring the comparison and weighted matrixes, the decision problem can be fully analysed, using a scoring model. The last step in the AHP is to calculate the weighted average scores for each decision alternative. The result will immediately rank the alternatives in terms of one another, as the total sum of all the weighted average scores ads up to unity.

5.2   Evaluation tool implementation example

As indicated above, the first step is to create a pairwise comparison matrix for each criterion, including all alternatives. As the criteria have been quantified, the pairwise comparison for each case study will be the same. The only input which changes is the criterion weights. The results of the accuracy are in the following order:

1. CMM   base
2. Renishaw   Δ2μ
3. GOM   Δ10μ
4. Arm   Δ16μ

The pairwise comparison for the accuracy criterion is made up of the above (Figure 34). The grey area shows the values assigned as the inputs to the matrix. These values are scaled to the quantified values obtained from the measurement, all other values are defined as explained. The matrix is normalised and the sores are averaged for each alternative. The consistency ratio is worked out to be 0.035 which is lower than 0.1 and therefore makes the consistency in the pairwise comparison matrix acceptable. The accuracy scores can be seen in column G, in orange, in Figure 34. These scores are also obtained for the other remaining three criteria and are presented in Appendix I. The different criteria scores are summarised in Table 11. As explained, the criteria of the pairwise comparison do not change for any task, as they have been quantified by this study. The inputs that change are the criteria weights assigned to each criterion. An example is set out to illustrate the algorithm.

Figure 34: AHP example calculation

Table 11: Pairwise comparison scores of different criteria

	Accuracy	Repeatability	Speed	Work Envelope	User-friendliness
CMM	0.520	0.525	0.165	0.094	0.165
ARM	0.044	0.120	0.506	0.629	0.506
GOM	0.094	0.052	0.289	0.218	0.289
RENISHAW	0.342	0.304	0.040	0.059	0.040

The example that will determine the weights is a hypothetical scenario that is often found in the blow moulding industry. This example is chosen due to the fact that the benchmark is designed to imitate typical features, found in tools for manufacturing. The example is a blow-mould tool that includes four cavities (Figure 35). The tool needs to be reverse engineered, when a new mould, with more cavities needs to be manufactured or the tool is worn and needs to be replicated and no current CAD data exist. The assumption is made that a part similar to this needs to be RE. The weights are as follows: The accuracy is fairly important as the bottle needs to be replicated to fit the production line and tool-making is regarded as a fine tuned profession. The repeatability is also important as there are four cavities and the repeatability should not include avoidable uncertainty.

Note that one cavity may also be reverse engineered and then copied along three equi-spaced axes. If using this RE strategy, repeatability is not that important. Speed is always important however, due to the fact that the quantified results all fall within a day, in this case the speed of measurement is not important. The work envelope is also not important, as all alternatives accommodate this work volume. The user friendliness is rather important as there are freeform shapes within the cavity itself and holes are present in any tool. The criterion weights can be seen in orange in Figure 36 and the evaluation of them is shown in Appendix I.

Figure 35: Four cavity Blow mould tools for a bottle

Final AHP Scoring Model

Criterion	CMM	ARM	GOM	RENISHAW	Criterion Weights
Accuracy	0.520	0.044	0.094	0.342	0.457
Repeatability	0.525	0.120	0.052	0.304	0.240
Speed	0.165	0.506	0.289	0.040	0.081
Work Envelope	0.094	0.629	0.218	0.059	0.042
User-friendliness	0.165	0.506	0.289	0.040	0.180
SCORE	0.411	0.207	0.140	0.242	1.000

Key Cell Formulas		
Cell	Formula	Copied to
C11	=SUMPRODUCT(C6:C10,$H$6:$H$10)	D11:F11

Figure 36: Final scoring model including outcomes

The AHP model evaluated that the CMM is the most suitable hardware for the task. The next best hardware is the RENISHAW, followed closely by the ARM and lastly by the GOM. An economical investigation can be executed now that the technical performance, or so called capability profile, has been defined, if acquisition of the hardware still needs to be done.

The model does not account for a few scenarios and has a few shortcomings. If an object needs to be scanned and the work envelope of one or more of the hardware does not accommodate the size, a score is still assigned to that alternative. That alternative however should be thrown out completely. Furthermore, if an object consists of almost completely free-form shapes and the accuracy does not need to be within a 100th of a mm, then in almost all cases the GOM is used. The user-friendliness includes free-form shapes; however, this criterion could possibly be a criterion by itself, although this can easily be changed. Another possibility is to create two models, one for mechanical shapes, and one for freeform shapes. This is for example a function within the REX software extension. The user states if the model includes mechanical features (edges, classical geometries, holes, etc) or if the model includes mostly 'softer', freeform surfaces. The main shortcoming of the model is that it is not practically validated. The model is assumed to be accepted, because it is well defined, widely accepted and originates in literature. The inputs that are used for the model are validated, as the CMM is traceable and its uncertainty was evaluated. Combining these two, the model and the input, it is assumed that the output is acceptable and validated.

6   Acquiring new hardware

The study considered an evaluation tool that helps the decision maker to choose the appropriate hardware for a specific task, with the assumption that all devices have already been acquired. The following is a step-by-step procedure for a decision maker wanting to acquire digitizing hardware. The majority of this information is common sense; however, it is still useful for potential end users. It is a procedure that looks at the requirement profile of the task at hand and tries to balance it with the capability profile of potential digitizers.
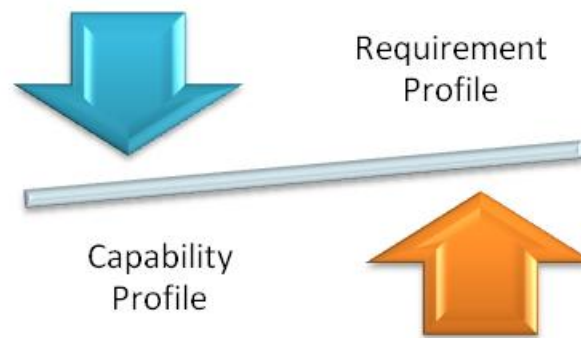
Figure 37: Balancing of requirement vs. capability profiles

- The decision maker should familiarise him-/ herself with the different technologies available in industry. A good start is to have a look at the Wohlers report table that lists all major commercial companies that offer such products. The websites of the different companies are listed and it is a good idea to start communicating with them. It is a sound plan to then make contact with a representative of the company, in the decision maker's country, and arrange for a demonstration. The larger companies will most of the time have trained salesmen assigned for these types of consultations.

- A clear specification sheet should be drawn up prior to this visit. The decision maker needs to carefully decide which capabilities of the hardware are desired. In other words, the capabilities of the hardware need to be decided on. For example, how accurate does the hardware need to be or does the device call for mobility? This is often not clearly thought out by the decision maker and the salesman could aid in this thought process, after hearing a description of the problem.

- If possible, the salesperson should be asked to reverse engineer the desired object, in order to evaluate the ease of the use of the machinery. If intellectual property is at stake it might be a good decision to design a benchmark part that best represents the actual object. In this study the benchmark part represented a typical production tool (mould). This can be done to various suppliers of digitizing equipment in the decision maker's area. It should be noted that the salesperson is trying to sell a product, so all information gathered should be verified and compared to other technology. The different visits may also bring up the types of questions which are important to ask in the RE industry. One example is how the accuracy of a device is evaluated and guaranteed.

- The decision maker will have a better understanding of the important criterion and will be exposed to different alternatives. Once this is known and the decision maker has confidence

in his understanding of the objective an Analytic Hierarchy Process may be executed. As stated above, the model is designed to work at whatever level the decision maker is at, in fully understanding the problem.

- Once this has been done the decision maker is able to align the available hardware with the budget available. This is conducted afterwards, because if price is included in the criteria of the AHP it may prevent the correct hardware from being chosen. As RE equipment is expensive, it would be senseless to spend a huge amount of money on an alternative which is cheaper than the alternative with the right criteria profile.

7   Conclusion

The study has identified a number of characteristics (accuracy, repeatability, measuring speed, work envelope and user-friendliness), which together define the capability profile of the four RE hardware systems available for the study.

A benchmark part was modified and manufactured, along with a measuring procedure that allows a comparison between the different hardware. The uncertainty for the measuring procedure was established to be 20µ for the CMM. The uncertainty analysis and procedure is adapted [**8**], to quantify the measurement uncertainty. It has been recognized that the uncertainty of the measurements is higher, than the value given by the certified uncertainty, from the calibration certificate. Other capability conclusions from the study are as follows:

- Measuring features with the CMM, using an automated process, gives better results than when individual points are manually measured.
- The 5 axis CNC machine has possibly a higher uncertainty than 10µ, as the average deviation from the CMM is at 41µ.
- The CMM is the most accurate device available, followed by the Renishaw, GOM and then ARM.
- The hardware with the highest repeatability is again the CMM followed by the Renishaw, ARM then GOM.
- The measuring speed of the Arm is the fastest followed by the GOM and CMM. The Renishaw is by far the slowest, when reverse engineering the benchmark.
- The largest work envelope belongs to the ARM followed by the GOM, CMM and Renishaw.
- The most user friendly hardware as defined in this study is the ARM followed by the GOM, CMM and then Renishaw.

The results of the study have succeeded in scientifically quantifying certain criteria that make up the capability profile of certain hardware technologies. It is however an ongoing endeavour to define capability profiles of RE techniques. This includes adding different hardware or including a RE software capability profile for the different packages available. As suggested a capability profile can be divided into two divisions: analytical surfaces and free-form surfaces.

As the results of the CMM capability in accuracy and repeatability were very high, although they were lower for the user friendliness and speed of measurement, it is suggested that the use of a laser scanner, used along with the CMM, should be investigated. Prior to the study the acquisition of a laser scanner for the ARM was suggested but it should rather be included in the CMM, as the accuracy for the ARM is already poor. Including a laser scanner will increase the user-friendliness and speed of the CMM, giving it high scores for all the defined criteria.

Bibliography

[1] K. Schreve, *Reverse Engineering Class Notes.* University of Stellenbosch: Unpublished Document, 2005.

[2] T.T. Wohlers, *Wohlers Report 2007*, Additive Manufacturing: State of the Industry, Annual Worldwide Progress Report, Wohlers Associates Inc., Fort Collins, CO, 2007.

[3] T. Varady, R.R. Martin and J. Coxt, *Reverse engineering of geometric models- an introduction, Computer-Aided Design*, pp. Vol.29, No.a, p.255-268, 1997.

[4] V. Raja and K. J. Fernandes, *Reverse Engineering - An Industrial Perspective.* London: Springer-Verlag , 2010.

[5] E. Savio, L. De Chiffre, and R. Schmitt, *Metrology of freeform shaped parts*, Annals of the CIRP Vol. 56(2), pp. 810-835, 2007.

[6] A. A. Baker et al., *An affordable methodology for replacing metallic aircraft panels with advanced composites*, Elsevier-Composites: Part A 33, pp. 687-696, 2002.

[7] Dong-Jin Yoo, *Three-dimensional surface reconstruction of human bone using a B-spline based interpolation approach* , Computer-Aided Design, Volume 43, Issue 8, pp. 934-947, 2011.

[8] B. R. Barbero and E. S. Ureta, *Comparative study of different digitization techniques and their accuracy*, Computer-Aided Design, 43 (2), pp. 188-206, 2011.

[9] Z.M. Bi and L. Wang, *Advances in 3D data acquisition and processing for industrial applications*, Robotics and Computer-Integrated Manufacturing, vol. 26, pp. 403-413, 2010.

[10] InnovMetric Software Inc., *3D Metrology Hardware Review*, 2010.

[11] G.T. Reid, R.C. Rixon, and H. Steward, *Moiré topography with large contour intervals*, Proc.SPIE, pp. 814:307-313, 1998.

[12] Nikon. (2011) Nikon Metrology. [Online]. www.nikonmetrology.com/

[13] Toshiba. (2002) [Online]. www.toshiba-itc.com/cat/en

[14] A. Weckenmann and M. Knauer, *The Influence of Measurement Strategy on the Uncertainty of CMM-Measurements*, Annals of the CIRP, Vol47, No.1, pp. 451-454, 1998.

[15] S. Martı´nez, E.Cuesta, J.Barreiro, and B.A´ lvarez, *Methodology for comparison of laser digitizing versus contact systems in dimensional control*, Optics and Lasers in Engineering, vol. 48, pp. 1238-1246, 2010.

[16] GOM, *ATOS v6 User Manual*, Braunschweig, 2007.

[17] Y. Jun, *A piecewise hole filling algorithm in reverse engineering*, Computer-Aided Design 37, pp. 263–270, 2005.

[18] T.T. Wohlers, *Wohlers Report 2011, Additive Manufacturing: State of the Industry*, Annual Worldwide Progress Report, Wohlers Associates Inc., Fort Collins, CO, 2011

[19] Z. Terék and T. Várady, *Digital shape reconstruction*, Third Hungarian Conference on Computer Graphics and Geometry, Budapest, 2005.

[20] T. Varady, M.A. Facello and Z. Terek, A*utomatic extraction of surface structures in digital shape reconstruction,* Computer-Aided Design, vol. 39, pp. 379-388, 2007.

[21] S. Hsiao and J. Chuang, *A reverse engineering based approach for product form design*, Elsevier Science Ltd. - Design Studies 24, pp. 155-171, 2003.

[22] Y. Ke et al., *Feature-based reverse modeling strategies*, Computer-Aided Design, vol. 38, pp. 485-506, 2006.

[23] M. Chang and S.C. Park, *Reverse engineering of a symmetric object*, Computers & Industrial Engineering, vol. 55, pp. 311-320, 2008.

[24] X. Ye, H. Liu, L. Chen, Z. Chen, X.Pan and S. Zhang, *Reverse innovative design—an integrated product design methodology,* Computer-Aided Design, vol. 40, pp. 812-827, 2008.

[25] L. Luliano, P. Minetola, and Alessandro Salmi, *Proposal of an innovative benchmark for comparison of the performance of contactless digitizers*, Measurement Science and Technology, pp. 1-13, 2010.

[26] J. Wirandi and A. Lauber, *Uncertainty and traceable calibration - how modern measurement concepts improve product quality in process industry*, Measuremen, 39(7), pp. 612-620, 2006.

[27] N. De Beer, *An Investigation towards developing capability profiles of rapid prototyping technologies with the focus on 3D-printing*, MScEng Thesis, University of Stellenbosch, Stellenbosch, 2004.

[28] D. Dimitrov, W. van Wijck, K. Schreve, N. de Beer, A*n Investigation of the Capability Profile of the Three Dimensional Printing Process with an Emphasis on the Achievable Accuracy*, Annals of the CIRP Vol.52/01, pp. 189-192, 2003.

[29] P. De Bièvre, *Accuracy versus Uncertainty*, Accreditation and Quality Assurance: Journal for Quality, Comparability and Reliability in Chemical Measurement, 10 (12), pp. 645-646, 2006.

[30] ISO/IEC Guide 98-3:, *Uncertainty of Measurement-part 3: guide to the expression of uncertainty in measurements (GUM:1995)*, 2008.

[31] ISO 14253-2:2011(E), *Guidence for the estimation of uncertainty in GPS measurement, in calibration of measuring equipment and in product verification*, 2011.

[32] R. S. Figliola and D. E. Beasley, *Theory and design for mechanical measurements.* USA: John Wiley & Sons, Inc, 2006.

[33] ISO/TS 15530-3: , *Geometric product specificatios (GPS) - coordinate measuring machines (CMM): Techniques for determining the uncertainty of measurement-part 3: use of calibrated workpieces or standards*, 2004(E).

[34] L. Hall, *Traceability & Calibration of an Articulated Arm Coordinate Measuring Machine*, BEng final year project, Stellenbosch, 2009.

[35] L. Luliano and P. Minetola, *Enhancing moulds manufacturing by means of reverse engineering*, Int. J. Adv. Manuf. Technol. 43, pp. 551-562, 2009.

[36] C. T. Ragsdale, *Spreadsheet Modeling and Decision Analysis.* Ohio, USA: South-Western College Publishing, 1998.

[37] T. L. Saaty, *Decision making with the analytic hierarchy process*, Int. J. Services Sciences, Vol. 1, No. 1, pp. 83-98, 2008.

Appendix

Appendix A – 3D scanning systems (Wohlers Report 2011)

Wohlers Report 2011

Appendix G: 3D scanning systems

Appendix G: 3D scanning systems

The following table lists 3D scanning and digitizing (CMM, touch probe, and other) systems from around the world. All company information and product specification data is subject to change. Please refer to the company websites for additional information. The company websites were live as of March 2011. Visit wohlersassociates.com for a list of companies that offer 3D scanning and scan data processing services.

The following abbreviations are used in the table.

acc	accuracy	H	height
acq	acquisition	horiz	horizontal
approx	approximately	lp	line pairs
CMM	coordinate measuring machine	lp/mm	line pairs per mm (image sharpness)
config	configuration	m	meter
CT	computed tomography	max	maximum
d	depth	meas	measure, measuring
DOF	depth of field	min	minimum or minutes (speed column)
DOV	depth of view	min/scan	minutes/scan
dia	diameter	mm	millimeter
diag	diagonal	ms	millisecond (1/1000 second)
dist	distance	msec	millisecond (1/1000 second)
dpi	dots per inch (resolution)	mult	multiple
ext	extended	n/a	not applicable, not available
feat	feature	nom	nominal
ft	feet	obj	object
FOV	field of view	pos	position

pts	points
pts/s	point per second
res	resolution
rot	rotation(al)
sec	second(s)
sec/scan	seconds/scan
SO	stand off distance
std	standard
TOF	time of flight
uncal	uncalibrated
μ	micron (10^{-6} m)
μm	micrometer (10^{-6} m)
vert	vertical
vol	volume
w/	with
W	width

Company	Product	Technology	Work volume	Accuracy[1]	Speed
Automated Precision, Inc. Rockville, MD apisensor.com	Axxis6 Arm	articulating CMM arm	2600-3200 mm diameter	0.06 – 0.09 mm	n/a
	Axxis7 with AxxisScan	articulating CMM arm & scanner	2600 mm diameter	0.09 mm	39,000 pts/s
Artec Palo Alto, CA artec3d.com	Artec L	structured light triangulation	0.8 – 1.6 m DOF	0.2 mm	500,000 pts/s
	Artec MHT		0.4 – 1.0 m DOF	0.1 mm	500,000 pts/s
	Artec M		0.4 – 1.0 m DOF	0.1 mm	500,000 pts/s
	Artec MH		0.4 – 1.0 m DOF	0.1 mm	500,000 pts/s
	Artec S		0.15 – 0.25 m DOF	0.05 mm	500,000 pts/s
Breuckmann Meersburg, Germany breuckmann.com	stereoSCAN[25]	Miniaturized Projection Technique (structured light triangulation)	75–750 mm FOV @ 360–880 mm dist	min depth res 2 μm	<1 s/frame
	optoTOP-HE, optoTOP-SE		50–800 mm FOV mm diag	min depth res 2 μm	<1 s/frame
	optoSCAN, (HE-100, HE-200)		HE-100: 80 x 60 mm, HE-200: 160 x 120 mm	feat acc ±10–15 μm	approx 1 s/frame
	μikroTOP-zoom		continuous between 8 x 11 and 33 x 24 mm	depth res better than 2 μm	approx 300–400 msec
	dermaTOP-blue		[mm] 20 x 15 x 6d, 40 x 30 x 20d and 60 x 60 x 40d	depth res 2, 4 and 8 μm	approx 300–400 msec
	faceSCAN-II		field: 600 x 460 mm @170°, depth 340 mm	feat acc ± 200 μm	acq time 0.9 sec
	faceSCAN-III		field: 600 x 460 mm @160°, depth 400 mm	feat acc ± 200 μm	acq time 0.8 sec
	bodySCAN		1200 x 800 x 2000 mm high	feat acc ± 250 μm	acq time 2.5 sec
	triTOS		[mm] 100 to 700, 60 to 900, 400 to 1700	± 15 μm, ± 30 μm, ± 60 μm	980 ms

1

WOHLERS ASSOCIATES, INC.

Wohlers Report 2011   Appendix G: 3D scanning systems

Company	Product	Technology	Work volume	Accuracy[1]	Speed
Capture Geometry Internally CGI Eden Prairie, MN, USA cgiinspection.com	CSS-300 CSS-1000 CSS-3000	Cross Sectional Scanning Cross Sectional Scanning Cross Sectional Scanning (destructive imaging)	7 x 5 x 9 in 12 x 10.5 x 8 in 14 x 16 x 15 in	repeatability ± 0.0005 in	n/a (automated milling of layers and imaging technique)
CogniTens (A Division of Hexagon Metrology) Ramat Hasharon, Israel cognitens.com	WLS400M/A	structured light triangulation	H x W x D [mm] 500 x 500 x 230	n/a	n/a
Creaform 3D Levis, Quebec, Canada creaform3d.com	REVscan EXAscan VIUScan MAXscan ERGOscan UNIscan Cyclops Gemini MegaCapturor	self-positioning laser triangulation self-positioning laser triangulation self-positioning laser triangulation self-positioning laser triangulation self-positioning laser triangulation self-positioning laser triangulation structured white light structured white light structured white light	50–1000 mm range (portable) 50–1000 mm range (portable) 50–1000 mm range (portable) 50–1000 mm range (portable) 50–1000 mm range (portable) 50–1000 mm range (portable) 680 x 510 x 400 mm 690 x 520 x 650 mm 1530 x 2020 x 1800 mm	± 0.05 mm ± 0.04 mm ± 0.05 mm ± 0.05 mm ± 0.05 mm ± 0.08 mm n/a n/a n/a	18,000 pts/s 25,000 pts/s 18,000 pts/s 18,000 pts/s 18,000 pts/s 18,000 pts/s 800,000 pts/s 800,000 pts/s 1,900,000 pts/s
Cyberware Monterey, CA, USA cyberware.com	Whole Body X 3D Scanner Head & Face Color 3D Scanner	laser stripe triangulation laser stripe triangulation	whole body scanning head scanning	n/a n/a	60,000 pts/s 30,000 pts/s
DataPixel Bilbao, Spain datapixel.com	OptiScan 1015L OptiScan 1040L OptiScan 2040L OptiScan 2080L	laser line scanner laser line scanner laser line scanner laser line scanner	SO 100 mm, DOV 10 mm, FOV 15 mm SO 100 mm, DOV 40 mm, FOV 40 mm SO 200 mm, DOV 40 mm, FOV 40 mm SO 200 mm, DOV 4060 mm, FOV 80 mm	± 0.006 mm ± 0.010 mm ± 0.025 mm ± 0.050 mm	60,000 pts/s 60,000 pts/s 60,000 pts/s 60,000 pts/s
Ecs Systems Inc. Vancouver, BC, Canada photomodeler.com	PhotoModeler	uses multiple images to create 3D geometry (photogrammetry)	n/a	n/a	Camera lens shutter speed dependent
Faro Technologies Lake Mary, FL, USA faro.com	Gage FaroArm (series) ScanArm ION Laser Tracker Focus Scanner	touch probe / gage 6-, 7-axis articulated arms 7-axis arm with laser scanner, ultra-precise laser beam, TOF phase-shift	1200 mm sphere varies based on scan arm varies based on scan arm horiz ± 270, vert +75 to -50, max range 110 m dia 20 – 120 m range (varies based on model)	0.010/500–0.020/500 mm 0.0005 in 2σ: 50µ 0.049 mm at 10 m ± 2 mm at 10 m and 25 m	varies varies 19,200 pts/second angular velocity 180°/s 976,00 pts/s
Geodetic Systems Melbourne, FL, USA geodetic.com	V-STARS E4X V-STARS S8 (INCA3) V-STARS M8	photogrammetry photogrammetry photogrammetry	67" x 47" FOV 77" x 56" FOV varies	8 µm + 8 µm per m 5 µm + 5 µm per m n/a	n/a 4–5 sec / shot (typical) n/a
GOM Braunschweig, Germany gom.com	ATOS I ATOS I 2M ATOS II Triple Scan ATOS III Triple Scan TRITOP Std/HR	structured white light (fringe) structured white light (fringe) structured white light (fringe) structured white light (fringe) optical photogrammetry	40 x 30 – 1000 x 800 mm 55 x 44 – 500 x 400 mm 38 x 29 – 1500 x 1130 mm 38 x 29 – 2000 x 1500 mm 0.1–20 m (and over)	n/a n/a n/a n/a 0.02 mm per 1 m of obj size	1 m pts / 7 seconds 2 m pts / 7 seconds 5 m pts / 7 seconds 8 m pts / 7 seconds 6–12 m pts/scan
Konica Minolta Ramsey, NJ, USA konicaminolta.com	VIVID 9i VIVD 910 Range7 Scanner Range5 Scanner	laser range finder laser range finder laser range finder laser range finder	198 x 69 x 26 mm – 1495 x 1121 x 1750 mm 111 x 83 x 40 mm – 1196 x 897 x 800 mm 79 x 99 x 54 mm – 267 x 334 x 194 mm 150 x 188 x 109 mm – 267 x 334 x 194 mm	± 0.05 mm ± 0.05 mm ± 0.04 mm ± 0.08 mm	2.5 sec/scan 0.3–2.5 sec/scan 2.0 sec/scan 2.0 sec/scan
Kreon Technologies Limoges, France kreon3d.com	Zephyr K2 25 Zephyr K2 50 Zephyr K2 100 Aquilon Solano	laser line scanner laser line scanner laser line scanner laser line scanner laser line scanner	varies by implementation varies by implementation varies by implementation varies by implementation varies by implementation	3 µm 6 µm 12 µm 5 µm 50 µm	30,000 pts/s 30,000 pts/s 30,000 pts/s 1,000,000 pts/s 40,000 pts/s

Wohlers Report 2011

Appendix G: 3D scanning systems

Company	Product	Technology	Work volume	Accuracy[1]	Speed
LDI Minneapolis, MN, USA laserdesign.com	AM-3R CS – Series DM – Series DT – Series PS – Series DS – Series FA – Series	laser line continuous laser line manual laser line laser line scattered light continuous laser line arm-mounted laser line	100 x 100 x 50 mm up to 1005 mm range 400 x 500 x 350 mm 200 mm line length 300–900 mm depth varies by implementation varies based on scan arm	±20 µm 3.0 µm + 3.5 L 4.5 µm + L/150 µm ±0.1 mm ±20 µm at 300 mm .015–.034 mm .25–.127 µm	14,400 pts/s 14,400 pts/s 14,400 pts/s 50,000 pts/s 7.5 frames/sec 14,400 pts/s 48,000 pts/s
Leica Geosystems AG (of Hexagon Metrology) Heerbrugg, Switzerland leica-geosystems.com	Tracker (many models) T-Scan T-Probe II HDS 3000 HDS 6000	TOF portable CMM, laser beam portable CMM, touch probe TOF phase-shift	80 m range (varies by model) 30 m 30 m vert 270° x horiz 360°, 100 m range vert 310° x horiz 360°, 10 m or 50 m range	25 µm 50 µm for <8.5 m (2σ) 60 µm in 17 m vol (2σ) 6 mm (pos) @ 50 m (range) 6–10 mm (pos) @range	up to 3000 pts/s 7000 pts/s output 1000 pts/s up to 1800 pts/s up to 500,000 pts/s
Metron Snoqualmie WA USA metronsys.com	MSG2	laser scanner	152–455 mm range	± 0.001 in	n/a
Nextec Tirat Hacarmel, Israel nextec-wiz.com	WizBlade WizInspect Hawk	laser scanner laser scanner laser scanner	1200 x 650 x 500 mm n/a 1400 x 650 x 500 mm	14 µm (2 σ) 6 µm (3 σ) 10 µm (1 σ)	50 pts/s 50 pts/s 40 pts/s
NextEngine Santa Monica, CA, USA nextengine.com	Desktop 3D Scanner	multistripe laser triangulation	130 x 97 mm (macro mode at 400 dpi) 343 x 257 mm (wide mode at 150 dpi)	± 0.005" (Macro mode) ± 0.015" (Wide mode)	50,000 processed pts/s
Nikon Metrology Leuven, Belgium nikonmetrology.com	XC65D LC15 LC60Dx MV260 MMDx MMC	laser line scanner (cross) laser line scanner laser line scanner laser radar arm-mounted laser scanner arm-mounted laser scanner	150 x 150 mm FOV 15 x 15 mm FOV 60 x 60 mm FOV 1–60 m range varies on arm length varies on arm length	15 µm (1 σ) 8 µm (1 σ) 7 µm (1 σ) 16–100 µm 10–15 µm 12-34 µm	19,200 pts/s 19,200 pts/s 75,000 pts/s 1,000 pts/s 150,000 pts/s 30,000 pts/s
Noomeo France noomeo.eu	OptiNum	vision-based self-positioning	0.1 m to 1.0 m FOV; 150 mm DOF	± 100 µm	n/a
Northern Digital Inc, Waterloo, Ontario, Canada ndigital.com	ScanTRAK VibraSCAN	optically tracked laser scanner self-positioning laser triangulation	1.34 x 1.28 m FOV 500 x 500 x 500 mm	40 µm 50 µm	Up to 150,000 pts/s 30,000 pts/s
North Star Imaging, Inc Rogers, MN, USA 4nsi.com	M50 M500 M5000	x-ray scanner x-ray scanner x-ray scanner	12 x 12 x 12 in 24 x 24 x 24 in 48 x 24 x 24 in	n/a n/a n/a	n/a n/a n/a
Nub3d Barcelona, Spain nub3d.com	SIDIO Pro SIDIO XR	structured white light structured white light	330 x 1200 mm 330 x 1200 mm	0.009 – 0.024 mm 0.009 – 0.019 mm	n/a n/a
Optimet Jerusalem, Israel optimet.com	ConoLine Smart Conoprobe	conoscopic holography (line) conoscopic holography (point)	45 mm DOF 1.8–120 mm range	2-25 µm 1–60 µm	18,000 pts/s 3000 pts/s
Perceptron Plymouth, MI, USA perceptron.com	Scanworks Contour Probe v5 Scanworks Contour Probe v4i	laser line scanner laser line scanner	varies on arm length varies on arm length	24µm, 2 σ 24µm, 2 σ	458,400 pts/s 23,040 pts/s
phoenix|x-ray Wunstorf, Germany microfocus-x-ray.com	v|tome|x 240 v|tome|x m v|tome|x 450 nanotom	X-ray computed tomography (CT) X-ray computed tomography (CT) X-ray computed tomography (CT) X-ray computed tomography (CT)	600 mm (h) x 500 mm (dia) 400 mm (h) x 250 mm (dia) 1000 mm (h) x 800 mm (dia) 127 mm (h) x 154 mm (dia)	4.0 µm (res) 4.0 µm (res) 4.0 µm (res) 0.5 µm (res)	n/a n/a n/a n/a

COPYRIGHT © 2011

3

WOHLERS ASSOCIATES, INC.

Wohlers Report 2011 — Appendix G: 3D scanning systems

Company	Product	Technology	Work volume	Accuracy[1]	Speed
Polhemus Inc. Colchester, VT, USA polhemus.com	FastScan Cobra/Scorpion	laser scan with magnetic tracking	0.75-75 cm	1 mm	50 lines/s
	Liberty	electromagnetic tracking	36 in range (up to 72 with decreased accuracy)	0.03 in RMS	240 updates/s
	Patriot	electromagnetic tracking	30–42 in range (up to 60 with decreased accuracy)	0.1 in RMS	60 updates/s
	Liberty Latus	large-area magnetic tracking	96 in range	0.1 in at 30 in (1–3 in typical)	94–188 updates/s
Riegl Horn, Austria riegl.com	LMS-Z420i	laser rangefinder	2–1000 m range, 360° H x 80° V	± 5 mm (multi-shot)	Up to 12,000 pts/s
	LMS-Z360i	laser rangefinder	1–200 m range, 360° H x 90° V	± 6 mm (multi-shot)	Up to 12,000 pts/s
	LMS-Z210i	laser rangefinder	4–400 m range, 360° H x 90° V	± 15 mm (multi-shot)	Up to 12,000 pts/s
	LPM-i800HA	laser profiler	10–800 m range, 360° H x 90° V	± 15 mm (multi-shot)	1000 pts/s
	LPM-2K	laser profiler	10–2500 m range, 360° H x 190° V	± 50 mm	4 pts/s
Roland DG Tokyo, Japan rolanddg.com	LPX-1200	laser line scanner	130 mm dia and 203.2 mm high	± 0.05 mm	n/a
	LPX-600	laser line scanner	254 mm dia and 406.4 mm high	± 0.05 mm	n/a
	LPX-60	laser line scanner	203 mm dia and 304.8 mm high	± 0.10 mm	n/a
Romer, Inc. (of Hexagon Metrology) Farmington Hills, MI, USA romer.com	Absolute Arm – 6 Axis	articulating arm	5 – 15 ft measuring range (varies by model)	± .037mm – ±.170 mm	n/a
	Absolute Arm – SE	articulating arm w/laser mount	7 – 15 ft measuring range (varies by model)	± .044mm – ±.156 mm	n/a
	Absolute Arm – SI	articulating arm w/laser scanner	7 – 15 ft measuring range (varies by model)	± .079mm – ±.214 mm	30,000 pts/s
RSI 3D Systems GmbH Oberursel, Germany rsi-gmbh.de	MicroScan 3D	laser line scanner	1200 x 800 x 400 mm	0.10 – 0.30 mm	28,000 pts/s
Scantech Ringsted, Denmark scantech.dk	St400 (Tympanon III)	laser line scanner	400 x 600 x 400 mm	± 0.02–0.1 mm	n/a
	St600	laser line scanner	400 x 600 x 400 mm (relief & cylindrical scanning)	± 0.02–0.1 mm	n/a
Shapegrabber, Ottawa, Ontario, Canada shapegrabber.com	AI300	laser line scanner	300 x 150 x 150 mm	0.04 mm	15,000–100,000 pts/s
	AI600	laser line scanner	600 x 150 x 150 mm	0.04 mm	
	AI810	laser line scanner	80 x 60 x 60 cm (single: 125 x 80 x 70 cm)	0.04 mm	
	LM600	laser line scanner	600 mm x 160 mm x 165 mm	0.03 mm	
	LM1250	laser line scanner	1250 mm x 750 mm x 1150 mm	0.1 mm	
	LM1750	laser line scanner	1750 mm x 750 mm x 1150 mm	0.1 mm	
Solutionix Seoul, Korea solutionix.com	Rexcan 4	phase-shifting optical triangulation	55 x 1715 mm	n/a	300,000 pts/0.7 sec
	Rexcan III	phase-shifting optical triangulation	75 x 420 – 880 x 587 mm	n/a	300,000 pts/0.7 sec
Steinbichler Optotechnik Neubeuern, Germany steinbichler.com	COMET5	white light triangulation	100 x 75 – 1200 x 1200 mm	n/a	~1 sec/scan
	T-SCAN 2	position-tracked laser scanner	90 mm scan width	±30 μm	n/a
	ABIS II	white light surface scanning	220–300 mm FOV	n/a	< 0.1 ms/scan
Surphaser West Chester, PA, USA surphaser.com	25HSX	phase-shift laser	1.5–22.5 m range, 360° H x 270° V	< 0.5 mm	190,000 pts/s
3D Digital Corp. (RealScan) Danbury, CT, USA 3ddigitalcorp.com	Optix 400H	laser line triangulation	350–550 mm DOF, 15° FOV	±30–80 μm	not specified
	Optix 400L	laser line triangulation	300–900 mm DOF, 30° FOV	±20–120 μm	not specified
	Optix 400M	laser line triangulation	300–650 mm DOF, 30° FOV	±35–100 μm	not specified
	Optix 400S	laser line triangulation	100–200 mm DOF, 30° FOV	±15–50 μm	not specified
	EScan	laser line triangulation	300–650 mm DOF, 40° FOV	±150–250 μm	not specified
3D3 Solutions Burnaby, BC, Canada 3d3solutions.com	HDI 3D	white light triangulation	200 x 200 cm	0.02 – 0.2 mm	500,000 pts/s
threeRivers 3D Gibsonia, PA 3rivers3d.com	LC-2	structured light triangulation	280 mm x 230 mm	n/a	500,000 pts/s

Wohlers Report 2011

Appendix G: 3D scanning systems

Company	Product	Technology	Work volume	Accuracy[1]	Speed
Trimble Navigation Sunnyvale, CA, USA trimble.com	GX Scanner VX Scanner	TOF (std and ext range models) TOF	horiz 360° x vert 60° FOV, 200 m std, 350 m ext horiz 360° x vert 60° FOV, 300–1600 m range	pos 12 mm @ 100m 10 mm @ 150 m	5000 pts/s up to 5000 pts/s
Vialux Chemnitz, Germany vialux.com	zSnapper	structured light triangulation	350 mm FOV	40 µm	300,000 pts/s
Wenzel Greding, Germany wenzel.com	MobileScan3D	laser line scanner	200–3000 mm (spherical)	0.01–0.25 mm	74,400 pts/s
Wolf & Beck Germany wolfbeck.com	WBRetro MAN	laser line scanner (CMM retrofit)	55–250 mm range	50–200 µm	250,000 pts/s
YXLON International X-Ray Hamburg, Germany yxlon.com	CT Precision CT Compact CT Modular CT Universal	cone beam volume CT cone beam volume CT cone beam volume CT cone beam volume CT	409 x 409 mm sensor area, 200 mm dia turntable 409 x 409 mm sensor area, 300 mm dia turntable 409 x 409 mm sensor area, 320 mm dia turntable 409 x 409 mm sensor area, 400 mm dia turntable	< 10 µm n/a < 10 µm n/a	1.8–15 min/scan ~100 sec/scan ~100 sec/scan ~100 sec/scan
Z Corporation Burlington, MA, USA zcorp.com	Z Scanner 600 Z Scanner 700 Z Scanner 800 Z Scanner 700 CX Z Scanner 800 PX	self-positioning laser triangulation self-positioning laser triangulation self-positioning laser triangulation self-positioning laser triangulation self-positioning laser triangulation	50–1000 mm range (portable) 50–1000 mm range (portable) 50–1000 mm range (portable) 50–1000 mm range (portable) 50–1000 mm range (portable)	± 0.05 mm ± 0.05 mm ± 0.04 mm ± 0.05 mm ± 0.05 mm	18,000 pts/s 18,000 pts/s 25,000 pts/s 18,000 pts/s 18,000 pts/s
Zoller+Fröhlich Wangen, Austria zf-laser.com	LARA 25200 LARA 53500 Imager 5003 – 25200 Imager 5003 – 53500	single spot laser (1D) single spot laser (1D) 2D deflected spot laser (360°) 2D deflected spot laser (360°)	1–25.2 m 1–53.5 m 1–25.2 m range, 360° H x 310° V 1–53.5 m range, 360° H x 310° V	≤ 3 mm ≤ 5 mm ≤ 3 mm, 0.02° ≤ 5 mm, 0.02°	≤ 625,000 pts/s ≤ 500,000 pts/s ~100 sec/scan ~100 sec/scan

Table created by Ping Fu and Kevin Scofield in cooperation with Wohlers Associates, Inc.

Footnote:
1. Accuracy as reported by vendor in technical specifications. Vendors that publish only repeatability or resolution are identified. For more information, contact the vendor directly.

5

WOHLERS ASSOCIATES, INC.

COPYRIGHT © 2011

Appendix B - Benchmark part – Drawings
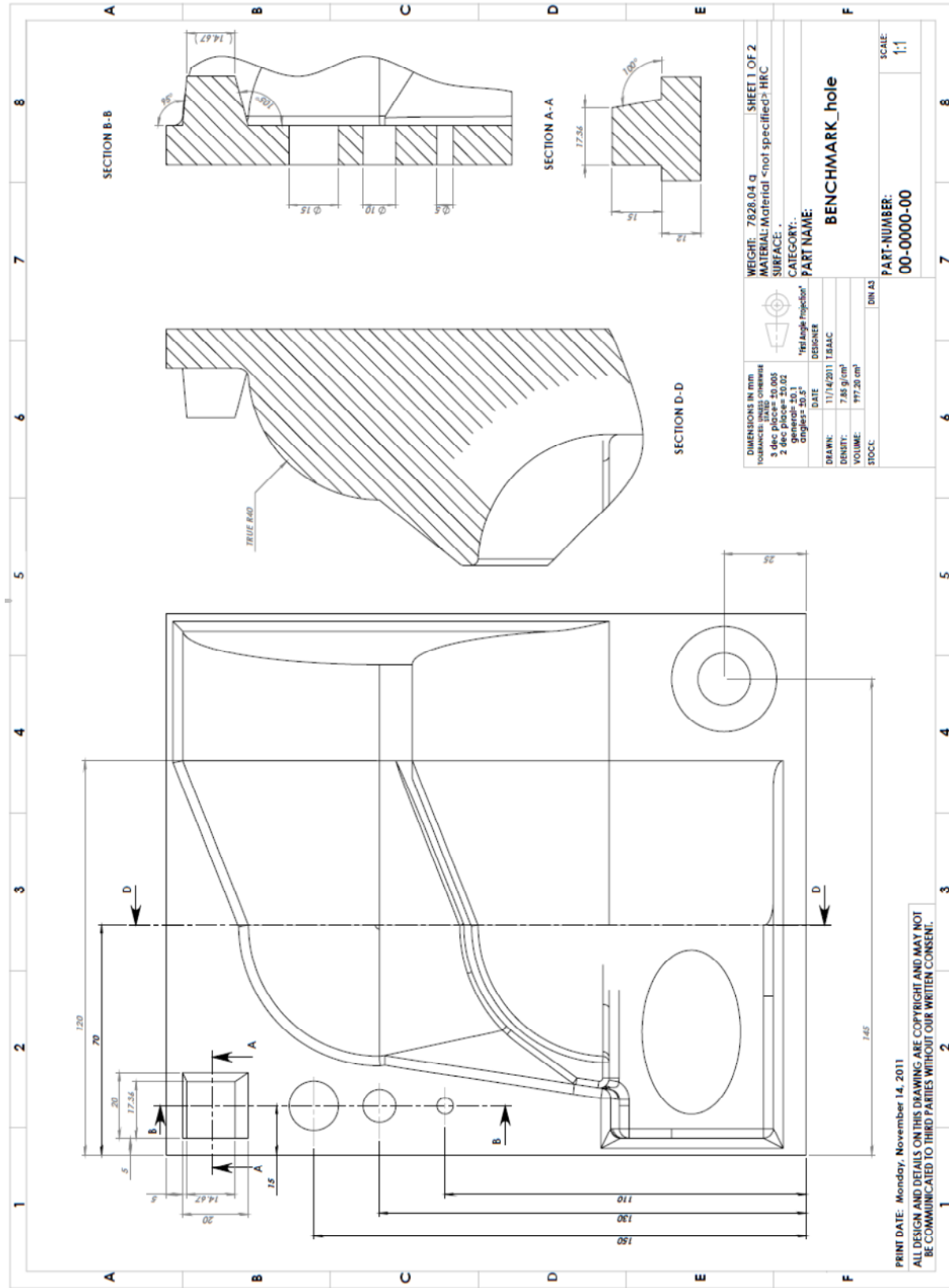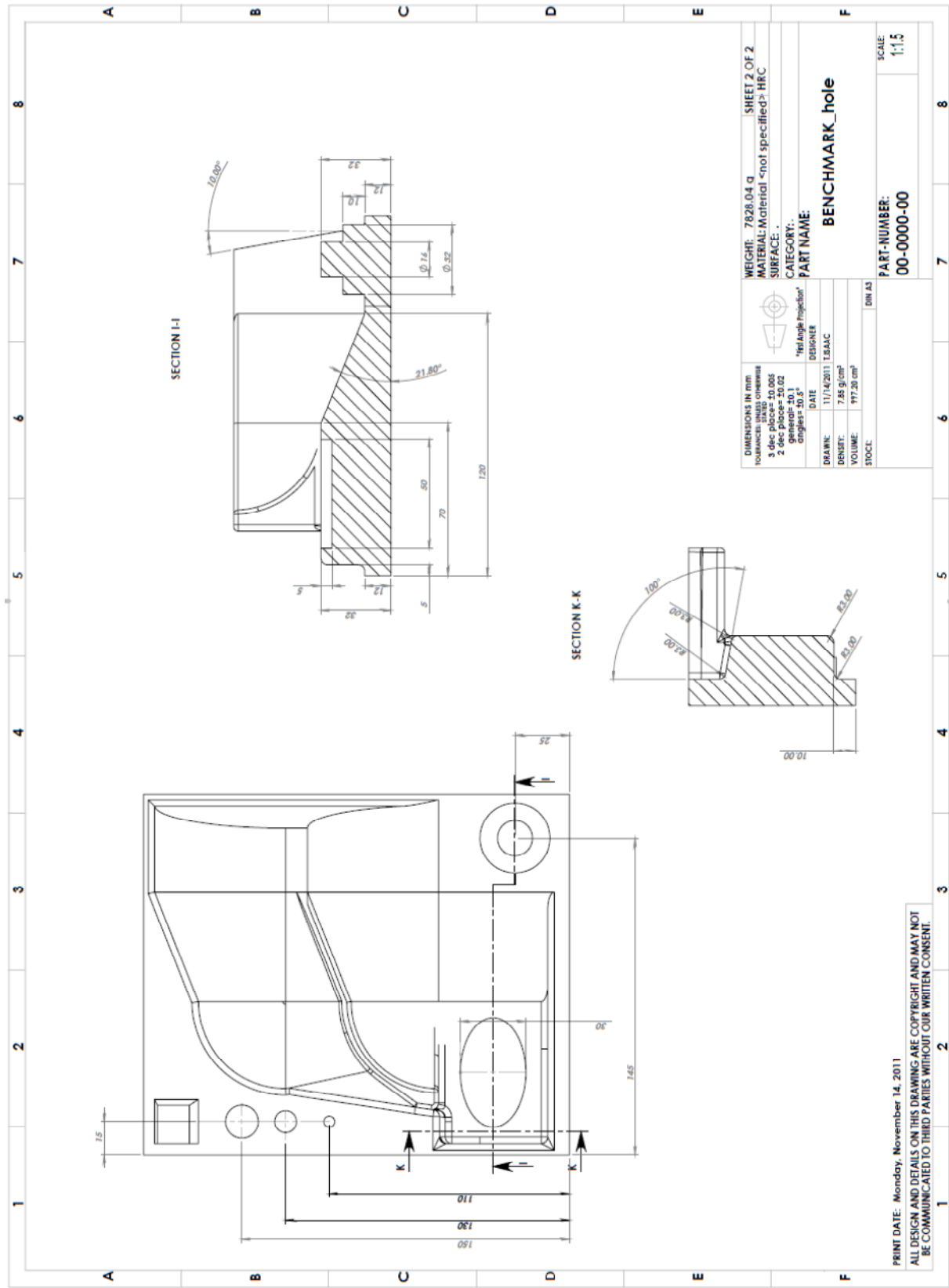
Appendix C – Data CMM (Benchmark Part)

Feature	Measurand	Unit	CAD model	1st replication	2st replication	3st replication	Mean	Std. Deviation	Difference
TSP1	Z	mm	15.000	15.061	15.040	15.051	15.051	0.011	-0.051
TSP2	X	mm	5.000	4.924	4.975	4.968	4.956	0.028	0.044
	α	degrees	0.000	0.043	0.040	0.450	0.178	0.236	-0.178
TSP3	α	degrees	5.000	5.335	5.333	5.055	5.241	0.161	-0.241
TSP4	α	degrees	10.000	9.963	10.194	10.009	10.055	0.122	-0.055
TSP5	α	degrees	15.000	15.014	15.087	15.031	15.044	0.038	-0.044
OS	R	mm	80.000	79.998	80.030	79.987	80.005	0.022	-0.005
	Xc	mm	70.000	69.929	69.939	69.928	69.932	0.006	0.068
	Yc	mm	130.000	129.932	129.932	129.935	129.933	0.002	0.067
	Zc	mm	0.000	0.006	0.012	0.003	0.007	0.005	-0.007
IS	R	mm	80.000	80.097	80.068	80.158	80.108	0.046	-0.108
	Xc	mm	70.000	69.929	69.975	70.004	69.969	0.038	0.031
	Yc	mm	60.000	59.888	59.917	59.863	59.889	0.027	0.111
	Zc	mm	60.000	60.035	60.030	60.061	60.042	0.017	-0.042
OC	R	mm	120.000	120.013	119.947	119.967	119.976	0.034	0.024
	Ya	mm	130.000	129.962	129.985	129.965	129.971	0.013	0.029
	Za	mm	0.000	0.000	0.032	0.020	0.017	0.016	-0.017
IC	R	mm	120.000	120.077	120.114	120.139	120.110	0.031	-0.110
	Ya	mm	60.000	59.916	59.908	59.879	59.901	0.019	0.099
	Za	mm	60.000	60.032	60.050	60.055	60.046	0.012	-0.046
OTC	α	degrees	43.600	43.344	43.486	43.537	43.456	0.100	0.144
	Ya	mm	130.000	129.938	129.945	129.961	129.948	0.012	0.052
	Za	mm	0.000	-0.021	-0.005	0.009	-0.006	0.015	0.006
ITC	α	degrees	43.600	43.652	43.412	43.418	43.494	0.137	0.106
	Ya	mm	60.000	59.881	59.825	59.839	59.848	0.029	0.152
	Za	mm	60.000	60.038	60.090	60.075	60.068	0.027	-0.068
CC1	Z	mm	20.000	19.941	19.940	19.924	19.935	0.010	0.065
	R	mm	8.000	7.980	7.978	7.979	7.979	0.001	0.021
	Xa	mm	145.000	144.972	144.970	144.969	144.970	0.002	0.030
	Ya	mm	25.000	24.956	24.957	24.945	24.953	0.007	0.047
CC2	Z	mm	10.000	9.989	9.963	9.957	9.970	0.017	0.030
	R	mm	16.000	15.984	15.983	15.980	15.982	0.002	0.018
	Xa	mm	145.000	144.968	144.967	144.965	144.967	0.002	0.033
	Ya	mm	25.000	24.958	24.957	24.943	24.953	0.008	0.047
EP	Min. R	mm	15.000	14.994	14.994	14.998	14.995	0.002	0.005
	Max. R	mm	25.000	24.993	24.999	24.994	24.995	0.003	0.005
HP1	Z	mm	0.000	0.053	0.059	0.062	0.058	0.005	-0.058
HP2	Z	mm	60.000	60.008	60.001	60.019	60.009	0.009	-0.009
HP3	Z	mm	20.000	20.000	19.999	20.000	20.000	0.001	0.000
HP4	Z	mm	15.000	15.014	15.013	15.009	15.012	0.003	-0.012
TP1	α	degrees	10.000	9.998	9.989	9.979	9.989	0.010	0.011
TP2	α	degrees	21.800	21.797	21.801	21.799	21.799	0.002	0.001
TP3	α	degrees	10.000	9.991	9.978	9.944	9.971	0.024	0.029
VP1	Y	mm	10.000	9.949	9.935	9.923	9.936	0.013	0.064
VP2	X	mm	5.000	4.955	4.967	4.949	4.957	0.009	0.043
H1	R	mm	7.500	7.461	7.466	7.468	7.465	0.004	0.035
	Xa	mm	15.000	14.932	14.930	14.929	14.930	0.002	0.070
	Ya	mm	150.000	149.951	149.931	149.927	149.936	0.013	0.064
H2	R	mm	5.000	4.967	4.957	4.962	4.962	0.005	0.039
	Xa	mm	15.000	14.939	14.927	14.899	14.922	0.021	0.078
	Ya	mm	130.000	129.945	129.932	129.923	129.933	0.011	0.067
H3	R	mm	2.500	2.454	2.445	2.456	2.452	0.006	0.048
	Xa	mm	15.000	14.927	14.929	14.930	14.929	0.002	0.071
	Ya	mm	110.000	109.946	109.930	109.932	109.936	0.009	0.064

Appendix D – CMM Uncertainty

Ring Ø 79.37557mm

n=5	Ø	d
1	79.381	0.006
2	79.383	0.011
3	79.382	0.007
4	79.379	0.006
5	79.381	0.026
avg	79.381	0.011
std	0.001	
dev	0.006	

n=10	Ø	d
1	79.380	0.021
2	79.382	0.010
3	79.381	0.004
4	79.383	0.007
5	79.375	0.026
avg	79.380	0.014
std	0.003	
dev	0.005	

n=20	Ø	d
1	79.381	0.017
2	79.382	0.029
3	79.382	0.015
4	79.382	0.016
5	79.378	0.011
avg	79.381	0.017
std	0.002	
dev	0.005	

Sphere Ø 24.99992mm

n=10	Ø	d
1	24.977	0.058
2	24.989	0.010
3	24.972	0.056
4	24.985	0.029
5	24.984	0.011
avg	24.981	0.033
std	0.007	
dev	-0.019	

n=20	Ø	d
1	24.994	0.052
2	24.995	0.071
3	25.004	0.040
4	25.004	0.114
5	25.000	0.046
avg	24.999	0.064
std	0.005	
dev	-0.001	

Block 100mm

point	distance
1	99.992
2	99.989
3	99.992
4	99.992
5	99.993
avg	99.992
std	0.002
dev	-0.008

line	distance
1	99.993
2	99.993
3	99.989
4	99.993
5	99.991
avg	99.992
std	0.002
dev	-0.008

plane	distance
1	99.989
2	99.976
3	99.970
4	100.019
5	100.038
avg	99.998
std	0.029
dev	-0.002

The data obtained from the experiment are shown above. The Ring is used as the sample calculation to show the steps taken in calculating the Uncertainty. The mean of the data set is calculated with the following formula:

$$\bar{x} = \frac{1}{n} \times \sum_1^n X_i = \frac{79.381+79.382+79.382+79.382+79.378}{5} = 79.381 mm$$

The standard deviation is calculated as follows:

$$S_x = \sqrt{\frac{\sum_1^n (\bar{x}-X_i)^2}{(n-1)}}$$

$$= \sqrt{\frac{(79.381-79.381)^2+(79.381-79.382)^2+(79.381-79.382)^2+(79.381-79.382)^2+(79.381-79.388)^2}{(5-1)}} = 0.002mm$$

Using equation 4 and reading off the student t-distribution graph for an experiment of 5 measurements and a desired probability of 95% the t value is 2.776.

$$u_{ring} = S_{ring,5} \times t_{4,95} = 0.002 * 2.776 = 0.0048mm$$

The ring is calibrated and is given with an uncertainty of 0.14μ therefore

$$u_{cal} = 0.00014mm$$

The uncertainty in the temperature is calculated as in Chapter 3 with the following formula, note the thermal expansion coefficient of steel is $1.1 \times 10^{-5}/°C$ at 20°C. The temperature difference is taken as ± 2 degrees over a normal distribution.

$$u_{\Delta t} = l \cdot \alpha \cdot \frac{\Delta t}{\sqrt{3}} = 80 \cdot 1.1 \cdot 10^{-5} \cdot \frac{2}{\sqrt{3}} = 0.001mm$$

The combined uncertainty is calculated as follows:

$$u_c = \sqrt{u_{ring}^2 + u_{cal}^2 + u_{\Delta t}^2} = \sqrt{0.0048^2 + 0.00014^2 + 0.001^2} = 0.0049mm$$

The extended Uncertainty is calculated including the coverage factor of k=2 and the bias error.

$$b = \bar{x} - x_b = 79.381 - 79.37557 = 0.0054mm$$

$$U_{ring} = k \cdot u_c + |b| = 2 * 0.0049 + |0.0054| = 0.015mm$$

This is repeated for the ceramic sphere (thermal expansion coefficient changes) and steel gauge block. Their extended uncertainty are as follows:

$$U_{sphere} = 0.027mm$$
$$U_{block} = 0.017mm$$

TABLE of CRITICAL VALUES for STUDENT'S *t* DISTRIBUTIONS

Column headings denote probabilities (α) **above** tabulated values.

d.f.	0.40	0.25	0.10	0.05	0.04	0.025	0.02	0.01	0.005	0.0025	0.001	0.0005
1	0.325	1.000	3.078	6.314	7.916	12.706	15.894	31.821	63.656	127.321	318.289	636.578
2	0.289	0.816	1.886	2.920	3.320	4.303	4.849	6.965	9.925	14.089	22.328	31.600
3	0.277	0.765	1.638	2.353	2.605	3.182	3.482	4.541	5.841	7.453	10.214	12.924
4	0.271	0.741	1.533	2.132	2.333	2.776	2.999	3.747	4.604	5.598	7.173	8.610
5	0.267	0.727	1.476	2.015	2.191	2.571	2.757	3.365	4.032	4.773	5.894	6.869
6	0.265	0.718	1.440	1.943	2.104	2.447	2.612	3.143	3.707	4.317	5.208	5.959
7	0.263	0.711	1.415	1.895	2.046	2.365	2.517	2.998	3.499	4.029	4.785	5.408
8	0.262	0.706	1.397	1.860	2.004	2.306	2.449	2.896	3.355	3.833	4.501	5.041
9	0.261	0.703	1.383	1.833	1.973	2.262	2.398	2.821	3.250	3.690	4.297	4.781
10	0.260	0.700	1.372	1.812	1.948	2.228	2.359	2.764	3.169	3.581	4.144	4.587
11	0.260	0.697	1.363	1.796	1.928	2.201	2.328	2.718	3.106	3.497	4.025	4.437
12	0.259	0.695	1.356	1.782	1.912	2.179	2.303	2.681	3.055	3.428	3.930	4.318
13	0.259	0.694	1.350	1.771	1.899	2.160	2.282	2.650	3.012	3.372	3.852	4.221
14	0.258	0.692	1.345	1.761	1.887	2.145	2.264	2.624	2.977	3.326	3.787	4.140
15	0.258	0.691	1.341	1.753	1.878	2.131	2.249	2.602	2.947	3.286	3.733	4.073
16	0.258	0.690	1.337	1.746	1.869	2.120	2.235	2.583	2.921	3.252	3.686	4.015
17	0.257	0.689	1.333	1.740	1.862	2.110	2.224	2.567	2.898	3.222	3.646	3.965
18	0.257	0.688	1.330	1.734	1.855	2.101	2.214	2.552	2.878	3.197	3.610	3.922
19	0.257	0.688	1.328	1.729	1.850	2.093	2.205	2.539	2.861	3.174	3.579	3.883
20	0.257	0.687	1.325	1.725	1.844	2.086	2.197	2.528	2.845	3.153	3.552	3.850
21	0.257	0.686	1.323	1.721	1.840	2.080	2.189	2.518	2.831	3.135	3.527	3.819
22	0.256	0.686	1.321	1.717	1.835	2.074	2.183	2.508	2.819	3.119	3.505	3.792
23	0.256	0.685	1.319	1.714	1.832	2.069	2.177	2.500	2.807	3.104	3.485	3.768
24	0.256	0.685	1.318	1.711	1.828	2.064	2.172	2.492	2.797	3.091	3.467	3.745
25	0.256	0.684	1.316	1.708	1.825	2.060	2.167	2.485	2.787	3.078	3.450	3.725
26	0.256	0.684	1.315	1.706	1.822	2.056	2.162	2.479	2.779	3.067	3.435	3.707
27	0.256	0.684	1.314	1.703	1.819	2.052	2.158	2.473	2.771	3.057	3.421	3.689
28	0.256	0.683	1.313	1.701	1.817	2.048	2.154	2.467	2.763	3.047	3.408	3.674
29	0.256	0.683	1.311	1.699	1.814	2.045	2.150	2.462	2.756	3.038	3.396	3.660
30	0.256	0.683	1.310	1.697	1.812	2.042	2.147	2.457	2.750	3.030	3.385	3.646
31	0.256	0.682	1.309	1.696	1.810	2.040	2.144	2.453	2.744	3.022	3.375	3.633
32	0.255	0.682	1.309	1.694	1.808	2.037	2.141	2.449	2.738	3.015	3.365	3.622
33	0.255	0.682	1.308	1.692	1.806	2.035	2.138	2.445	2.733	3.008	3.356	3.611
34	0.255	0.682	1.307	1.691	1.805	2.032	2.136	2.441	2.728	3.002	3.348	3.601
35	0.255	0.682	1.306	1.690	1.803	2.030	2.133	2.438	2.724	2.996	3.340	3.591
36	0.255	0.681	1.306	1.688	1.802	2.028	2.131	2.434	2.719	2.990	3.333	3.582
37	0.255	0.681	1.305	1.687	1.800	2.026	2.129	2.431	2.715	2.985	3.326	3.574
38	0.255	0.681	1.304	1.686	1.799	2.024	2.127	2.429	2.712	2.980	3.319	3.566
39	0.255	0.681	1.304	1.685	1.798	2.023	2.125	2.426	2.708	2.976	3.313	3.558
40	0.255	0.681	1.303	1.684	1.796	2.021	2.123	2.423	2.704	2.971	3.307	3.551
60	0.254	0.679	1.296	1.671	1.781	2.000	2.099	2.390	2.660	2.915	3.232	3.460
80	0.254	0.678	1.292	1.664	1.773	1.990	2.088	2.374	2.639	2.887	3.195	3.416
100	0.254	0.677	1.290	1.660	1.769	1.984	2.081	2.364	2.626	2.871	3.174	3.390
120	0.254	0.677	1.289	1.658	1.766	1.980	2.076	2.358	2.617	2.860	3.160	3.373
140	0.254	0.676	1.288	1.656	1.763	1.977	2.073	2.353	2.611	2.852	3.149	3.361
160	0.254	0.676	1.287	1.654	1.762	1.975	2.071	2.350	2.607	2.847	3.142	3.352
180	0.254	0.676	1.286	1.653	1.761	1.973	2.069	2.347	2.603	2.842	3.136	3.345
200	0.254	0.676	1.286	1.653	1.760	1.972	2.067	2.345	2.601	2.838	3.131	3.340
250	0.254	0.675	1.285	1.651	1.758	1.969	2.065	2.341	2.596	2.832	3.123	3.330
inf	0.253	0.674	1.282	1.645	1.751	1.960	2.054	2.326	2.576	2.807	3.090	3.290

Appendix E – Data Cimcore

Feature	Measurand	Unit	CAD model	1st replication	2st replication	3st replication	Mean	Std. Deviation	Difference
TSP1	Z	mm	15.000	15.036	15.027	14.975	15.013	0.033	-0.013
TSP2	X	mm	5.000	4.968	4.884	4.964	4.939	0.047	0.061
	α	degrees	0.000	0.003	0.045	-0.061	-0.004	0.053	0.004
TSP3	α	degrees	5.000	5.138	5.092	5.137	5.122	0.026	-0.122
TSP4	α	degrees	10.000	10.044	10.021	10.058	10.041	0.019	-0.041
TSP5	α	degrees	15.000	15.229	15.052	15.013	15.098	0.115	-0.098
OS	R	mm	80.000	80.005	79.839	80.013	79.952	0.098	0.048
	Xc	mm	70.000	70.039	69.865	69.981	69.962	0.089	0.038
	Yc	mm	130.000	129.891	129.948	129.881	129.907	0.036	0.093
	Zc	mm	0.000	0.039	0.083	-0.003	0.040	0.043	-0.040
IS	R	mm	80.000	80.147	80.176	80.142	80.155	0.018	-0.155
	Xc	mm	70.000	70.072	69.957	70.078	70.036	0.068	-0.036
	Yc	mm	60.000	59.776	59.804	59.799	59.793	0.015	0.207
	Zc	mm	60.000	60.044	60.095	60.102	60.080	0.032	-0.080
OC	R	mm	120.000	119.680	119.676	119.638	119.665	0.023	0.335
	Ya	mm	130.000	130.056	130.045	130.063	130.055	0.009	-0.055
	Za	mm	0.000	0.148	0.184	0.134	0.155	0.026	-0.155
IC	R	mm	120.000	120.255	120.047	120.276	120.193	0.127	-0.193
	Ya	mm	60.000	59.725	59.841	59.719	59.762	0.069	0.238
	Za	mm	60.000	60.111	60.059	60.159	60.110	0.050	-0.110
OTC	α	degrees	43.600	43.418	43.458	43.574	43.483	0.081	0.117
	Ya	mm	130.000	130.021	130.015	130.010	130.015	0.006	-0.015
	Za	mm	0.000	0.060	0.061	0.905	0.342	0.488	-0.342
ITC	α	degrees	43.600	43.796	43.650	43.610	43.685	0.098	-0.085
	Ya	mm	60.000	59.830	59.815	59.738	59.794	0.049	0.206
	Za	mm	60.000	60.003	60.051	60.081	60.045	0.039	-0.045
CC1	Z	mm	20.000	20.097	20.042	19.588	19.909	0.279	0.091
	R	mm	8.000	7.959	7.960	7.953	7.957	0.004	0.043
	Xa	mm	145.000	145.015	144.942	145.029	144.995	0.047	0.005
	Ya	mm	25.000	24.990	24.958	24.934	24.961	0.028	0.039
CC2	Z	mm	10.000	10.007	10.047	9.894	9.983	0.079	0.017
	R	mm	16.000	15.966	15.951	15.962	15.959	0.008	0.041
	Xa	mm	145.000	145.012	144.952	144.983	144.982	0.030	0.018
	Ya	mm	25.000	24.983	24.947	24.944	24.958	0.022	0.042
EP	Min. R	mm	15.000	15.001	14.994	14.997	14.997	0.004	0.003
	Max. R	mm	25.000	24.963	24.978	24.976	24.972	0.008	0.028
HP1	Z	mm	0.000	-0.002	0.050	0.032	0.027	0.026	-0.027
HP2	Z	mm	60.000	59.981	60.039	59.969	59.996	0.037	0.004
HP3	Z	mm	20.000	19.978	20.003	20.016	19.999	0.019	0.001
HP4	Z	mm	15.000	15.002	15.026	15.022	15.017	0.013	-0.017
TP1	α	degrees	10.000	9.965	9.972	9.989	9.975	0.012	0.025
TP2	α	degrees	21.800	21.800	21.791	21.795	21.795	0.005	0.005
TP3	α	degrees	10.000	9.978	10.032	10.053	10.021	0.039	-0.021
VP1	Y	mm	10.000	9.931	9.924	9.911	9.922	0.010	0.078
VP2	X	mm	5.000	5.015	4.941	4.927	4.961	0.047	0.039
H1	R	mm	7.500	7.495	7.502	7.497	7.498	0.003	0.002
	Xa	mm	15.000	14.961	14.913	14.955	14.943	0.026	0.057
	Ya	mm	150.000	149.897	149.930	149.897	149.908	0.019	0.092
H2	R	mm	5.000	5.011	4.953	4.982	4.982	0.029	0.018
	Xa	mm	15.000	14.967	14.989	14.896	14.951	0.049	0.049
	Ya	mm	130.000	129.890	129.924	129.902	129.905	0.017	0.095
H3	R	mm	2.500	NA	NA	NA	NA	NA	NA
	Xa	mm	15.000	NA	NA	NA	NA	NA	NA
	Ya	mm	110.000	NA	NA	NA	NA	NA	NA

Appendix F – Data GOM

Feature	Measurand	Unit	CAD model	1st replication	2st replication	3st replication	Mean	Std. Deviation	Difference
TSP1	Z	mm	15.000	14.893	14.945	14.948	14.929	0.031	0.071
TSP2	X	mm	5.000	4.965	5.004	4.990	4.986	0.020	0.014
	α	degrees	0.000	0.225	-0.089	0.142	0.093	0.163	-0.093
TSP3	α	degrees	5.000	5.207	4.683	4.940	4.943	0.262	0.057
TSP4	α	degrees	10.000	10.831	10.731	10.621	10.728	0.105	-0.728
TSP5	α	degrees	15.000	15.432	15.382	15.481	15.432	0.050	-0.432
OS	R	mm	80.000	79.802	79.884	79.966	79.884	0.082	0.116
	Xc	mm	70.000	69.869	69.933	69.964	69.922	0.048	0.078
	Yc	mm	130.000	130.060	130.127	130.139	130.109	0.043	-0.109
	Zc	mm	0.000	0.063	0.046	0.015	0.041	0.024	-0.041
IS	R	mm	80.000	80.065	79.989	80.015	80.023	0.039	-0.023
	Xc	mm	70.000	70.009	70.061	70.076	70.049	0.035	-0.049
	Yc	mm	60.000	59.905	59.961	59.950	59.939	0.030	0.061
	Zc	mm	60.000	60.099	60.037	60.057	60.064	0.032	-0.064
OC	R	mm	120.000	119.946	120.296	120.158	120.133	0.176	-0.133
	Ya	mm	130.000	130.029	130.037	130.088	130.051	0.032	-0.051
	Za	mm	0.000	0.055	-0.049	0.028	0.011	0.054	-0.011
IC	R	mm	120.000	120.016	120.128	120.112	120.085	0.061	-0.085
	Ya	mm	60.000	59.924	59.962	59.954	59.947	0.020	0.053
	Za	mm	60.000	59.999	60.040	60.053	60.031	0.028	-0.031
OTC	α	degrees	43.600	43.734	43.670	43.658	43.687	0.041	-0.087
	Ya	mm	130.000	130.099	130.161	130.157	130.139	0.035	-0.139
	Za	mm	0.000	0.119	0.093	0.082	0.098	0.019	-0.098
ITC	α	degrees	43.600	43.734	43.700	43.700	43.711	0.020	-0.111
	Ya	mm	60.000	59.864	59.927	59.931	59.907	0.038	0.093
	Za	mm	60.000	60.058	60.073	60.052	60.061	0.011	-0.061
CC1	Z	mm	20.000	20.011	20.003	20.021	20.012	0.009	-0.012
	R	mm	8.000	7.892	7.983	7.947	7.941	0.046	0.059
	Xa	mm	145.000	145.025	145.138	145.111	145.091	0.059	-0.091
	Ya	mm	25.000	24.917	24.992	24.982	24.964	0.041	0.036
CC2	Z	mm	10.000	9.971	9.988	10.002	9.987	0.016	0.013
	R	mm	16.000	15.945	15.983	15.878	15.935	0.053	0.065
	Xa	mm	145.000	144.938	145.131	144.938	145.002	0.111	-0.002
	Ya	mm	25.000	24.891	24.968	25.013	24.957	0.062	0.043
EP	Min. R	mm	15.000	15.020	15.012	14.982	15.004	0.020	-0.004
	Max. R	mm	25.000	25.063	25.033	25.045	25.047	0.015	-0.047
HP1	Z	mm	0.000	-0.003	-0.025	-0.018	-0.015	0.011	0.015
HP2	Z	mm	60.000	60.020	60.099	60.104	60.074	0.047	-0.074
HP3	Z	mm	20.000	20.106	20.067	20.063	20.079	0.024	-0.079
HP4	Z	mm	15.000	15.039	15.010	15.130	15.060	0.063	-0.060
TP1	α	degrees	10.000	9.943	9.952	9.962	9.952	0.010	0.048
TP2	α	degrees	21.800	21.951	21.904	21.893	21.916	0.031	-0.116
TP3	α	degrees	10.000	10.319	10.007	10.422	10.249	0.216	-0.249
VP1	Y	mm	10.000	9.958	9.932	9.931	9.940	0.015	0.060
VP2	X	mm	5.000	4.944	5.007	4.968	4.973	0.032	0.027
H1	R	mm	7.500	7.443	7.365	7.368	7.392	0.044	0.108
	Xa	mm	15.000	14.948	15.052	14.992	14.997	0.052	0.003
	Ya	mm	150.000	149.948	150.078	150.152	150.059	0.103	-0.059
H2	R	mm	5.000	4.797	4.774	4.770	4.780	0.014	0.220
	Xa	mm	15.000	14.946	15.026	15.114	15.029	0.084	-0.029
	Ya	mm	130.000	129.859	130.028	130.070	129.986	0.112	0.014
H3	R	mm	2.500	2.169	2.482	2.343	2.331	0.157	0.169
	Xa	mm	15.000	15.010	15.109	14.829	14.983	0.142	0.017
	Ya	mm	110.000	109.938	109.957	110.033	109.976	0.050	0.024

Appendix G – Data Renishaw

Feature	Measurand	Unit	CAD model	1st replication	2st replication	3st replication	Mean	Std. Deviation	Difference
TSP1	Z	mm	15.000	15.025	15.011	15.017	15.018	0.007	-0.018
TSP2	X	mm	5.000	4.750	4.950	5.000	4.900	0.132	0.100
	α	degrees	0.000	2.018	0.474	0.000	0.831	1.055	-0.831
TSP3	α	degrees	5.000	6.177	6.356	4.961	5.831	0.759	-0.831
TSP4	α	degrees	10.000	10.054	10.130	10.032	10.072	0.051	-0.072
TSP5	α	degrees	15.000	14.990	15.054	15.001	15.015	0.034	-0.015
OS	R	mm	80.000	80.053	80.215	80.040	80.103	0.098	-0.103
	Xc	mm	70.000	69.928	69.996	69.948	69.957	0.035	0.043
	Yc	mm	130.000	129.910	129.899	129.934	129.914	0.018	0.086
	Zc	mm	0.000	-0.012	-0.090	-0.013	-0.038	0.045	0.038
IS	R	mm	80.000	80.037	79.933	80.026	79.999	0.057	0.001
	Xc	mm	70.000	69.962	69.966	70.003	69.977	0.023	0.023
	Yc	mm	60.000	59.889	59.927	59.899	59.905	0.020	0.095
	Zc	mm	60.000	60.017	59.953	59.984	59.985	0.032	0.015
OC	R	mm	120.000	119.988	120.002	119.970	119.987	0.016	0.013
	Ya	mm	130.000	129.976	129.997	130.007	129.993	0.016	0.007
	Za	mm	0.000	0.022	0.000	0.020	0.014	0.012	-0.014
IC	R	mm	120.000	119.862	119.880	119.876	119.873	0.009	0.127
	Ya	mm	60.000	59.960	59.982	59.982	59.975	0.013	0.025
	Za	mm	60.000	59.942	59.936	59.942	59.940	0.003	0.060
OTC	α	degrees	43.600	43.622	43.620	43.616	43.619	0.003	-0.019
	Ya	mm	130.000	129.970	129.998	129.999	129.989	0.016	0.011
	Za	mm	0.000	0.029	0.019	0.032	0.027	0.007	-0.027
ITC	α	degrees	43.600	43.622	43.628	43.618	43.623	0.005	-0.023
	Ya	mm	60.000	59.891	59.945	59.912	59.916	0.027	0.084
	Za	mm	60.000	59.980	59.924	59.974	59.959	0.031	0.041
CC1	Z	mm	20.000	20.019	20.001	20.010	20.010	0.009	-0.010
	R	mm	8.000	8.296	7.933	7.971	8.066	0.200	-0.066
	Xa	mm	145.000	145.185	145.016	144.916	145.039	0.136	-0.039
	Ya	mm	25.000	25.089	25.065	24.930	25.028	0.086	-0.028
CC2	Z	mm	10.000	10.020	10.002	10.009	10.010	0.009	-0.010
	R	mm	16.000	16.156	15.956	15.941	16.018	0.120	-0.018
	Xa	mm	145.000	144.854	144.979	144.916	144.916	0.063	0.084
	Ya	mm	25.000	24.988	25.013	24.930	24.977	0.043	0.023
EP	Min. R	mm	15.000	15.252	15.007	14.813	15.024	0.220	-0.024
	Max. R	mm	25.000	25.033	25.016	25.122	25.057	0.057	-0.057
HP1	Z	mm	0.000	-0.003	-0.016	-0.010	-0.010	0.007	0.010
HP2	Z	mm	60.000	60.008	59.996	60.004	60.003	0.006	-0.003
HP3	Z	mm	20.000	20.000	19.993	19.989	19.994	0.006	0.006
HP4	Z	mm	15.000	15.013	15.001	15.000	15.005	0.007	-0.005
TP1	α	degrees	10.000	9.989	9.989	9.995	9.991	0.003	0.009
TP2	α	degrees	21.800	21.791	21.788	21.807	21.795	0.010	0.005
TP3	α	degrees	10.000	9.961	10.059	9.975	9.998	0.053	0.002
VP1	Y	mm	10.000	9.750	9.750	9.750	9.750	0.000	0.250
VP2	X	mm	5.000	4.750	4.950	4.957	4.886	0.118	0.114
H1	R	mm	7.500	7.445	7.573	7.442	7.487	0.075	0.014
	Xa	mm	15.000	15.281	14.697	14.709	14.896	0.334	0.104
	Ya	mm	150.000	149.910	150.253	149.984	150.049	0.181	-0.049
H2	R	mm	5.000	4.985	4.788	4.876	4.883	0.099	0.117
	Xa	mm	15.000	14.953	14.768	14.730	14.817	0.119	0.183
	Ya	mm	130.000	129.962	129.829	130.025	129.939	0.100	0.061
H3	R	mm	2.500	2.946	2.433	2.782	2.720	0.262	-0.220
	Xa	mm	15.000	15.002	15.031	14.968	15.000	0.032	0.000
	Ya	mm	110.000	109.944	109.923	109.748	109.872	0.108	0.128

Appendix H –Data Repeatability

Ø= 79.37557

	CMM	*ARM*	*GOM*	*RENISHAW*
1	79.376	79.375	79.427	79.366
2	79.378	79.373	79.415	79.378
3	79.377	79.369	79.448	79.356
4	79.377	79.352	79.469	79.358
5	79.378	79.382	79.481	79.372
6	79.377	79.401	79.384	79.376
7	79.378	79.391	79.384	79.376
8	79.377	79.392	79.384	79.374
9	79.378	79.417	79.424	79.376
10	79.377	79.411	79.436	79.370
11	79.378	79.390	79.413	79.368
12	79.378	79.405	79.406	79.364
13	79.376	79.376	79.398	79.370
14	79.377	79.386	79.379	79.360
15	79.377	79.358	79.439	79.376
16	79.377	79.384	79.421	79.368
17	79.378	79.378	79.407	79.358
18	79.378	79.372	79.378	79.364
19	79.379	79.409	79.433	79.374
20	79.378	79.366	79.452	79.372
avg.	79.377	79.384	79.419	79.369
std.	0.001	0.018	0.030	0.007
dev.	0.002	0.009	0.043	-0.007

Appendix I – Analytical Hierarchy Process

The quantified scores of the different repeatability results are listed and evaluated below (standard deviation from Section 4.4):

1. CMM   1μ
2. RENISHAW   7μ
3. ARM   18μ
4. GOM   30μ

		CMM	ARM	GOM	RENISHAW		
Repeatability Criterion Pairwise Comparison							
	CMM	1	5	8	2		
	ARM	0.200	1	3	0.333		
	GOM	0.125	0.333	1	0.167		
	RENISHAW	0.500	3	6	1		
	SUM	1.825	9.333	18.000	3.500		

		Normalised Comparison				Repeatability	Consistency
		CMM	**ARM**	**GOM**	**RENISHAW**	**Score**	**Measure**
	CMM	0.548	0.536	0.444	0.571	0.525	4.087
	ARM	0.110	0.107	0.167	0.095	0.120	4.023
	GOM	0.068	0.036	0.056	0.048	0.052	4.011
	RENISHAW	0.274	0.321	0.333	0.286	0.304	4.071

					Consistency Ratio:		0.018

	Key Cell Formulas		
Cell	Formula		Copied to
C10	= SUM(C6:C9)		D10:F10
C14	=C6/C$10		C15:F17
G14	=AVERAGE(C14:F14)		G15:G17
H14	=MMULT(C6:F9,$G$14:$G$17)/G14		H15:H17
H19	=(AVERAGE(H14:H17)-4)/(3*0.9)		-

The quantified scores for the speed of measurement results are listed and evaluated below (from Section 4.5):

1. ARM 13:00 min
2. GOM 21:40 min
3. CMM 29:30 min
4. RENISHAW 5:47 hours

		C	D	E	F	G	H
		Speed Criterion Pairwise Comparison					
		CMM	ARM	GOM	RENISHAW		
	CMM	1	0.250	0.500	6		
	ARM	4	1	2	9		
	GOM	2	0.500	1	8		
	RENISHAW	0.167	0.111	0.125	1		
	SUM	7.167	1.861	3.625	24.000		
		Normalised Comparison				**Speed**	**Consistency**
		CMM	ARM	GOM	RENISHAW	Score	Measure
	CMM	0.140	0.134	0.138	0.250	0.165	4.080
	ARM	0.558	0.537	0.552	0.375	0.506	4.161
	GOM	0.279	0.269	0.276	0.333	0.289	4.118
	RENISHAW	0.023	0.060	0.034	0.042	0.040	4.014
						Consistency Ratio:	0.035

		Key Cell Formulas			
	Cell	Formula			Copied to
	C10	= SUM(C6:C9)			D10:F10
	C14	=C6/C$10			C15:F17
	G14	=AVERAGE(C14:F14)			G15:G17
	H14	=MMULT(C6:F9,$G$14:$G$17)/G14			H15:H17
	H19	=(AVERAGE(H14:H17)-4)/(3*0.9)			-

The quantified score for the work envelope as obtained and verified from literature are as follows (from Section 4.6):

1. ARM $\qquad$ 3.71m^3
2. GOM $\qquad$ 1.98 m^3
3. CMM $\qquad$ 0.35 m^3
4. RENISHAW $\qquad$ 0.12 m^3

	A	B	C	D	E	F	G	H
1								
2			**Work Envelope Criterion**					
3			**Pairwise Comparison**					
4								
5			CMM	ARM	GOM	RENISHAW		
6		CMM	1	0	0	2		
7		ARM	7	1	4	8		
8		GOM	3	0.250	1	4		
9		RENISHAW	0.500	0	0	1		
10		SUM	11.500	1.518	5.583	15.000		
11								
12			Normalised Comparison				Work Envelope	Consistency
13			CMM	ARM	GOM	RENISHAW	Score	Measure
14		CMM	0.087	0.094	0.060	0.133	0.094	4.006
15		ARM	0.609	0.659	0.716	0.533	0.629	4.179
16		GOM	0.261	0.165	0.179	0.267	0.218	4.100
17		RENISHAW	0.043	0.082	0.045	0.067	0.059	4.033
18								
19							Consistency Ratio:	0.029
20								
21					Key Cell Formulas			
22		Cell	Formula					Copied to
23		C10	= SUM(C6:C9)					D10:F10
24		C14	=C6/C$10					C15:F17
25		G14	=AVERAGE(C14:F14)					G15:G17
26		H14	=MMULT(C6:F9,$G$14:$G$17)/G14					H15:H17
27		H19	=(AVERAGE(H14:H17)-4)/(3*0.9)					-
28								
29								

The user-friendliness scores as defined are listed and evaluated below (from Section 4.7):

1. ARM   18 stars
2. GOM   17 stars
3. CMM   16 stars
4. RENISHAW   10 stars

	A	B	C	D	E	F	G	H	I
1									
2				**User-friendliness**					
3				**Pairwise Comparison**					
4									
5			CMM	ARM	GOM	RENISHAW			
6		CMM	1	0.250	0.500	6			
7		ARM	4	1	2	9			
8		GOM	2	0.500	1	8			
9		RENISHAW	0.167	0.111	0.125	1			
10		SUM	7.167	1.861	3.625	24.000			
11									
12				Normalised Comparison			User-F.	Consistency	
13			CMM	ARM	GOM	RENISHAW	Score	Measure	
14		CMM	0.140	0.134	0.138	0.250	0.165	4.080	
15		ARM	0.558	0.537	0.552	0.375	0.506	4.161	
16		GOM	0.279	0.269	0.276	0.333	0.289	4.118	
17		RENISHAW	0.023	0.060	0.034	0.042	0.040	4.014	
18									
19							Consistency Ratio:	0.035	
20									
21				Key Cell Formulas					
22		Cell	Formula					Copied to	
23		C10	= SUM(C6:C9)					D10:F10	
24		C14	=C6/C$10					C15:F17	
25		G14	=AVERAGE(C14:F14)					G15:G17	
26		H14	=MMULT(C6:F9,$G$14:$G$17)/G14					H15:H17	
27		H19	=(AVERAGE(H14:H17)-4)/(3*0.9)					-	
28									
29									

The different Criterion Weights are calculated below:

	A	B	C	D	E	F	G	H	I
1									
2				**Criterion Weights**					
3				**Pairwise Comparison**					
4									
5			Accuracy	Repeatability	Speed	Work Envelope	User-F.		
6		**Accuracy**	1	3	7	6	3		
7		**Repeatability**	0.333	1	4	6	2		
8		**Speed**	0.143	0.250	1	4	0.250		
9		**Work Envelope**	0.167	0.167	0.250	1	0.200		
10		**User-F.**	0.333	0.500	4	5	1		
11		**SUM**	1.976	4.917	16.250	22.000	6.450		
12									
13				**Normalised Comparison**				Criterion	Consistency
14			Accuracy	Repeatability	Speed	Work Envelope	User-F.	Weight	Measure
15		**Accuracy**	0.506	0.610	0.431	0.273	0.465	0.457	5.550
16		**Repeatability**	0.169	0.203	0.246	0.273	0.310	0.240	5.530
17		**Speed**	0.072	0.051	0.062	0.182	0.039	0.081	5.174
18		**Work Envelope**	0.084	0.034	0.015	0.045	0.031	0.042	5.103
19		**User-F.**	0.169	0.102	0.246	0.227	0.155	0.180	5.488
20									
21						**Consistency Ratio:**			0.082
22									
23									
24					*Key Cell Formulas*				
25		*Cell*	*Formula*					*Copied to*	
26		C10	=SUM(C6:C10)					D11:G11	
27		C14	=C7/C$11					C15:G19	
28		G14	=AVERAGE(C15:G15)					H16:H19	
29		H14	=MMULT(C6:G6,$H$15:$H$19)/H15					I15:I17	
30		H19	=(AVERAGE(I15:I19)-5)/(4*1.12)					-	
31									